**Doctoral Dissertation**

# Visualization and Functional Control of Proteins in Living Cells by Using BL-tag Technology

**Akimasa Yoshimura**

**January 2014**

*Laboratory of Chemical Biology*

*Department of Material and Life Science*

*Division of Advanced Science and Biotechnology*

*Graduate School of Engineering*

*Osaka University*

# Contents

# Introduction

Proteins are involved in various chemical reactions in living systems, including metabolism. Thus, in order to understand fundamental biological processes, a comprehensive understanding of protein function is very important. This requires the development of protein research methods.

Fluorescent proteins (FPs) are some of the most robust tools available for studying protein function.[1] Green fluorescent protein (GFP) from the jellyfish *Aequorea victoria*, a typical FP used as a fluorescent label, is introduced into target proteins through genetic engineering (Figure I-1A).[2] The GFP chromophore, which absorbs blue light and emits green light, is encoded by the primary amino acid sequence at positions 65–67 (Ser-Tyr-Gly) among its 238 amino acids (27 kDa). GFP folds spontaneously without the requirement of cofactors or external enzyme components (Figure I-1B).[2b, 3] GFP-fused proteins can be expressed by introduction of genes into cells, which are localized to particular sites through the action of appropriate targeting signals; this allows imaging of a range of biological events. Furthermore, the emergence of spectral variants of *A. victoria* GFP, as well as the identification of GFP-like proteins in other organisms, has enabled simultaneous observation of multiple cellular events.[4] In addition to localization studies, FP-fusion proteins can be used to detect biochemical parameters such as metabolite concentrations, enzyme activity, or protein-protein interactions.[5] Thus, fusion proteins prepared by linking FPs can be used to image any target protein. However, FPs cannot be used in multicolor pulse-chase experiments because the timing of labeling and labeling efficiency cannot be controlled.[6] Moreover, some FPs become oligomerized and aggregated.[7] When GFP is expressed as a fusion

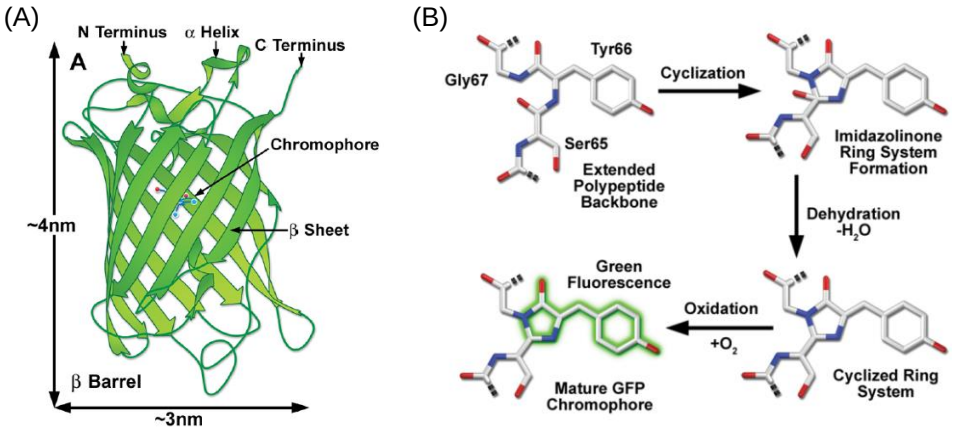


***Figure I-1.*** (A) Structure of GFP. (B) Formation of the GFP chromophore. Sequence of GFP choromophore after cyclization tripeptide made of Ser65, Tyr66, and Gly67.

construct with another protein in cells, the concentration is typically considered to be in the range at which protein molecules primarily exist as monomers. However, when specific cellular localization results in high local concentrations, fusion protein dimerization may be induced by the fluorescent protein, which can result in the loss of function or mislocalization of the protein.

**Protein labeling with fluorescent small molecules using BL-tag system**

Recently, labeling of proteins with small functional molecules has become an important research method.[8] This provides a wider range of methods for studying target proteins compared to labeling with fluorescent proteins.[9] Various protein labeling methods have been reported based on enzyme-catalyzed modification,[10] specific chelation of fluorescent ligands to short peptides[11], and protein tags.[12]

The author's group recently developed a specific protein-labeling system based on mutant β-lactamase (TEM-1) known as BL-tag system (Scheme I-1A).[13] This labeling system involves covalent modification of BL-tag with various functional probes. β-Lactamases are members of a bacterial enzyme family that efficiently cleave β-lactam moieties within compounds such as penicillins and cephalosporins.[14] Because the activity of β-lactamases has not been observed in eukaryotic cells, these proteins have been widely exploited as reporter enzymes in living mammalian cells.[15] One such well-characterized isoform is the 29-kDa TEM-1 β-lactamase from *Escherichia coli*, which is categorized as a class A β-lactamase.[16]

The reaction between wild-type (WT) TEM-1 and β-lactams involves both acylation

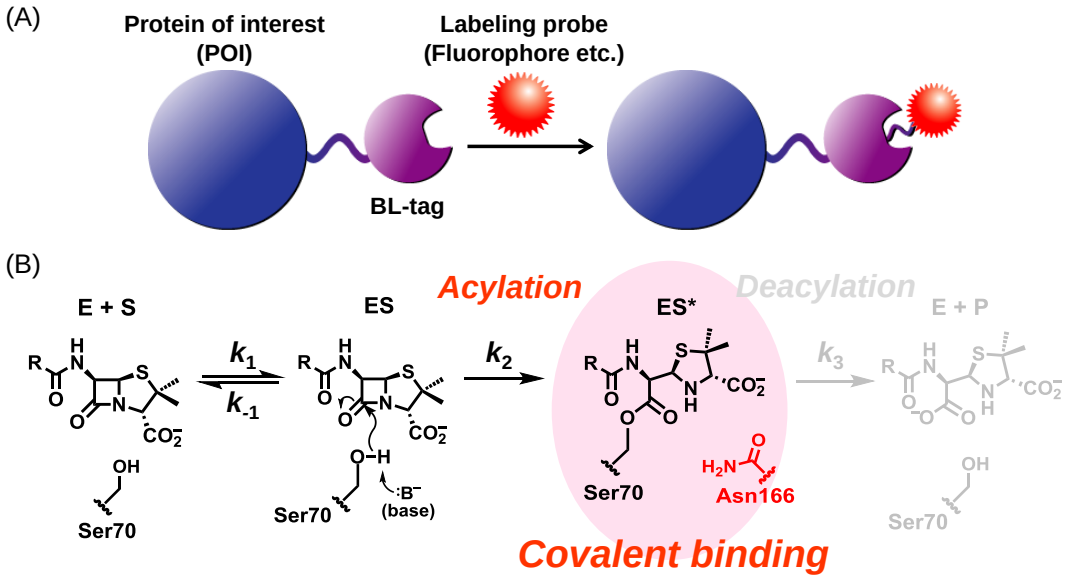


***Scheme I-1.*** (A) Protein labeling system based on mutant (E166N) TEM-1 β-lactamase (BL-tag). (B) Labeling reaction of BL-tag.

and deacylation steps. Nucleophilic attack on the β-lactam ring by Ser70 leads to the formation of a covalent acyl-enzyme intermediate.[17] In WT TEM-1, Glu166 acts as a base to catalyze hydrolysis of the intermediate, resulting in release of the product and regeneration of WT TEM-1. In E166N TEM, Asn166 is ineffective as a base; hence, the intermediate accumulates as a stable covalent adduct (Scheme I-1B).[18]

Various functional probes for labeling cell-surface proteins have been developed. These probes are composed of ampicillin and fluorescent dyes (Scheme I-2A). Moreover, fluorescent probes for labeling intracellular proteins have also been developed (Scheme I-2B)[19]. These probes contain bacampicillin as BL-tag ligand structure. Bacampicillin is a prodrug of ampicillin; the carboxylate is modified to a non-charged ester to improve the oral bioavailability.[20] Bacampicillin-based probes permeate the cell membrane to covalently bind to BL-tag-fused intracellular proteins. This technology is quite versatile and can be used in various applications, such as

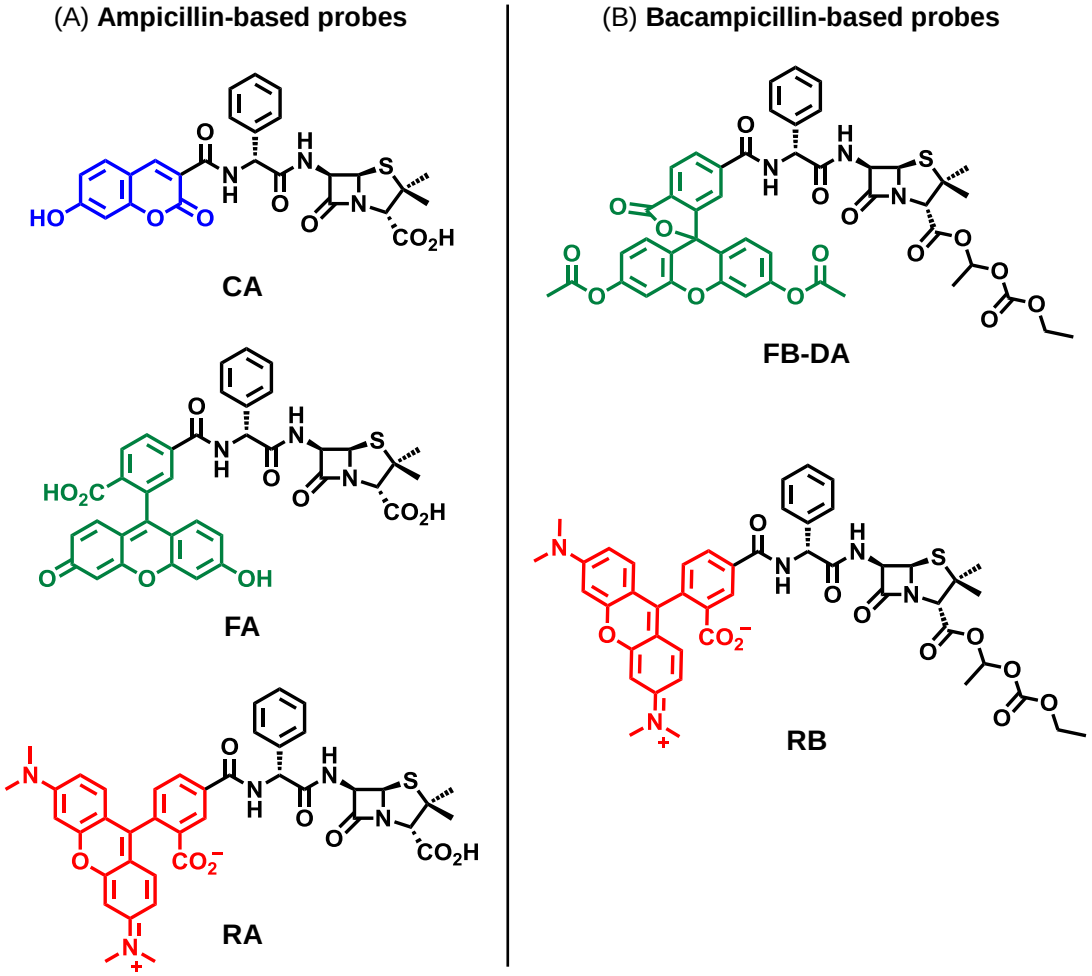


***Scheme I-2.*** Fluorescent labeling probes for BL-tag. (A) Ampicillin-based probes. (B) Bacampicillin-based probes.

time-resolved fluorescence imaging using a lanthanide-based probe.[21] Labeling probes that can be turned on using fluorescence switches based on Förster resonance energy transfer (FRET)[13, 22] or aggregation quenching[23] have been developed.

Although there are many benefits to the use of fluorescence imaging, it is not applicable for the imaging of deep regions in living animals. Therefore, detection of proteins of interest (POIs) by means other than fluorescence imaging is required. Moreover, fluorescence-labeled POIs should be analyzed in detail to examine protein function using techniques such as single-molecule imaging.[24] Moreover, techniques for controlling protein function are required in order to better understand complex living systems.

**Purpose of research**

The author investigated the development of multilateral protein research tools using BL-tag technology. First, multilateral imaging methods were developed that enabled both fluorescence imaging and magnetic resonance imaging (MRI). Next, the structure of a cell-permeable probe was optimized and applied to single-molecule imaging, allowing individual POIs to be visualized. This method was used to analyze immune system function. Finally, a protein dimerization system based on a protein-labeling system was developed in order to control protein function. Using this system, manipulation of epidermal growth factor receptor (EGFR) signaling in living cells was demonstrated. Moreover, manipulation of cell signaling through EGFR regulated by ultraviolet (UV) light irradiation was successfully achieved using a photoactivatable molecule.

## References


1. (a) N.C. Shaner, G.H. Patterson, M.W. Davidson, *J. Cell. Sci.* **2007**, *120*, 4247–4260. (b) M. Zimmer *Chem. Soc. Rev.* **2009**, *38*, 2823–2832. (c) A. Miyawaki, *Nat. Rev. Mol. Cell Biol.* **2011**, *12*, 656–668. (d) M. Chalfie, Y. Tu, G. Euskirchen, W.W. Ward, D.C. Prasher, *Science* **1994**, *263*, 802–805.
2. (a) R.Y. Tsien, *Annu. Rev. Biochem.* **1998**, *67*, 509–544. (b) M.A. Rizzo, M.W. Davidson, D.W. Piston, *Cold Spring Harb. Protoc.* **2009**, pdb.top63.
3. (a) C.W. Cody, D.C. Prasher, W.M. Westler, F.G. Prendergast, W.W. Ward, *Biochemistry* **1993**, *32*, 1212–1218. (b) R. Heim, D.C. Prasher, R.Y. Tsien, *Proc. Natl. Acad. Sci. U. S. A.* **1994**, *91*, 12501–12504.

4. (a) A. Miyawaki, *Neuron* **2005**, *48*, 189–199. (b) N.C. Shaner, P.A. Steinbach, R.Y. Tsien, *Nat. Methods* **2005**, *2*, 905–909. (c) N.C. Shaner, G.H. Patterson, M.W. Davidson, *J. Cell Sci.* **2007**, *120*, 4247–4260. (d) R.N. Day, M.W. Davidson, *Chem. Soc. Rev.* **2009**, *38*, 2887–2921. (e) D.M. Chudakov, M.V. Matz, S. Lukyanov, K. Lukyanov, *Physiol. Rev.* **2010**, *90*, 1103–1163.
5. (a) J. Zhang, R.E. Campbell, A.Y. Ting, R.Y. Tsien, *Nat. Rev. Mol. Cell Biol.* **2002**, *3*, 906–918. (b) A. Miyawaki, A. Sawano, T. Kogure, *Nat. Cell Biol.* **2003**, *5*, S1–S7. (c) J. Lippincott-Schwartz, N. Altan-Bonnet, G.H. Patterson, *Nat. Cell Biol.* **2003**, *5*, S7–S14.
6. G. Gaietta, T.J. Deerinck, S.R. Adams, J. Bouwer, O. Tour, D.W. Laird, G.E. Sosinsky, R.Y. Tsien, M.H. Ellisman, *Science* **2002**, *296*, 503–507.
7. J. Wiedenmann, F. Oswald, G.U. Nienhaus, *Iubmb Life* **2009**, *61*, 1029–1042.
8. (a) D. Jung, K. Min, J. Jung, W. Jang, Y. Kwon, *Mol. Biosyst.* **2013**, *9*, 862–872. (b) H.M. O'Hare, K. Johnsson, A. Gautier, *Curr. Opin. Struct. Biol.* **2007**, *17*, 488–494. (c) I. Chen, A.Y. Ting, *Curr. Opin. Biotechnol.* **2005**, *16*, 35–40.
9. B.N.G. Giepmans, S.R. Adams, M.H. Ellisman, R.Y. Tsien, *Science* **2006**, *312*, 217–224.
10. (a) I. Chen, M. Howarth, W. Lin, A.Y. Ting, *Nat. Methods* **2005**, *2*, 99–104. (b) N. George, H. Pick, H. Vogel, N. Johnsson, K. Johnsson, *J. Am. Chem. Soc.* **2004**, *126*, 8896–8897.
11. (a) B.A. Griffin, S.R. Adams, R.Y. Tsien, *Science* **1998**, *281*, 269–272. (b) S.R. Adams, R.E. Campbell, L.A. Gross, B.R. Martin, G.K. Walkup, Y. Yao. J. Llopis, R.Y. Tsien, *J. Am. Chem. Soc.* **2002**, *124*, 6063–6076. (c) C.T. Hauser, R.Y. Tsien, *Proc. Natl. Acad. Sci. U. S. A.* **2007**, *104*, 3693–3697.
12. (a) G.V. Los, L.P. Encell, M.G. McDougall, D.D. Hartzell, N. Karassina, C. Zimprich, M.G. Wood, R. Learish, R.F. Ohana, M. Urh, D. Simpson, J. Mendez, K. Zimmerman, P. Otto, G. Vidugiris, J. Zhu, A. Darzins, D.H. Klaubert, R.F. Bulleit, K.V. Wood, *ACS Chem. Biol.* **2008**, *3*, 373–382. (b) A. Keppler, S. Gendreizig, H. Pick, H. Vogel, K. Johnsson, *Nat. Biotechnol.* **2003**, *21*, 86–89. (c) A. Gautier, A. Juillerat, C. Heinis, I.R. Corrêa. Jr, M. Kindermann, F. Beaufils, K. Johnsson, *Chem. Biol.* **2008**, *15*, 128–136. (d) S.S. Gallagher, J.E. Sable, M.P. Sheetz, V.W. Cornish, *ACS Chem. Biol.* **2009**, *4*, 547–556. (e) Z. Chen, C. Jing, S.S. Gallagher, M.P. Sheetz, V.W. Cornish, *J. Am. Chem. Soc.* **2012**, *134*, 13692–13699. (f) Y. Hori, H. Ueno, S. Mizukami, K. Kikuchi, *J. Am. Chem. Soc.* **2009**, *131*, 16610–16111. (g) Y. Hori, K. Nakaki, M. Sato, S. Mizukami, K. Kikuchi, *Angew. Chem. Int. Ed.*, **2012**, *51*, 5611–5614.

13. S. Mizukami, S. Watanabe, Y. Hori, K. Kikuchi, *J. Am. Chem. Soc.* **2009**, *131*, 5016–5017.
14. H. Christensen, T.M. Martin, S.G. Waley, *Biochem. J.* **1990**, *266*, 853–861.
15. (a) J.T. Moore, S.T. Davis, I.K. Dev, *Anal. Biochem.* **1997**, *247*, 203–209. (b) G. Zlokarnik, P.A. Negulescu, T.E. Knapp, L. Mere, N. Burres, L. Feng, M. Whitney, K. Roemer, R.Y. Tsien, *Science* **1998**, *279*, 84–88. (c) W. Gao, B. Xing, R.Y. Tsien, J. Rao, *J. Am. Chem. Soc.* **2003**, *125*, 11146–11147.
16. A. Matagne, J. Lamotte-Blasseur, J.-M. Fre´re, *Biochem. J.* **1998**, *330*, 581–598.
17. G. Guillaume, M. Vanhove, J. Lamotte-Brasseur, P. Ledent, M. Jamin, B. Joris, J.-M. Fre´re, *J. Biol. Chem.* **1997**, *272*, 5438–5444.
18. H. Adachi, T. Ohta, H. Matsuzawa, *J. Biol. Chem.* **1991**, *266*, 3186–3191.
19. S. Watanabe, S. Mizukami, Y. Akimoto, Y. Hori, K. Kikuchi, *Chem. Eur. J.* **2011**, *17*, 8342–8349.
20. N.-O. Bodin, B. Ekström, U. Forsgren, L.-P. Jalar, L. Magni, C.-H. Ramsay, B. Sjöberg, *Antimicrob. Agents Chemother.* **1975**, *8*, 518–525.
21. S. Mizukami, T. Yamamoto, A. Yoshimura, S. Watanabe, K. Kikuchi, *Angew. Chem. Int. Ed.* **2011**, *50*, 8750–8752.
22. (a) S. Watanabe, S. Mizukami, Y. Hori, K. Kikuchi, *Bioconjugate Chem.* **2010**, *21*, 2320–2326. (b) S. Mizukami, S. Watanabe, Y. Akimoto, K. Kikuchi, *J. Am. Chem. Soc.* **2012**, *134*, 1623–1629.
23. (a) K.K. Sadhu, S. Mizukami, S. Watanabe, K. Kikuchi, *Chem. Commun.*, **2010**, *46*, 7403–7405. (b) K.K. Sadhu, S. Mizukami, S. Watanabe, K. Kikuchi, *Mol. BioSyst.* **2011**, *7*, 1766–1772.
24. A.D. Mehta, M. Rief, J.A. Spudich, D.A. Smith, R.M. Simmons, *Science* **1999**, *283*, 1689–1695.

# **Chapter 1.** Development of Multilateral Imaging Methods for Cell-Surface Proteins by Using Protein Tag and Functional Nanoparticles

Cell surface proteins play important roles in various biological processes. Most of these proteins are classified into groups based on their functions, such as membrane receptors, ion channels, or transporters. These proteins transduce biological signals in response to extracellular signals or transport biological substances from the outside of the cell to the interior. Thus, it is important to investigate the activities and localization of cell surface proteins. Multilateral detection of cell surface proteins was performed by focusing on the biotinylation of target proteins as biotin strongly binds to commercially available streptavidin-conjugated molecules. Thus, biotinylation of proteins of interest (POIs) enabled the introduction of various types of functional molecules onto proteins. Biotinylation is typically performed using a biotin ligase[1] or HaloTag.[2] In addition, other protein-labeling methods using tag proteins,[3] tag peptides,[4] or enzymes[5] have been reported.

Previously, the author's group achieved visualization of cell-surface proteins using a BL-tag and fluorescent probes.[6] Using the biotinylation probe, BL-tag technology is useful because it combines streptavidin-conjugated functional molecules.

First, luminescent quantum dots (QDs) were used as a streptavidin-conjugated functional molecule. Fluorescence imaging using luminescent QDs as fluorophores has been reported for surface protein identification.[7] QDs are semiconductor nanoparticles with many unique functions, such as stronger emission intensity compared to small molecular dyes and remarkable resistance to photobleaching. QDs of different sizes can simultaneously display different colors when excited at a single wavelength; thus, multicolor imaging can be achieved via simple experiments.

Although fluorescence imaging has many benefits, it is not applicable for imaging of deep regions in living animals. Comparatively, many in vivo imaging methods have been established, such as bioluminescence imaging, X-ray computed tomography (CT), positron-emission tomography (PET), single-photon emission computed tomography (SPECT), and magnetic resonance imaging (MRI).[8] Bioluminescence imaging is also often used to visualize gene expression[9]; however, its detectable emission is prone to attenuation with increased tissue thickness and this method does not allow absolute

signal quantification.[10] Visualization of gene expression using other in vivo imaging methods remains challenging, although some pioneering studies have been reported.[11] Therefore, the author investigated the detection of cell-surface proteins using MRI and superparamagnetic iron oxide (SPIO) nanoparticles,[12] which were introduced into proteins. SPIO alters the longitudinal and transverse relaxation times of $^{1}H$ atoms in biological tissues. SPIO is known to be a negative contrast agent in MRI, producing dark signals on MR images and providing a drastic signal change per unit of metal, particularly $T_2$-weighted images. The method enables multilateral detection of cell-surface proteins by fluorescence and MRI achieved using biotinylated proteins and commercially available streptavidin-conjugated functional molecules.

## Biotinylation of BL-tag-fused POIs

First, a biotinylation probe **BHA** was designed and synthesized (Scheme 1-1A). The labeling scheme is illustrated in Scheme 1-1B.

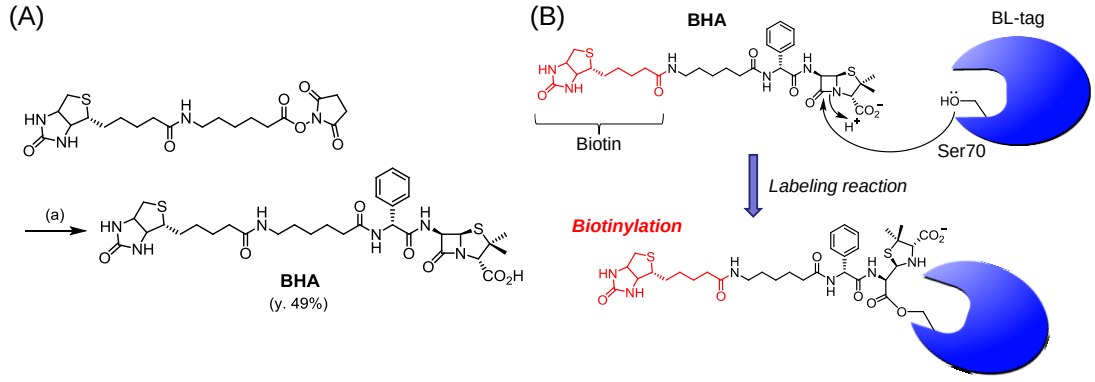


***Scheme 1-1.*** (A) Synthetic scheme of **BHA**. (a) ampicillin, TEA, DMF. (B) Labeling mechanism of BL-tag and **BHA**.

The purified BL-tag was incubated with **BHA** in 10 mM Tris-HCl buffer (pH 7.0) at 25°C and then analyzed by western blotting. The biotinylated protein, which was detected using streptavidin-horseradish peroxidase (HRP) and its substrate, were observed at ~29 kDa. (Figure 1-1A). Next, the reaction rate of **BHA** and BL-tag protein were investigated over time as the band signal on the western blot (Figure 1-1B). The reaction was completely finished within 60 min under the reaction conditions.

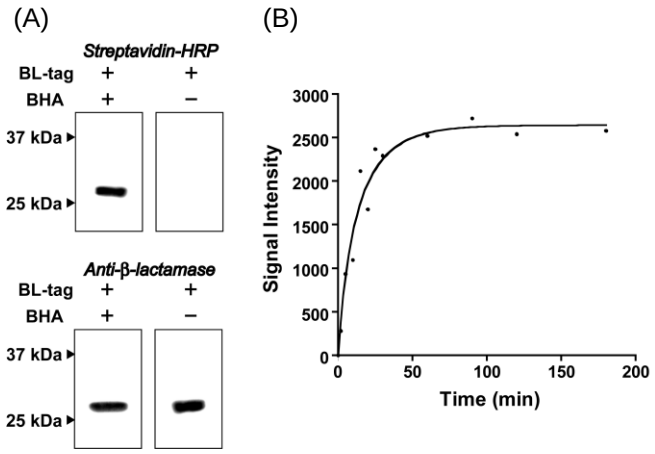


***Figure 1-1.*** (A) Western blot of BL-tag incubated with **BHA**. Protein bands were visualized with streptavidin conjugated-HRP (top) and anti-β-lactamase antibody (bottom). (B) Binding reaction rate of **BHA** (2 μM) and BL-tag (1 μM) at room temperature in 10 mM Tris-HCl buffer (pH 7.0). Aliquots of the solution mixture were analyzed at the indicated time points. Signal intensities were determined from the bands on the western blot.

## Fluorescence imaging of cell-surface proteins with QDs

Fluorescence imaging of cell-surface proteins was examined using **BHA** and QDs. Labeling of cell surface proteins with QDs facilitates the investigation of protein localization and movement, among other parameters.

Cell surface proteins were labeled with QDs. Cell surface proteins fused with BL-tag at the extracellular terminus can be labeled with **BHA** and streptavidin-conjugated QDs. Epidermal growth factor receptor (EGFR) was selected as the POI because EGFR is known to be overexpressed in several types of cancers, including lung and stomach cancer.[13] It has also been reported that internalization of EGFR transduces cell proliferation signals to the intracellular milieu. EGFR fused with BL-tag at the N-terminus (BL-EGFR) was overexpressed on the plasma membrane of mammalian HEK293T cells. Next, BL-EGFR was labeled with QD605 ($\lambda_{em\ max}$ = 605 nm) in two steps using **BHA** and streptavidin-conjugated QD605. When the cells were observed

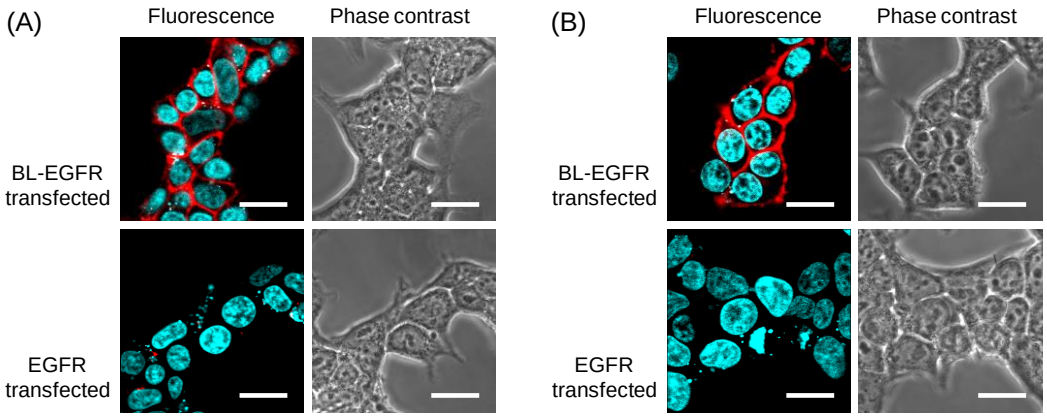


***Figure 1-2.*** Labeling of BL-EGFR fusion proteins with **BHA** and streptavidin-conjugated QDs through (A) two steps or (B) one step co-stained with Hoechst 33342. For fluorescence microscopic images, QDs and Hoechst 33342 were excited at 405 nm. Scale bar: 20 μm.

under a confocal laser scanning microscope, only cells overexpressing BL-EGFR showed red fluorescence at the plasma membranes (Figure 1-2A). No fluorescence was observed at the plasma membrane of cells overexpressing EGFR. One-step QD labeling was also performed. **BHA** was mixed with QD605 to form **BHA**-QD605 conjugates before incubation with HEK293T cells. QD605 fluorescence was detected from the plasma membranes of cells overexpressing BL-EGFR (Figure 1-2B).

Next, pulse-chase imaging of EGFR in living HEK293T cells was performed using **BHA** and three different QDs. BL-EGFR was labeled with QD605, QD525, and QD655 at 18 h, 24 h, and 30 h after transfection, respectively. The purpose of this experiment was to label newly expressed proteins with different colors of QDs and to visualize time-dependent changes in their localization induced by low amounts of EGF included in fetal bovine serum (FBS). BL-EGFR expressed in the first 18 h after transfection was selectively visualized as red fluorescence, whereas proteins expressed 18–24 h and 24–30 h after transfection were labeled as green and blue, respectively (Figure 1-3). Although QD fluorescence was mostly detected at the plasma membrane immediately after labeling, some QDs were internalized and fluorescent vesicles could be detected inside cells 6 h after labeling. In the merged fluorescence images of different QDs, red and green fluorescent dots could be observed. Thus, internalized EGFRs could be distinguished from newly expressed EGFRs. Thus, pulse-chase imaging of EGFR was successful using a simple experimental setup with BL-tag and QDs; these results cannot be achieved using fluorescent proteins. Imaging was successful using a single excitation laser and a single expressed protein; thus, the photochemical characteristics of QDs are well suited for tracking the timing of protein expression.

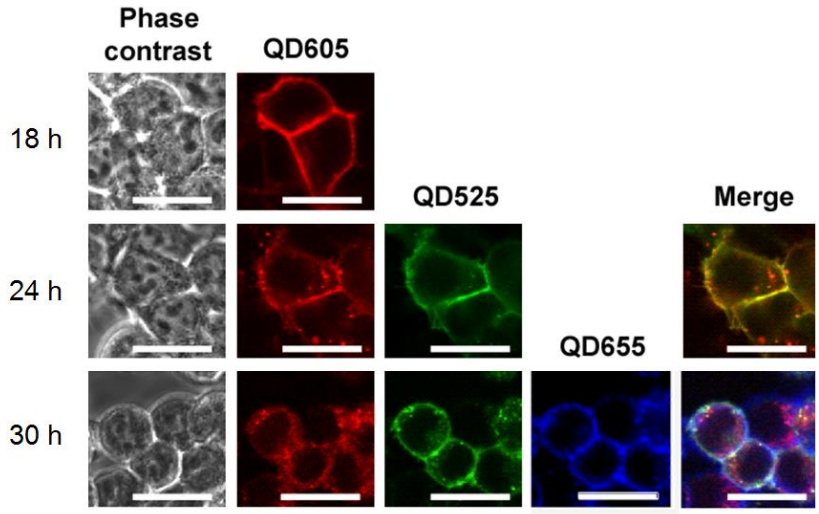


***Figure 1-3.*** Fluorescence images of QDs-labeled BL-EGFR at 18 h, 24 h, and 30 h after transfection. Scale bar: 20 μm.

**Detection of POI expression in living cells by MRI**

The author attempted to detect target POI expression using MRI. As a streptavidin-conjugated functional molecule, SPIO nanoparticles were used. First, the specific introduction of SPIO onto cell-surfaces displaying BL-tag protein was confirmed. BL-EGFR was overexpressed in mammalian HEK293T cells. As a control, cells were transfected with a plasmid encoding EGFR or an empty vector and the cells were detached and treated with **BHA**. Next, unreacted **BHA** was removed by washing with phosphate-buffered saline (PBS) and incubating with streptavidin-conjugated SPIO (diameter: 20 nm). Unreacted SPIO was removed by washing with PBS, after which the cells were suspended in PBS. Relaxation times of the suspension were measured using a 0.47 T nuclear magnetic resonance (NMR) instrument. Both $T_1$ and $T_2$ of the suspension containing BL-EGFR-expressing cells were decreased to a greater extent than the control suspensions containing wild-type EGFR-expressing cells or empty vector-transfected cells (Figure 1-4). This result indicates that streptavidin-conjugated SPIO was specifically introduced onto cell-surface BL-tag proteins through **BHA**. Because of the significant decrease in $T_2$, SPIO-labeled cells can be negatively imaged using an appropriate pulse sequence for highlighting changes in $T_2$.

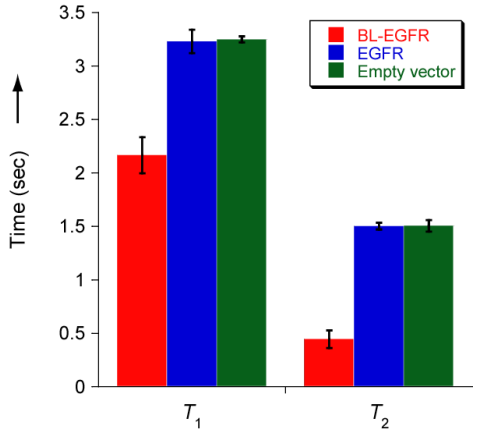


***Figure 1-4.*** Longitudinal relaxation time ($T_1$) and transverse relaxation time ($T_2$) of suspensions containing HEK293T cells transfected with *BL-EGFR*, *EGFR*, and the empty vector at 37°C. Results are means ± S.E.M. of triplicate determination.

Next, $^1$H MRI visualization of gene expression in living cells was performed. The plasmid encoding BL-EGFR was transfected into HEK293T cells and the fusion protein was overexpressed on the cell-surface. Next, cells were detached and incubated with **BHA** (50 μM in 200 μL PBS) at 37°C for 60 min. Unreacted **BHA** was removed by washing with PBS and incubation with streptavidin-conjugated SPIO (0.4 μM/mL (Fe) in 200 μL PBS, diameter: 20 nm) at 4°C for 30 min. Unreacted SPIO was removed by washing with PBS; $1.0 \times 10^6$ cells were pelleted in a polymerase chain reaction (PCR) tube by centrifugation. $^1$H images were captured using an 11.7 T MRI scanner (Figure

1-5A). The pellet of the cells treated with **BHA** and streptavidin-conjugated SPIO were only negatively visualized on the $^{1}$H MR image when the plasmid encoding BL-EGFR was transfected (Figure 1-5B). In comparison, the pellets of wild-type EGFR-transfected cells and empty vector-transfected cells were not clearly visible using $^{1}$H MRI (Figure 1-5C and 1-5D).

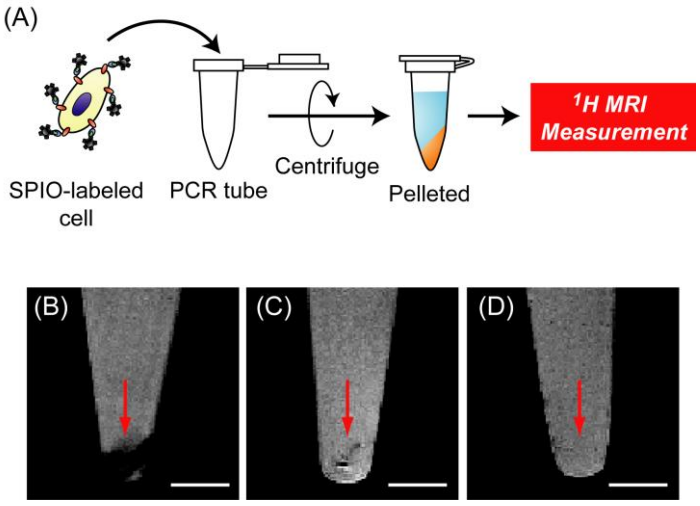


***Figure 1-5.*** $^{1}$H MRI detection of target gene expression in living cells. (A) Illustration of the experimental protocol to detect expression of the BL-EGFR gene in pelleted HEK293T cells by $^{1}$H MRI. (B–D) $^{1}$H MRI images of pelleted cells transfected with *BL-EGFR* (B), *EGFR* (C), and the empty vector (D) in PCR tubes. Red arrows indicate cell pellets. Scale bar: 3 mm. RARE sequence was used with the following parameters; *T*E, 8.9 ms; *T*R, 4000 ms; NEX, 2; matrix size, 256 × 256; FOV, 20 mm × 20 mm; and slice thickness, 0.5 mm).

Finally, gene expression was detected in living cells that were dispersed in an agarose gel using MRI. Living HEK293T cells transfected with the BL-EGFR gene were labeled with streptavidin-conjugated SPIO through **BHA**. In this experiment, larger-sized SPIO nanoparticles (diameter: 100 nm) were used to ensure sensitivity, as relaxivity is enhanced with increasing size.[14] Next, a suspension of SPIO-labeled cells was mixed with agarose solution and fixed in a dispersed state. $^{1}$H MRI images of the gels containing dispersed cells were captured using an 11.7 T MRI scanner. On MR images, SPIO-labeled cells that expressed an extrinsic reporter gene of BL-EGFR were imaged as several black dots in the agarose gel (Figure 1-6A). By contrast, a dark spot for SPIO nanoparticles was not observed on MR images of control cells, which had been transfected with a wild-type EGFR gene or an empty vector (Figure 1-6B and 1-6C). In addition, by mixing a gadolinium-based positive contrast agent, Omniscan® (Gd-DTPA-BMA),[15] in the gel, background signals were notably decreased and the MRI signal contrast was greatly enhanced (Figure 1-6D–F). As a result, BL-EGFR gene expression in dispersed living cells was detected using $^{1}$H MR imaging with a higher

signal-to-noise ratio by using a combination of positive and negative MRI contrast agents.

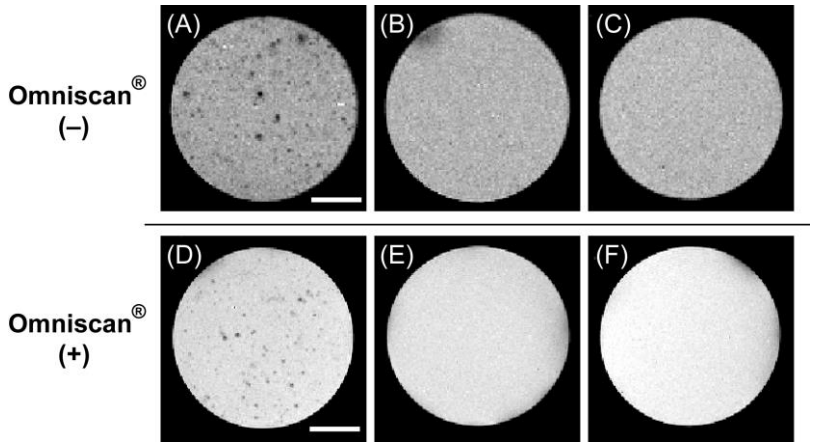


***Figure 1-6.*** $^{1}$H MRI images of target gene expression in dispersed living HEK293T cells. The cells transfected with *BL-EGFR* (A,D), *EGFR* (B,E), and empty vector (C,F) were dispersed in agarose gel. $^{1}$H images were taken in the presence (A–C) and absence (D–F) of Omniscan®. Scale bar: 3 mm. FLASH sequence was used with following parameters: *T*E, 8.0 ms; *T*R, 200 ms; NEX, 64; matrix size, 512 × 512; FOV, 20 mm × 20 mm; and slice thickness, 0.5 mm). In the presence of Omniscan®, the following parameters were changed: *T*R, 80 ms and *T*E, 4.9 ms.

## Experimental Section

**Materials.** The chemicals used in the experiment were supplied by Wako Pure Chemical and Tokyo Chemical Industries. These were of the highest grade available and used without further purification. EZ-Link NHS-LC-Biotin was purchased from Pierce. The synthesized probe was dissolved in dimethylsulfoxide (DMSO, biochemical grade, Wako Pure Chemical) and diluted with aqueous buffer prior to experiments to ensure it was solubilized in the aqueous solvents. Kanamycin and inorganic chemicals were purchased from Wako Pure chemical or Nacalai Tesque. *E. coli* BL21 (DE3) (Novagen) was the host for target gene expression. Luria-Bertani (LB) medium or Terrific Broth (TB) was used as the growth medium for all bacterial strains. Bacto Agar (Wako Pure Chemical) was added at concentrations up to 1.5% for the preparation of solid media.

**Instruments.** NMR spectra were recorded on a JEOL JNM-AL400 instrument at 400 MHz for $^{1}$H and at 100.4 MHz for $^{13}$C NMR, using tetramethylsilane as an internal standard. Mass spectra were measured on a JEOL JMS-700 mass spectrometer for FAB and on a Waters LCT-Premier XE mass spectrometer for ESI.

## Synthesis of Compound

**Synthesis of BHA.** Ampicillin (30.7 mg, 0.0879 mmol) was dissolved in anhydrous dimethylformamide (DMF; 2 mL), and triethylamine (25 µL, 0.176 mmol) was added. The reaction mixuture was stirred at room temperature for 10 min under argon, and EZ-Link NHS-LC-Biotin (20 mg, 0.0440 mmol) was added. The reaction mixuture was stirred at room temperature for 2 h under argon and then evaporated. The compound was purified with reversed-phase HPLC to produce pure **BHA** (14.9 mg, 0.0217 mmol, y. 49%). $^{1}$H NMR (400 MHz, DMSO-$d_6$) $\delta$ 9.08 (d, 1H, $J$ = 8.3 Hz), 8.47 (d, 1H, $J$ = 8.8 Hz), 7.71 (t, 1H, $J$ = 5.1 Hz), 7.40 (t, 1H, $J$ = 7.3 Hz), 7.31 (d, 2H, $J$ = 7.3 Hz), 7.26 (d, 2H, $J$ = 7.3 Hz), 6.37 (s, 2H), 5.70 (d, 1H, $J$ = 8.8 Hz), 5.51 (t, 1H, $J$ = 8.3 Hz), 5.37 (d, 1H, $J$ = 8.3 Hz), 4.18 (s, 1H), 4.11–4.08 (m, 2H, m), 2.98 (d, 1H, $J$ = 6.0 Hz), 2.18 (t, 2H, $J$ = 5.1 Hz), 2.02 (t, 2H, $J$ = 6.8 Hz), 1.48–1.20 (m, 16H), 1.53 (s, 1H), 1.40 (s, 1H); $^{13}$C NMR (100 MHz, DMSO-$d_6$) $\delta$ 174.3, 172.5, 172.0, 171.8, 170.3, 164.9, 134.3, 129.2, 127.1, 79.5, 72.3, 64.5, 63.7, 62.1, 60.7, 59.2, 55.4, 41.5, 38.3, 35.6, 35.3, 30.4, 29.4, 28.2, 28.0, 25.8, 25.3, 25.1, 24.4; HRMS (FAB$^+$) *m/z*: 689.2783 (Calcd for $[M+H]^+$ 689.2785).

## Experimental Procedures

**HPLC analysis.** HPLC analyses were performed with an Inertsil ODS-3 column (4.6 mm×250 mm, GL Sciences Inc.) using an HPLC system composed of a pump (PU-2080, JASCO) and a detector (MD-2010 and FP-2020, JASCO). Preparative HPLC was performed with an Inertsil ODS-3 column (10.0 mm × 250 mm, GL Sciences Inc.) using an HPLC system with a pump (PU-2087, JASCO) and a detector (UV-2075, JASCO).

**Plasmid constructs.** The pET-24a(+)-BL-tag, pCDNA3.1(+)-BL-EGFR, and pCDNA3.1(+)-EGFR plasmids were constructed previously.[6a]

**Expression and purification of mutant β-lactamase (BL-tag).** For protein purification, *E. coli* BL21 (DE3) cells were cultured overnight in LB medium supplemented with 20 µg/mL kanamycin and subsequently diluted 100-fold in TB supplemented with 20 µg/mL kanamycin, 500 mM sorbitol, and 2.5 mM betaine. After incubation for 4–5 h at 37 °C with shaking (260–280 rpm) until the optical density of the culture medium was 0.6 at 600 nm, isopropyl-β-D-thiogalactopyranoside (IPTG) was added to the medium at a final concentration of 0.4 mM, and the culture was incubated overnight at 25°C. The cells were pelleted by centrifugation, and the supernatant containing the enzyme was concentrated and replaced by 10 mM Tris-HCl

buffer (pH 7.0) using a Vivaspin centrifugal concentrator (membrane molecular weight cut off: 10,000; Sartorius). The concentrated proteins were loaded onto a DEAE Sephadex column equilibrated with the same buffer. BL-tag was eluted with a stepwise gradient elution (10–100 mM Tris-HCl buffer, pH 7.0).

**Blotting analysis of BHA labeling.** BL-tag (1 μM) was added to a solution of **BHA** (2 μM) in 10 mM Tris-HCl buffer (pH 7.0) at room temperature for 1 h. For the analysis of the binding reaction rate of BL-tag and **BHA**, the reaction mixture was sampled at 0, 2, 5, 10, 15, 20, 25, 30, 60, 90, 120, and 180 min. They were mixed with 2 × sample buffer (100 mM Tris-HCl buffer (pH 6.8), 2.5% sodium dodecyl sulfate (SDS), 20% glycerol, and 10% mercaptoethanol) and subjected to SDS-PAGE, followed by transfer onto a polyvinylidene fluoride (PVDF) membrane (Millipore). The immunodetection of BL-tag was performed with anti-β-lactamase antibody (1:3000 dilution) (Millipore) and horseradish peroxidase (HRP)-conjugated anti-rabbit IgG antibody (1:2000 dilution) (GE Healthcare). The chemiluminescence signal using western blotting substrate (Thermo Scientific) was detected with ImageQuant LAS 4000 mini (GE Healthcare). After removing the anti-β-lactamase antibody by washing with the stripping buffer (pH 2.0, 2.5 mM glycine, 1% SDS), the membrane was treated with streptavidin-conjugated HRP (1:5000 dilution) (Thermo Scientific) and detected by chemiluminescence.

**Cell culture and BL-tag fusion protein expression in HEK293T cells.** HEK293T cells were cultured in high-glucose Dulbecco's Modified Eagle Medium (DMEM) +Gluta Max-I (Invitrogen) supplemented with 10% fetal bovine serum (FBS, Sigma Aldrich), penicillin (100 units/mL), and streptmycin (100 μg/mL) (Invitrogen). Cells were incubated at 37°C in a humidified atmosphere of 5% $CO_2$ in air. A subculture was performed every 2–3 days from subconfluent (<80%) cultures using a trypsin-EDTA solution (Invitrogen). Transfection of plasmids was carried out in a glass-bottomed dish (Matsunami) using Lipofectamine 2000 (Invitrogen) according to the general protocol.

**Fluorescence microscopy.** Fluorescence microscopic images were recorded using a confocal laser scanning microscope (Olympus, FLUOVIEW FV10i) equipped with a 60× lens and the appropriate emission filters. Quantum dots (QD525, 605, 655) and Hoechst 33342 were excited with a 405 nm laser.

**General procedures for BL-tag-fused EGFR labeling.**

**(a) Two-step labeling.** HEK293T cells incubated in 10% FBS in DMEM at 37°C under 5% $CO_2$ were transfected with the pcDNA3.1(+)-BL-EGFR and pcDNA3.1(+)-EGFR plasmids using Lipofectamine 2000 (Invitrogen). After 3 h, the culture medium was replaced with DMEM, and the cells were incubated at 37°C for 24 h. Then, the cells were washed three times with phosphate-buffered saline (PBS) and incubated with 10

μM **BHA** in DMEM for 1 h in a $CO_2$ incubator. Then, the cells were washed three times with Hank's balanced salt solution (HBSS, Invitrogen), incubated with 10 nM QD605-streptavidin (Invitrogen), and costained with Hoechst 33342 (Invitrogen) for 1 h at room temperature. After the culture medium was replaced, microscopic images were acquired. The fluorescence microscopic images were deconvoluted using ImageJ software.

**(b) One-step labeling. BHA** was mixed with the streptavidin-QD605 conjugate at a ratio of 50:1 in HBSS for 30 min at room temperature, and free ligand was removed with three washes using Vivaspin (membrane molecular weight cut off: 3,000) by centrifugation at 7000 rpm for 5 min at 4°C. Final QD/**BHA** complexes were collected with HBSS for concentration determination. Cells were prepared using previous protocols for labeling. After washing twice with HBSS, transfected cells were incubated with 20 nM QD/**BHA** ligand conjugates and costained with Hoechst 33342 for 1 h at room temperature. The incubation buffer was removed, and the cells were washed three times with HBSS before imaging. The fluorescence microscopic images were deconvoluted using ImageJ software.

**Pulse-chase labeling of BL-EGFR internalization.** BL-EGFR overexpressed on HEK293T cell surfaces was labeled by treatment with 10 μM **BHA** in DMEM. The dish was incubated for 60 min in a $CO_2$ incubator. After removing the probe solution, the cells were washed with HBSS three times. Next, the biotinylated cells were labeled by treatment with 10 nM streptavidin-conjugated QD605 in HBSS. Unreacted QD605-streptavidin was washed by HBSS three times, and the cells were observed by fluorescence microscopy. The cells were incubated in a $CO_2$ incubator for 6 h again and treated with **BHA** (10 μM) and QD525-streptavidin (10 nM). After incubation in a $CO_2$ incubator for 6 h, the cells were treated with **BHA** (10 μM) and QD655-streptavidin (10 nM).

**Relaxation time measurements of SPIO-labeled cell suspensions.** Transfected cells were washed three times with phosphate-buffered saline (PBS) and detached and suspended in 200 μL of PBS. The cells were incubated with 50 μM of **BHA** for 1 h in a $CO_2$ incubator, followed by washing three times with PBS. Next, the cells were incubated with 0.4 μM/mL (Fe) streptavidin-conjugated nanomag® D-spio (Micromod, 79-19-201, diameter: 20 nm) for 30 min at 4°C. Finally, the cells were washed with PBS three times, and 500 μL of cell suspension containing $1.0 \times 10^5$ cells were aliquoted into an NMR tube (diameter: 10 mm, Bruker Optics). Relaxation times were measured by a Minispec mq20 (Bruker Optics) at 37°C. The inversion-recovery sequence and Carr–Purcell–Meiboom–Gill sequence were used for the measurements of

both $T_1$ and $T_2$.

**$^1$H MRI visualization of BL-EGFR expression in living HEK293T cells.** Transfected cells were detached and labeled with 50 μM **BHA** in DMEM. The cells were incubated for 60 min in a $CO_2$ incubator. After removing the probe solution, the cells were washed with PBS three times. Next, the cells were incubated with 0.4 μM/mL (Fe) streptavidin-conjugated nanomag® D-spio (Micromod, 79-19-201, diameter: 20 nm) for 30 min at 4°C. The cells were washed with PBS three times and then, $1.0 \times 10^6$ cells were pelleted in a PCR tube. Finally, $^1$H images were captured using an 11.7 T MRI scanner at 37°C.

**$^1$H MRI visualization of gene expression in dispersed cells.** Transfected cells were detached, labeled with 50 μM **BHA** in DMEM, and then incubated for 60 min in a $CO_2$ incubator. After removing the probe solution, the cells were washed with PBS three times. Next, the cells were incubated with 0.4 μM/mL (Fe) streptavidin-conjugated nanomag® D-spio (Micromod, 79-19-102, diameter: 100 nm) for 30 min at 4°C. The cells were washed with PBS three times and then, 100 μL of the cell suspension containing $2 \times 10^4$ cells was mixed with 100 μL of PBS containing 1% low-melting point agarose gel (Agarose XP, Wako) solution and cooled on ice for 1 h in a PCR tube. Then, $^1$H images were captured by an 11.7 T MRI scanner at 25°C. Finally, the gadolinium-based contrast agent Omniscan® (Daiichi-sankyo) was added to the agarose gel (1 drop), and the $^1$H images were captured.

**$^1$H MRI measurement procedure.** $^1$H MRI images were captured by an 11.7 T MRI (Bruker BioSpin). For taking images of the SPIO-labeled HEK293T cell pellets, a rare sequence was used with the following parameters; *T*E, 8.9 ms; *T*R, 4000 ms; NEX, 2; matrix size, 256 × 256; FOV, 20 mm × 20 mm; and slice thickness, 0.5 mm). For taking images of the SPIO-labeled HEK293T cells dispersed in agarose gel, a flash sequence was used with following parameters: *T*E, 8.0 ms; *T*R, 200 ms; NEX, 64; matrix size, 512 × 512; FOV, 20 mm × 20 mm; and slice thickness, 0.5 mm). When Omniscan® was added, the following parameters were changed: *T*R, 80 ms and *T*E, 4.9 ms.

## References


1. M. Howarth, K. Takao, Y. Hayashi, A.Y. Ting, *Proc. Natl. Acad. Sci. U. S. A.* **2005**, *102*, 7583–7588.
2. M.K. So, H. Yao, J. Rao, *Biochem. Biophys. Res. Commun*. **2008**, *374*, 419–423.
3. (a) G.V. Los, L.P. Encell, M.G. McDougall, D.D. Hartzell, N. Karassina, C. Zimprich, M.G. Wood, R. Learish, R.F. Ohana, M. Urh, D. Simpson, J. Mendez, K.

Zimmerman, P. Otto, G. Vidugiris, J. Zhu, A. Darzins, D.H. Klaubert, R.F. Bulleit, K.V. Wood, *ACS Chem. Biol.* **2008**, *3*, 373–382. (b) A. Keppler, S. Gendreizig, H. Pick, H. Vogel, K. Johnsson, *Nat. Biotechnol.* **2003**, *21*, 86–89. (c) S.S. Gallagher, J.E. Sable, M.P. Sheetz, V.W. Cornish, *ACS Chem. Biol.* **2009**, *4*, 547–556.

4. (a) B.A. Griffin, S.R. Adams, R.Y. Tsien, *Science* **1998**, *281*, 269–272. (b) A. Ojida, K. Honda, D. Shinmi, S. Kiyonaka, Y. Mori, I. Hamachi, *J. Am. Chem. Soc.* **2006**, *128*, 10452–10459. (c) C.T. Hauser, R.Y. Tsien, *Proc. Natl. Acad. Sci. U. S. A.* **2007**, *104*, 3693–3697.
5. (a) I. Chen, M. Howarth, W. Lin, A.Y. Ting, *Nat. Methods.* **2005**, *2*, 99–104. (b) N. George, H. Pick, H. Vogel, N. Johnsson, K. Johnsson, *J. Am. Chem. Soc.* **2004**, *126*, 8896–8897.
6. (a) S. Mizukami, S. Watanabe, Y. Hori, K. Kikuchi, *J. Am. Chem. Soc.* **2009**, *131*, 5016–5017. (b) S. Watanabe, S. Mizukami, Y. Hori, K. Kikuchi, *Bioconjugate Chem.* **2010**, *21*, 2320–2326.
7. X. Michalet, F.F. Pinaud, L.A. Bentolia, J.M. Tsay, S. Doose, J.J. Li, G. Sundaresan, A.M. Wu, S.S. Gambhir, S. Weiss, *Science* **2005**, *307*, 538–544.
8. (a) T.F. Massoud, S.S. Gambhir, *Gene. Dev.* **2003**, *17*, 545–580. (b) K. Shah, A. Jacobs, X.O. Breakefield, R. Weissleder, *Gene Ther.* **2004**. *11*. 1175–1187.
9. (a) C.H. Contag, S.D. Spilman, P.R. Contag, M. Oshiro, B. Eames, P. Dennery, D.K. Stevenson, D.A. Benaron, *Photochem. Photobiol.* **1997**, *66*, 523–531. (b) K.V. Wood, Y.A. Lam, H.H. Seliger, W.D. McElroy, *Science* **1989**, *244*, 700–702. (c) W.W. Lorenz, R.O. McCann, M. Longiaru, M.J. Cormier, *Proc. Natl. Acad. Sci. U. S. A.* **1991**, *88*, 4438–4442.
10. (a) J.H. Kang, J.-K. Chung, *J. Nucl. Med.* **2008**, *49*, 164S–179S. (b) R. Weissleder, M.J. Pittet, *Nature* **2008**, *452*, 580–589.
11. (a) S.S. Gambhir, J.R. Barrio, M.E. Phelps, M. Iyer, M. Namavari, N. Satyamurthy, L. Wu, L.A. Green, E. Bauer, D.C. MacLaren, K. Nguyen, A.J. Berk, S.R. Cherry, H.R. Herschman, *Proc. Natl. Acad. Sci. U. S. A.* **1999**, *96*, 2333–2338. (b) M.A. Moroz, I. Serganova, P. Zanzonico, L. Ageyeva, T. Beresten, E. Dyomina, E. Burnazi, R.D. Finn, M. Doubrovin, R.G. Blasberg, *J. Nucl. Med.* **2007**, *48*, 827–836. (c) A.Y. Louie, M.M. Hüber, E.T. Ahrens, U. Rothbächer, R. Moats, R.E. Jacobs, S.E. Fraser, T.J. Meade, *Nat. Biotechnol.* **2000**, *18*, 321–325. (d) G. Genove, U. DeMarco, H. Xu, W.F. Goins, E.T. Ahrens, *Nat. Med.* **2005**, *11*, 450–454. (e) B.B. Bartelle, C.A. Berríos-Otero, J.J. Rodriguez, A.E. Friedland, O. Aristizábal, D.H. Turnbull, *Circ. Res.* **2012**, *110*, 938–947.
12. J.W.M. Bulte, D.L. Kraitchman, *NMR Biomed.* **2004**, *17*, 484–499.

13. (a) Q. Wang, G. Villeneuve, Z. Wang, *EMBO Rep.* **2005**, *6,* 942–948. (b) D.L. Wheeler, E.F. Dunn, P.M. Harari, *Nat. Rev. Clin. Oncol*. **2010**, *7*, 493–507.
14. Y.-W. Jun, J.-H. Lee, J. Cheron, *Angew. Chem. Int. Ed.* **2008**, *47*, 5122–5135.
15. M. Port, J.M. Idee, C. Medina, C. Robic, M. Sabatou, C. Corot, *Biometals* **2008**, *21*, 469–490.

# **Chapter 2.** Single-Molecule Imaging of Intracellular Proteins by Using BL-tag System

Single-molecule imaging is a robust method for studying biomolecules in living cells.[1] The obtained data are not obscured by the averaging that is inherent in conventional biochemical experiments. Therefore, it is possible to quantify dynamic and kinetic parameters of biological reactions. Kinetic parameters are difficult to determine using multiple-molecule techniques because the reactions of individual molecules occur stochastically inside of a cell. In addition, it is difficult to identify local and temporal heterogeneities in the dynamic movement of molecules using multiple-molecule techniques. Single-molecule techniques can therefore be used to avoid such difficulties.

In this chapter, BL-tag technology[2] was applied for single-molecule imaging of target intracellular proteins. With this method, fluorescently labeled proteins can be analyzed in more detail using BL-tag technology, enabling the clarification of various biological phenomena.

## References


1. (a) S. Weiss, *Nat. Struct. Biol.* **2000**, *7*, 724–729. (b) A. Ishijima, T. Yanagida, *Trends Biochem. Sci.* **2001**, *26*, 438–444. (c) S. Xie, *Single Mol.* **2001**, *2*, 229–236. (d) P. Hinterdorfer, G. Schütz, F. Kienberger, H. Schindler, *J. Biotechnol.* **2001**, *82*, 25–35. (e) Y. Sako, T. Uyemura, *Cell Struct. Funct.* **2002**, *27*, 205–213.
2. (a) S. Mizukami, S. Watanabe, Y. Hori, K. Kikuchi, *J. Am. Chem. Soc.* **2009**, *131*, 5016–5017. (b) S. Watanabe, S. Mizukami, Y. Hori, K. Kikuchi, *Bioconjugate Chem.* **2010**, *21*, 2320–2326. (c) S. Watanabe, S. Mizukami, Y. Akimoto, Y. Hori, K. Kikuchi, *Chem. Eur. J.* **2011**, *17*, 8342–8349.

## **Section 2.1.** Optimization of Cell-Permeable Probes for Single-Molecule Imaging

The author's group developed cell-permeable labeling probes for BL-tag technology utilizing a derivative of bacampicillin, **RB**, and **FB-DA**. Labeling of intracellular proteins with these previously developed permeable probes was successful.[1] In particular, the tetramethylrhodamine-conjugated probe **RB** has broad utility because rhodamine has (i) a high absorption coefficient and broad fluorescence and (ii) high fluorescence quantum yield and photostability.[2] Rhodamine dyes are often utilized to develop fluorescent probes.[3] Therefore, **RB** was thought to be the most suitable fluorescent probe for single-molecule imaging of intracellular proteins. However, when fluorescence imaging of intracellular proteins was performed with **RB**, a high background signal was detected immediately after washing out of unreacted probes. This high background signal makes single-molecule imaging difficult; thus, improving the probe is very important.

**Fluorescence imaging of BL-tag expressed in cytosol by RB**

First, fluorescence imaging of BL-tag expressed in cytosol (Cytoplasmic-BL) was performed with **RB** (Scheme 2-1). The protein was expressed in HEK293T cells by transfection with a plasmid encoding Cytoplasmic-BL. The cells were incubated with **RB**, washed three times, and observed using a confocal fluorescence microscope. A strong red fluorescence signal was detected from both BL-tag-expressing cells and control cells immediately after the washing procedure (Figure 2-1A). When labeled cells were incubated for 7 h, the background signal was decreased (Figure 2-1B). The average fluorescence intensity per pixel was calculated from Cytoplasmic-BL-expressing cells and compared. Values were slightly enhanced compared with the background signal immediately after the washing procedure, while the signal-to-noise (S/N) ratio was increased 7 h after preincubation. Since longer preincubation is necessary to perform fluorescence imaging with a high S/N ratio, optimization of the probe structure is important.

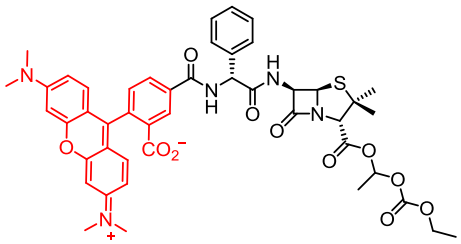

***Scheme 2-1.*** Structure of **RB**.

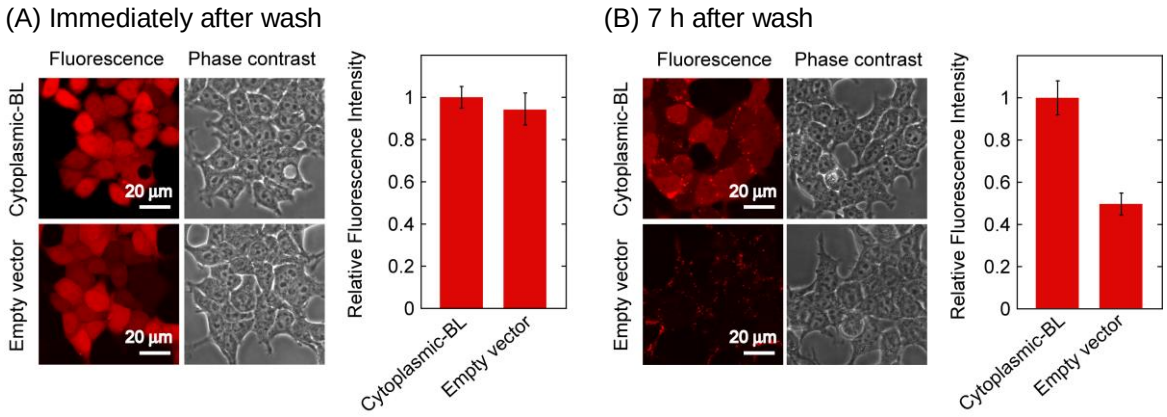


***Figure 2-1.*** Labeling of Cytoplasmic-BL expressed in HEK293T cells with **RB** (100 nM) for 30 min at 37°C. HEK293T cells were transfected with a plasmid encoding Cytoplasmic-BL. Fluorescence images were captured (A) immediately after the washing procedure or (B) 7 h after the washing procedure. Excitation at 559 nm. Detection at 570–670 nm. Average fluorescence intensity per pixel of labeled cells was analyzed using ImageJ software. Data are means ± S.E.M. of triplicate determinations from fluorescence images.

## Optimization and synthesis of labeling probe for intracellular protein

Rhodamine-based fluorescent probes often show non-specific accumulation in organelles such as mitochondria because of their positive charge and hydrophobicity.[4] However, **RB** fluorescence was uniformly detected inside cells. It was hypothesized that this non-specific accumulation may have been caused by non-specific adsorption on endogeneous proteins derived from the total hydrophobicity of the probe. In general, increased hydrophobicity is required for cell permeability; hydrophobicity can be increased by introduction of the hydrophobic region or by conversion of the anionic region into the non-charged region with an ester group such as acetoxymethyl (AM) ester.[5] However, high hydrophobicity of a fluorescent functional molecule induces non-specific accumulation inside cells.[6] Commercial fluorescent probes for HaloTag system contain a hydrophilic diethylene glycol-based linker between the fluorescent dyes and their ligands, and can be used to achieve specific labeling of intracellular proteins.[7] It was hypothesized that introduction of a hydrophilic linker may be important. Therefore, two types of cell-permeable probes with a hydrophilic linker between the fluorescent dye and BL-tag ligand were designed.

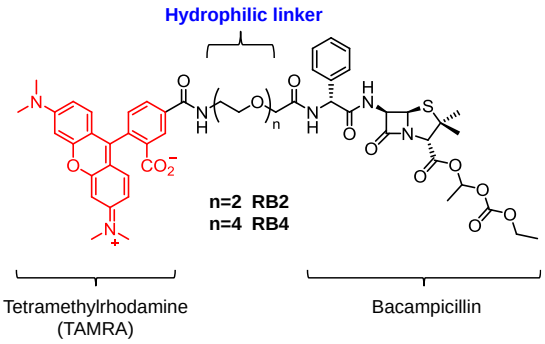


***Scheme 2-2.*** Design of new cell permeable probes **RB2** and **RB4**.

New bacampicillin-based labeling probes, **RB2** and **RB4**, were designed (Scheme 2-2). These molecules were synthesized using the procedure shown in Schemes 2-3 and 2-4. These final compounds were purified by reversed phase-high-performance liquid chromatography (HPLC), and the HPLC trace of purified **RB2** and **RB4** showed a single peak. These probes contain a different hydrophilic linker that can be used to study the relationship between non-specific accumulation of the probe and hydrophilicity.

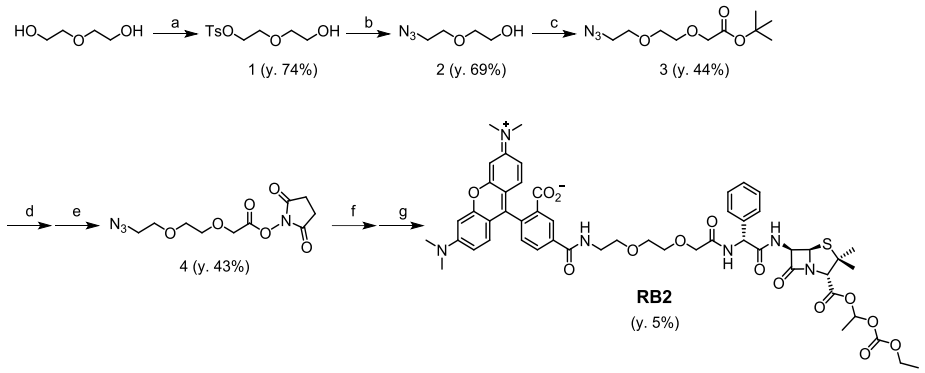


***Scheme 2-3***. Synthetic scheme of **RB2**. (a) TsCl, NaOH, $CH_2Cl_2$; (b) $NaN_3$, DMF, 80°C; (c) *tert*-butyl bromoacetate, NaH, DMF; (d) TFA, $CH_2Cl_2$; (e) WSCD·HCl, *N*-hydroxysuccinimide, TEA, DMF; (f) bacampicillin·HCl, WSCD·HCl, HOBt, TEA, DMF; (g) 5-carboxytetramethylrhodamine succinimidyl ester, TEA, DMF.

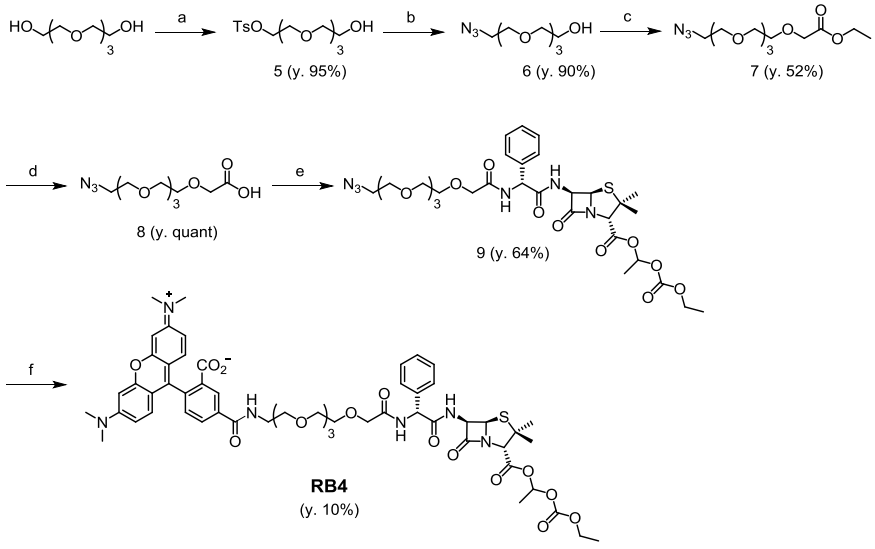


***Scheme 2-4***. Synthetic scheme of **RB4**. (a) TsCl, NaOH, $CH_2Cl_2$; (b) $NaN_3$, DMF, 80°C; (c) ethyl bromoacetate, NaH, DMF; (d) NaOH, MeOH; (e) bacampicillin·HCl, WSCD·HCl, HOBt, TEA, DMF; (f) 5 (6)-carboxytetramethylrhodamine succinimidyl ester, TCEP, TEA, DMF.

Absorption and emission spectra of all synthesized probes are shown in Figure 2-2. All synthesized probes showed similar spectroscopic properties and fluorescence quantum efficiencies.

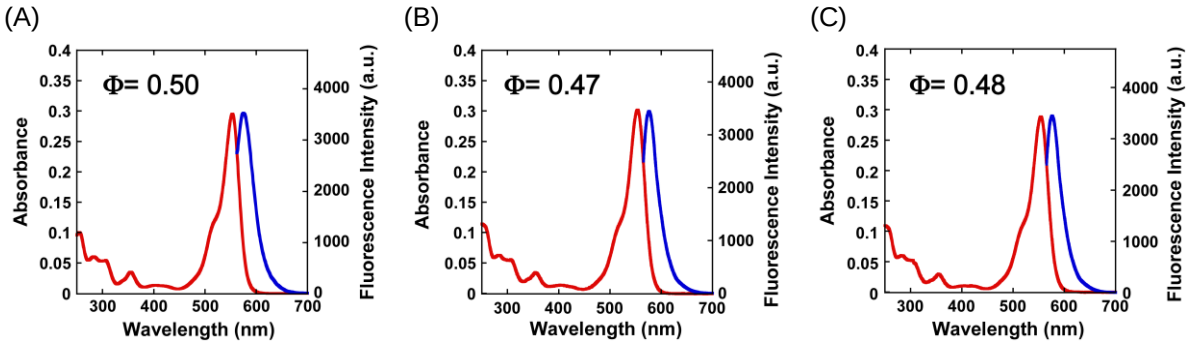


***Figure 2-2.*** Absorption spectra (red lines) and emission spectra (blue lines) of (A) **RB**, (B) **RB2**, and (C) **RB4** in 100 mM HEPES buffer (pH 7.4). In the absorption measurements, the concentration of probes was 5 μM. In the fluorescence measurements, the concentration of probes was 0.5 μM. Excitation wavelengths were 556 nm. Fluorescence quantum efficiencies of the probes are shown in the graphs.

BL-tag was incubated with the developed probes in 10 mM Tris-HCl buffer (pH 7.0) at 37°C, and protein labeling was assessed following sodium dodecyl sulfate-polyacrylamide gel electrophoresis (SDS-PAGE) (Figure 2-3). Fluorescent proteins were detected by irradiating the gels with green light. When the purified BL-tag was mixed with the probes, a protein band of approximately 29 kDa exhibited orange fluorescence. Coomassie Brilliant Blue (CBB) staining confirmed that this band corresponded to BL-tag. The labeling reaction was successful when the samples were mixed with the cell lysate.

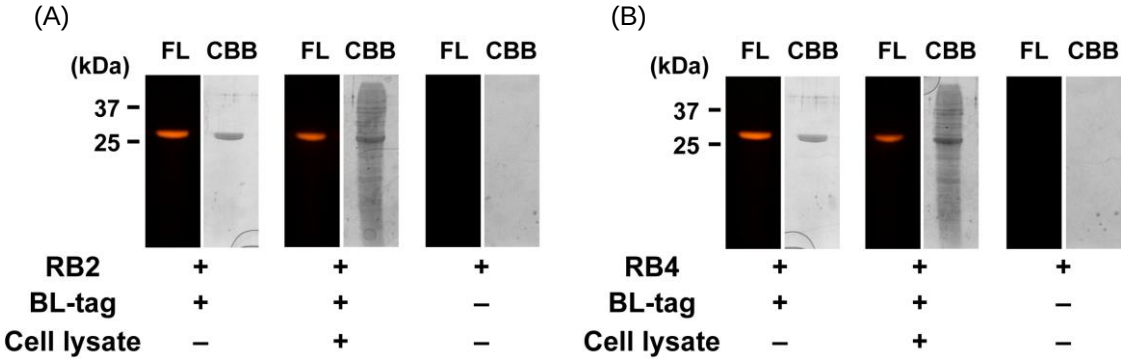


***Figure 2-3.*** Fluorescence (left) and Coomassie brilliant blue (CBB) -stained (right) gel images of BL-tag with (A) **RB2**, (B) **RB4**.

Moreover, the precise labeling kinetics of **RB**, **RB2**, and **RB4** toward BL-tag was examined. To a solution of the excess BL-tag (100 nM), 2.5–20 nM labeling probes were added and fluorescence polarization was measured (Figure 2-4). The initial

reaction rate calculated from the fluorescence polarization increase was plotted against probe concentration (Figure 2-5). Second-order labeling rate constants for **RB**, **RB2**, and **RB4** were determined to be $5.3 \times 10^4$, $4.1 \times 10^4$, and $4.2 \times 10^4$ $M^{-1}$ $s^{-1}$, respectively (Table 2-1). These results indicate that introduction of a hydrophilic linker does not affect the labeling reaction rate.

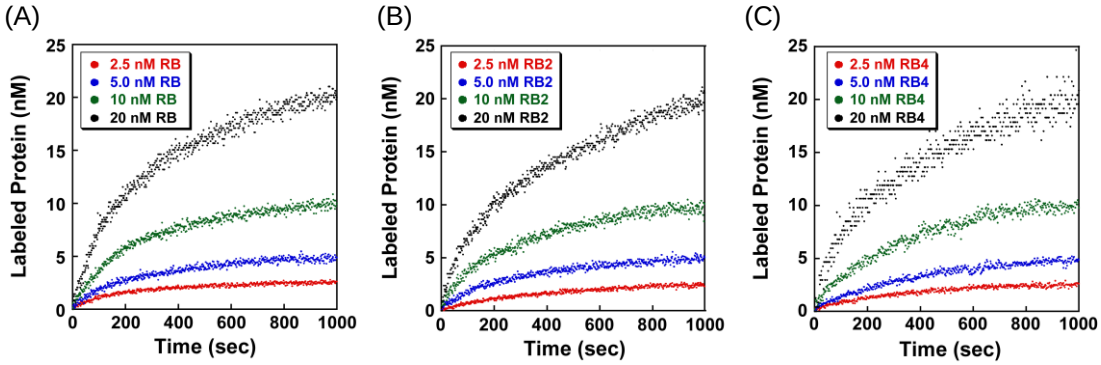


***Figure 2-4.*** Labeling kinetics of BL-tag and synthesized probes ((A) **RB**, (B) **RB2**, and (C) **RB4**). Reactions between 100 nM BL-tag protein and 20, 10, 5, and 2.5 nM probes at 25°C were monitored over time using fluorescence polarization.

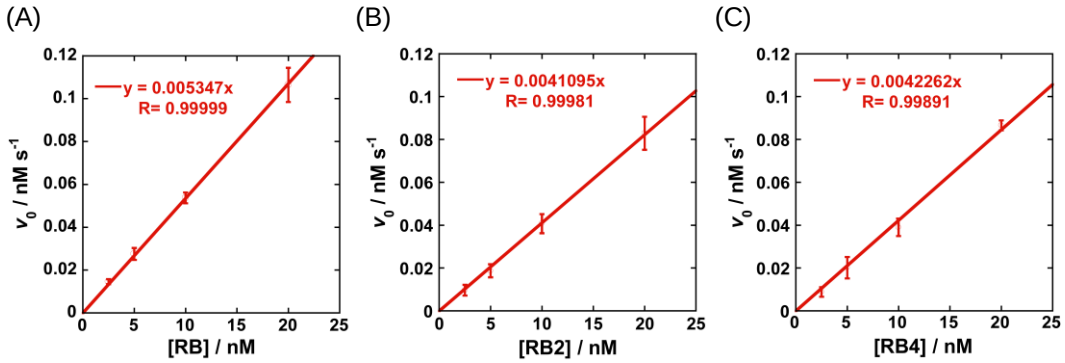


***Figure 2-5.*** Kinetic study of (A) **RB**, (B) **RB2**, and (C) **RB4**. Plot of initial labeling reaction rate $v_0$ versus probe concentration. [BL-tag] = 100 nM.

| compound | $\lambda_{abs,\,max}$/nm | $\lambda_{em,\,max}$/nm | Fluorescence quantum efficiency (Φ) –MBP-BL | Fluorescence quantum efficiency (Φ) +MBP-BL | $k_2$ ($M^{-1}$ $s^{-1}$) |
|---|---|---|---|---|---|
| RB | 553 | 575 | 0.50 | 0.37 | $5.3 \times 10^4$ |
| RB2 | 554 | 576 | 0.47 | 0.54 | $4.1 \times 10^4$ |
| RB4 | 554 | 576 | 0.48 | 0.47 | $4.2 \times 10^4$ |

***Table 2-1.*** Spectroscopic properties and calculated rate constants of the probes in 100 mM HEPES buffer (pH 7.4).

## Fluorescence labeling of intracellular BL-tag protein

The newly synthesized probes were used to label the intracellular protein BL-tag. First, BL-tag was expressed in the cytosol (Cytoplasmic-BL) of HEK293T cells. The cells were incubated with **RB2** or **RB4**, washed three times, and observed using a confocal fluorescence microscope. A fluorescence signal was detected only from BL-tag-expressing cells immediately after the washing procedure (Figure 2-6). Next, the average fluorescence intensity per pixel from Cytoplasmic-BL-expressing cells was calculated and the values were compared. The intensity was clearly enhanced compared with the background signal after the washing procedure. Therefore, the S/N ratio was largely improved with **RB2** and **RB4** relative to **RB**. The newly synthesized probes **RB2** and **RB4** showed successful fluorescence imaging of intracellular proteins with a higher S/N ratio; in addition, fluorescence imaging can be performed more immediately than when using the previous probe, **RB**. Introduction of a hydrophilic linker between the fluorescent dye and BL-tag substrate was effective for suppressing non-specific accumulation inside of cells.

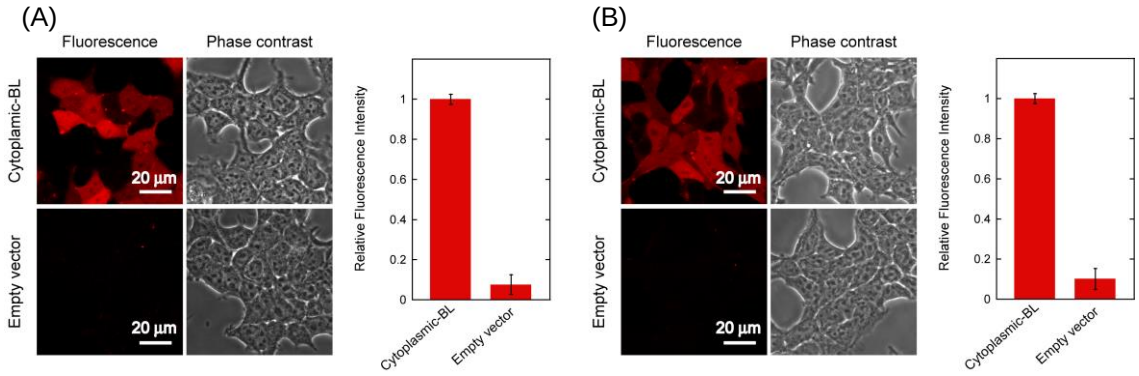


***Figure 2-6.*** Specific labeling of Cytoplasmic-BL expressed in HEK293T cells with (A) **RB2** (200 nM) or (B) **RB4** (1 μM) for 30 min at 37°C. HEK293T cells were transfected with a plasmid encoding Cytoplasmic-BL. Excitation at 559 nm. Detection at 570–670 nm. Relative fluorescence intensities of labeled cells. Average fluorescence intensity per pixel of labeled cells was analyzed using ImageJ software. Data are the means ± S.E.M. of triplicate determinations from fluorescence images.

## Comparing the cell permeability of probes

Introduction of a hydrophilic linker was highly effective for suppressing non-specific accumulation inside cells. However, a higher concentration of probe was needed to perform fluorescence microscopy, particularly in the case of **RB4** (1 μM). Next, the relationship between hydrophilic linker length and the cell permeability of synthesized probes was evaluated.

First, BL-tag was fused to the nuclear localization signal (NLS)[8] and expressed in the nuclei of HEK293T cells. The cells were incubated with various concentrations of **RB**, **RB2**, or **RB4** (100, 200, 500, and 1000 nM) and observed using a confocal fluorescence microscope (Figure 2-7A). The average fluorescence intensity in cell nuclei of BL-NLS-expressing cells was calculated for each condition (Figure 2-7B). From the cells incubated with **RB**, strong red fluorescence was detected at each concentration and the fluorescence intensity was only minimally decreased in response to lowering the concentration. The fluorescence intensity of BL-NLS-expressing cells incubated with **RB2** and **RB4** was lower than that of **RB** at 1 μM. Moreover, the fluorescence intensity of **RB2** and **RB4** detected in cell nuclei decreased at lower concentrations. In particular, the fluorescence intensity detected in cell nuclei labeled with **RB4** was largely decreased at lower concentrations.

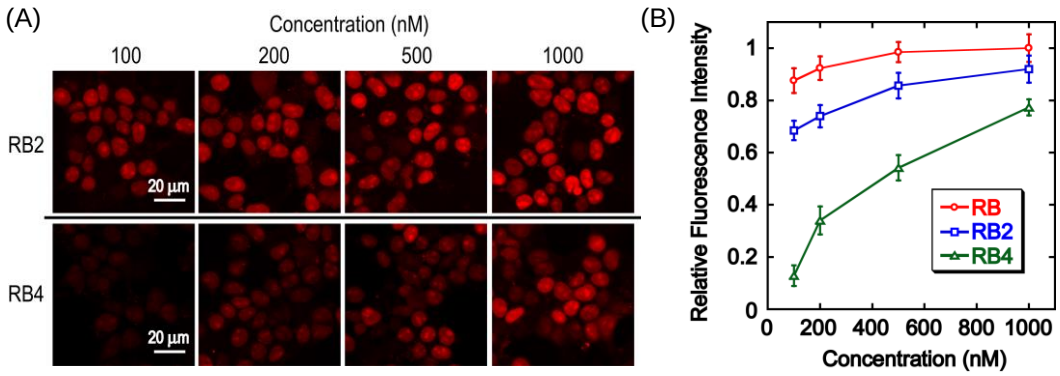


***Figure 2-7.*** Specific labeling of (A) BL-NLS expressed in HEK293T cells with **RB**, **RB2**, and **RB4** for 30 min at 37°C. HEK293T cells were transfected with a plasmid encoding BL-NLS. The concentrations of the probes were 1000 nM, 500 nM, 200 nM, and 100 nM. Excitation at 559 nm. Detection at 570–670 nm. (B) Plots of relative fluorescence intensities of labeled cells. Average fluorescence intensity per pixel of labeled cells was analyzed using ImageJ software. Data are the means ± S.E.M. of triplicate determinations from fluorescence images.

Next, HEK293T cells transfected with plasmids expressing the cell surface-targeted BL-tag (BL-GPI) were prepared.[9] Cells were incubated with synthesized probes as described above (Figure 2-8A). In these cells, BL-tag was anchored to the extracellular surface of the plasma membrane and labeled with synthesized probes without plasma membrane permeation. A strong red fluorescence signal was detected from the plasma membrane at each concentration (Figure 2-8B). The fluorescence intensity of both probes was similar at all concentrations.

Based on the comparable labeling rate constant ($k_2$) of synthesized probes, longer hydrophilic linkers may decrease the cell permeability of the probe. In particular, **RB4** showed the lowest cell permeability. Thus, introduction of a hydrophilic linker suppressed non-specific accumulation of synthesized probes, while a longer hydrophilic

linker suppressed cell permeability. The linker length can be optimized to design cell permeable probes; **RB2** has optimum cell permeability and shows limited non-specific intracellular accumulation. Thus, **RB2** is suitable for use in intracellular single-molecule imaging.

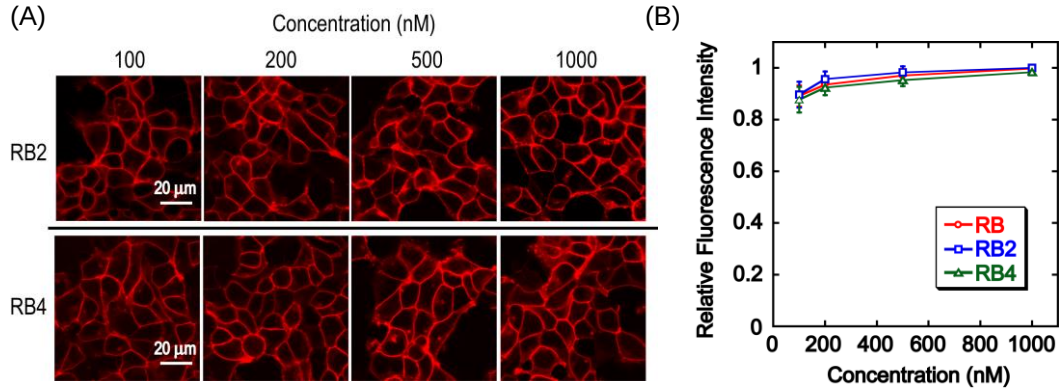


***Figure 2-8.*** Specific labeling of (A) BL-GPI expressed in HEK293T cells with **RB**, **RB2**, and **RB4** for 30 min at 37°C. HEK293T cells were transfected with a plasmid encoding BL-GPI. The concentrations of probes were 1000 nM, 500 nM, 200 nM, and 100 nM. Excitation at 559 nm. Detection at 570–670 nm. (B) Plots of relative fluorescence intensities of labeled cells. Average fluorescence intensity per pixel of labeled cells was analyzed using ImageJ software. Data are the means ± S.E.M. of triplicate determinations from fluorescence images.

## Experimental Section

**Materials.** General chemicals for organic synthesis were of the highest grade available and were supplied by Tokyo Chemical Industries, Wako Pure Chemical, and Sigma-Aldrich. Chemicals were used without further purification. Bacampicillin hydrochloride was a gift from Nichi-Iko Pharmaceutical Co. Ltd. Anti-β-lactamase antibody was purchased from Abcam (ab12251). Horseradish peroxidase-linked secondary antibody was purchased from GE Healthcare (anti-mouse NA931). The pcDNA 3.1(+) vector was purchased from Invitrogen (21083-027). Restriction endonucleases and PrimeSTAR® HS DNA polymerase were purchased from Takara Bio, Inc. Plasmid DNA was isolated using a QIAprep Spin Miniprep kit (Qiagen). 5(6)-Carboxytetramethylrhodamine succinimidyl ester and 5-carboxytetramethylrhodamine succinimidyl ester were purchased from AnaSpec. All labeling probes were dissolved in dimethyl sulfoxide (biochemical grade; Wako Pure Chemical) before fluorescence measurements to facilitate solubilization in aqueous solvents. Silica gel column chromatography was performed using BW-300 (Fuji Silysia Chemical, Ltd.). The pKmcl-BL-GPI plasmid was a kind gift from Dr. Atsushi Miyawaki.

**Instruments.** Nuclear magnetic resonance (NMR) spectra were recorded on a JEOL JNM-AL400 instrument at 400 MHz for $^{1}H$ and at 100.4 MHz for $^{13}C$ NMR, using tetramethylsilane as an internal standard. Mass spectra were measured on a JEOL JMS-700 mass spectrometer for FAB and on a Waters LCT-Premier XE mass spectrometer for electrospray ionization (ESI). Fluorescence spectra were measured using a Hitachi F4500 spectrometer. Ultraviolet-visible absorbance spectra were measured using a Shimadzu UV1650PC spectrometer. Fluorescence images of SDS-PAGE were visualized using a BSPEBV001 EtBr viewer (Biospeed).

## Synthesis of Compounds

**Synthesis of RB.** The synthesis of this compound is described elsewhere.[1]

**Synthesis of 1.** Diethylene glycol (14.4 g, 136 mmol) was dissolved in tetrahydrofuran (THF; 15 mL) and 2N NaOH aq. (15 mL) was added at 0°C. The mixture was stirred for 1 h, and then *p*-toluenesulfonyl chloride (5.18 g, 27.2 mmol) was added in a drop-wise manner at 0°C over a period of 1 h. The mixture was stirred for 17 h and then diluted with ethyl acetate. The organic layer was washed with water and dried with brine and $Na_2SO_4$. After removal of the organic solvent, the residue was purified with flash column chromatography to yield compound **1** (5.25 g, 20.2 mmol, y. 74%). $^{1}H$ NMR (400 MHz, $CDCl_3$) $\delta$ 7.80 (d, 2H, $J$ = 8.4 Hz), 7.35 (d, 2H, $J$ = 8.0 Hz), 4.20 (t, 2H, $J$ = 2.2 Hz), 3.70–3.66 (m, 4H), 3.53 (d, 2H, $J$ = 4.4 Hz), 2.45 (s, 3H); $^{13}C$ NMR (100 MHz, $CDCl_3$) $\delta$ 144.9, 132.9, 129.9, 127.9, 72.4, 69.1, 68.5, 61.6, 21.6; HRMS ($FAB^+$) *m/z*: 261.0713 (Calcd for $[M+H]^+$: 261.0971).

**Synthesis of 2.** Compound **1** (3.63 g, 13.9 mmol) was dissolved in anhydrous dimethylformamide (DMF; 10 mL) and sodium azide (4.51 g, 69.5 mmol) was added. The mixture was stirred at 0°C under argon (Ar). After 20 h, the organic solvent was removed by evaporation and the residue was dissolved in ethyl acetate, and then was washed with water. The organic layer was dried with brine and $Na_2SO_4$. The solvent was removed by evaporation and the residue was purified by flash column chromatography to yield compound **2** (1.26 g, 9.61 mmol, y. 69%). $^{1}H$ NMR (400 MHz, $CDCl_3$) $\delta$ 3.78–3.74 (m, 2H), 3.71 (t, 2H, $J$ = 5.0 Hz), 3.62 (t, 2H, $J$ = 4.6 Hz), 3.41 (t, 2H, $J$ = 5.0 Hz), 1.99 (t, 1H, $J$ = 6.2 Hz); $^{13}C$ NMR (100 MHz, $CDCl_3$) $\delta$ 71.9, 70.4, 69.1, 61.2; HRMS ($FAB^+$) *m/z*: 132.0732 (Calcd for $[M+H]^+$: 132.0767).

**Synthesis of 3.** Compound **2** (634 mg, 4.83 mmol) was dissolved in THF (8 mL), then sodium hydride (386 mg, 9.66 mmol) was added at 0°C under Ar. The reaction mixture was stirred for 1 h, and *tert*-butyl bromoacetate (1.42 mL, 9.66 mmol) was then added

in a drop-wise manner at 0°C over a period of 20 min. The reaction mixture was stirred for 16 h and then quenched using methanol and water. The organic solvent was removed and the mixture was extracted with ethyl acetate. The organic layer was washed with water and then dried with brine and $Na_2SO_4$. After removal of the solvent, the residue was purified with flash column chromatography to yield compound **3** (522 mg, 2.13 mmol, y. 44%). $^1$H NMR (400 MHz, $CDCl_3$) δ 4.03 (s, 2H), 3.74–3.68 (m, 6H), 3.41 (t, 2H, *J* = 5.2 Hz), 1.45 (s, 9H); $^{13}$C NMR (100 MHz, $CDCl_3$) δ 169.6, 81.6, 70.8, 70.7, 70.0, 69.1, 50.6, 28.1; HRMS ($FAB^+$) *m/z*: 246.1452 (Calcd for $[M+H]^+$: 246.1448).

**Synthesis of 4.** Compound **3** (203 mg, 0.828 mmol) was dissolved in $CH_2Cl_2$ (6 mL), then trifluoroacetic acid (TFA; 632 µL, 8.28 mmol) was added in a drop-wise manner at 0°C. The reaction mixture was stirred for 3 h at room temperature and then the organic solvent was removed. The residue was dissolved in $CH_2Cl_2$ (2.5 mL) and then *N*-hydroxysuccinimide (286 mg, 2.48 mmol) and WSCD·HCl (475 mg, 2.48 mmol) were added at 0°C. The mixture was stirred for 24 h under Ar. The organic solvent was removed by evaporation and the residue was dissolved in ethyl acetate and washed with 0.1 M phosphate buffer (pH 6.2) and water. The organic layer was dried with brine and $Na_2SO_4$. After removal of the organic solvent by evaporation, the residue was purified by flash column chromatography to yield compound **4** (102 mg, 0.357 mmol, y. 43%). $^1$H NMR (400 MHz, $CDCl_3$) δ 4.53 (s, 2H), 3.73–3.67 (m, 6H), 3.41 (t, 2H, *J* = 5.2 Hz), 2.86 (s, 4H); $^{13}$C NMR (100 MHz, $CDCl_3$) δ 168.7, 71.4, 70.6, 70.0, 66.6, 50.6, 37.9, 32.5, 25.5; HRMS ($FAB^+$) *m/z*: 287.0972 (Calcd for $[M+H]^+$: 287.0986).

**Synthesis of RB2.** Compound **4** (47.4 mg, 0.166 mmol) was dissolved in anhydrous DMF (1.5 mL), and then bacampicillin hydrochloride and TEA were added at 0°C. The reaction mixture was stirred at room temperature under Ar. After 24 h, the reaction mixture was diluted with ethyl acetate and washed with 10% citric acid aq. and water. The organic layer was then dried with brine and $Na_2SO_4$. The organic solvent was removed by evaporation. The residue was dissolved in DMF (1.5 mL), then TCEP·HCl (26.4 mg, 0.0921 mmol), TEA (33.8 mg, 0.334 mmol), and 5-carboxytetramethylrhodamine succinimidyl ester (23.3 mg, 0.0434 mmol) were added. The reaction mixture was stirred for 22 h under an Ar atmosphere, and the solvent was removed under reduced pressure. The residue was purified with reversed-phase HPLC and eluted with $H_2O$/acetonitrile containing 0.1% formic acid to yield **RB2** (8.74 mg, 0.00855 mmol, y. 5%). $^1$H NMR (400 MHz, dimethyl sulfoxide (DMSO)): 9.32 (t, 1H, *J* = 7.2 Hz), 8.89 (d, 1H, *J* = 7.3 Hz), 8.45 (s, 1H), 8.22 (dd, 1H, *J* = 8.0 Hz, 1.2 Hz), 8.15 (d, 1H, *J* = 8.0 Hz), 7.41-7.24 (m, 6H), 6.68 (q, 1H, *J* = 5.8 Hz) 6.58-6.43 (m, 6H), 5.76 (d, 1H, *J* = 7.8 Hz), 5.65 (dd, 1H, *J* = 7.3 Hz, 4.0 Hz), 5.41 (d, 1H, *J* = 4.0 Hz),

4.33 (s, 1H), 4.14 (q, 2H, $J$ = 7.2 Hz), 4.00 (s, 2H), 3.66–3.58 (m, 8H), 2.94 (s, 12H), 1.54–1.47 (m, 6H), 1.36 (s, 3H), 1.24 (t, 3H, $J$ = 7.2 Hz); HRMS ($FAB^+$) *m/z*: 1023.3806 (Calcd for $[M+H]^+$: 1023.3804).

**Synthesis of 5.** A solution of sodium hydroxide (1.37 g, 34.3 mmol) in water (7 mL) was added to a mixture of tetraethylene glycol (40.0 g, 206 mmol) and THF (8 mL) at 0°C. The reaction mixture was stirred at 0°C for 1 h, and a solution of *p*-toluenesulfonyl chloride (4.00 g, 21.0 mmol) in THF (20 mL) was added in a drop-wise manner. After stirring at 0°C for 3 h, the reaction mixture was poured into ice water (50 mL) and extracted with $CH_2Cl_2$. Next, the organic layer was washed with water and dried with brine and $Na_2SO_4$. The organic solvent was removed by evaporation and purified with flash column chromatography to yield compound **5** (6.96 g, 20 mmol, y. 95%). $^1H$ NMR (400 MHz, $CDCl_3$) $\delta$ 7.80(d, $J$ = 7.8 Hz, 2H), 7.30(d, $J$ = 7.8 Hz, 2H), 4.07–4.12(m, 2H), 3.55–3.72 (m, 14H), 2.38(s, 3H); $^{13}C$ NMR (100 MHz, $CDCl_3$) $\delta$ 144.5, 132.4, 129.5, 127.5, 72.2, 70.2, 70.1, 69.9, 69.8, 69.0, 68.2, 61.2, 21.3; HRMS ($FAB^+$) *m/z*: 349.1234 (Calcd for $[M+H]^+$: 349.1240).

**Synthesis of 6.** Compound **5** (5.00 g, 14.4 mmol) was dissolved in anhydrous DMF (50 mL) and sodium azide (4.67 g, 71.9 mmol) was added under Ar. The reaction mixture was heated at 60°C while stirring for 3 h. The organic solvent was removed by evaporation and the residue was placed in water and extracted with $CH_2Cl_2$. The organic layer was washed with water and dried with brine and $Na_2SO_4$. The organic solvent was removed by evaporation to yield compound **6** (2.84 g, 13.0 mmol, y. 90%). $^1H$ NMR(400MHz, $CDCl_3$) $\delta$ 3.73–3.58 (m, 14H), 2.53 (t, $J$ = 4.9 Hz, 2H); $^{13}C$ NMR (100 MHz, $CDCl_3$) $\delta$ 72.4, 70.6, 70.5, 70.4, 70.3, 69.9, 61.6; HRMS ($FAB^+$) *m/z*: 220.1284 (Calcd for $[M+H]^+$: 220.1291).

**Synthesis of 7.** Compound **6** (4.00 g, 18.3 mmol) was dissolved in anhydrous DMF (7 mL) and sodium hydride (0.480 g, 20.1 mmol) was added at 0°C under Ar. The reaction mixture was stirred for 1 h, and then ethyl bromoacetate (3.36 g, 20 mmol) was added drop-wise at 0°C. The reaction mixture was stirred for 16 h at room temperature. The reaction mixture was quenched with methanol and water on ice and the organic solvent was removed by evaporation. The residue was placed in water and extracted with ethyl acetate. The organic layer was washed with water and dried with brine and $Na_2SO_4$. The organic layer was removed by evaporation and the residue was purified by flash column chromatography to yield compound **7** (2.91 g, 9.52 mmol, y. 52%). $^1H$ NMR(400MHz, $CDCl_3$) $\delta$ 4.22–4.07 (m, 4H), 3.75–3.61(m, 14H), 3.40–3.34(m, 2H), 1.28–1.22(m, 3H); $^{13}C$ NMR (100 MHz, $CDCl_3$) $\delta$ 170.1, 72.3, 71.0, 70.5, 70.4, 70.1, 69.8, 67.0, 61.6, 61.0, 14.7; HRMS ($FAB^+$) *m/z*: 306.1654 (Calced for $[M+H]^+$ 306.1659).

**Synthesis of 8.** Compound **7** (2.80 g, 7.00 mmol) was dissolved in methanol and 2 M NaOH aq. (10 mL) was added at 0°C. The reaction mixture was stirred at room temperature for 30 min. Next, the excess NaOH was neutralized with Dowex-50 H+ resin, which was then filtered off. The methanol from the filtrate was removed by evaporation to yield compound **8** (1.94 g, quant.). $^{1}$H NMR (400MHz, $CDCl_3$) $\delta$ 4.28–4.10(m, 4H), 3.72–3.59 (m, 14H), 3.43–3.30 (m, 2H); $^{13}$C NMR (100 MHz, CDCl3) $\delta$ 173.0, 71.9, 70.9, 70.6, 70.4, 70.3, 69.6, 66.7, 62.0; HRMS ($FAB^+$) *m/z*: 278.1357 (Calcd for $[M+H]^+$ 278.1346).

**Synthesis of 9.** Compound **8** (200 mg, 0.722 mmol) was dissolved in anhydrous DMF (10 mL), and then WSCD·HCl (277 mg, 1.44 mmol), HOBt (195 mg, 1.44 mmol), and TEA were added under Ar. After 30 min of stirring at room temperature, bacampicillin hydrochloride (542 mg, 1.08 mmol) was added and the reaction was continued for 8 h. The solvent was removed by evaporation and the residue was diluted with ethyl acetate and washed with 10% citric acid aq., sat. $NaHCO_3$ aq., and water. The organic layer was dried with brine and $Na_2SO_4$. Next, the organic solvent was removed by evaporation and the residue was purified by flash column chromatography to yield compound **9** (328 mg, 0.453 mmol, 63%). $^{1}$H NMR (400MHz, $CDCl_3$) $\delta$ 8.80 (d, 1H, *J* = 6.2 Hz), 8.20 (d, 1H, *J* = 6.4 Hz), 7.26–7.40 (m, 5H), 6.77 (q, 1H, *J* = 5.1 Hz), 5.67(d, 1H, *J* = 6.4 Hz), 5.56 (dd, 1H, *J* = 3.8 Hz, 6.2 Hz), 5.47 (d, 1H, *J* = 4.0 Hz), 4.48 (s, 1H), 4.23 (q, 2H, *J* = 6.3 Hz), 3.88 (s, 2H), 3.66–3.45 (m, 16H), 1.29–1.34 (m, 9H), 1.25 (t, 3H, *J* = 6.3 Hz); $^{13}$C NMR (100.4 MHz, $CDCl_3$) $\delta$ 168.5, 168.1, 167.6, 167.0, 158.4, 133.2, 130.5, 129.4, 127.8, 98.0, 72.1, 71.5, 71.2, 70.6, 70.4, 70.2, 70.0, 69.7, 69.4, 65.0, 61.2, 60.9, 52.7, 32.4, 29.7, 26.8, 21.8, 14.7; HRMS ($FAB^+$) *m/z*: 725.2851 (Calcd for $[M+H]^+$ 725.2810).

**Synthesis of RB4.** Compound **9** (53.4 mg, 0.0737 mmol) was dissolved in anhydrous DMF (5 mL), then TCEP·HCl (42.3 mg, 0.148 mmol), TEA (29.9 mg, 0.295 mmol), and 5 (6)-carboxytetramethylrhodamine succinimidyl ester (35.3 mg, 0.0670 mmol) was added. The mixture was stirred for 10 h under Ar, and the solvent was removed by evaporation. The residue was purified by reversed-phase HPLC and eluted with $H_2O$/acetonitrile containing 0.1% formic acid to yield **RB4** (7.4 mg, 0.00666 mmol, y. 9%). $^{1}$H NMR (400 MHz, DMSO) $\delta$ 9.28 (t, 1H, *J* = 7.6 Hz), 8.90 (d, 1H, *J* = 7.0 Hz), 8.46 (s, 1H), 8.24 (dd, 1H, *J* = 7.8 Hz, 1.4 Hz), 8.14 (d, 1H, *J* = 7.8 Hz), 7.40–7.26 (m, 6 H), 6.68 (q, 1H, *J* = 5.4 Hz), 6.53–6.47 (m, 6H), 5.74 (d, 1H, *J* = 7.4 Hz), 5.67 (dd, 1H, *J* = 7.0 Hz, 4.4 Hz), 5.44 (d, 1H, *J* = 4.4 Hz), 4.33 (s, 1H), 4.16 (q, 2H, *J* = 7.2 Hz), 3.97 (s, 2H), 3.60–3.46 (m, 16H), 2.94 (s, 12H), 1.52–1.46 (m, 6H), 1.37 (s, 3H), 1.20 (t, 3H, *J* = 7.2 Hz); $^{13}$C NMR (100.4 MHz, DMSO) $\delta$174.2, 169.8, 168.7, 168.3, 167.2,

164.7, 158.7, 154.6, 153.2, 136.3, 134.2, 132.9, 130.2, 128.7, 128.5, 127.8, 125.0, 123.4, 110.8, 107.3, 105.9, 98.8, 92.7, 71.5, 71.0, 70.9, 70.6, 70.4, 70.3, 70.1, 69.9, 69.7, 67.6, 64.5, 59.8, 58.1, 41.1, 39.7, 32.6, 27.2, 21.3, 14.2. HRMS ($FAB^+$) *m/z*: 1111.4360 (Calcd for $[M+H]^+$: 1111.4328).

## Experimental Procedures

**HPLC analysis.** HPLC analyses were performed with an Inertsil ODS-3 column (4.6 × 250 mm; GL Sciences) using an HPLC system composed of a pump (PU-2080; JASCO) and a detector (MD-2010 and FP-2020; JASCO). Preparative HPLC was performed with an Inertsil ODS-3 column (10.0 × 250 mm; GL Sciences, Inc.) using an HPLC system with a pump (PU-2087; JASCO) and a detector (UV-2075; JASCO).

**Fluorometric analysis.** A slit width of 5.0 nm was used for both excitation and emission, and the photomultiplier voltage was set to 700 V. All fluorescent probes were dissolved in DMSO to obtain 1 mM stock solutions, and these solutions were diluted to the desired final concentrations in an appropriate aqueous buffer. The relative fluorescence quantum yields of the compounds were obtained by comparing the area under the emission spectrum of the sample with that of a 0.5 μM EtOH solution of rhodamine B (fluorescence quantum yield of 0.97 when excited at 545 nm).[10]

**Confocal laser scanning fluorescence microscopy.** Confocal fluorescence microscopic images were recorded using a confocal laser scanning microscope (Olympus, FLUOVIEW FV10i) equipped with a 60× lens. The probes were excited at 559 nm. The emission filter sets used were Olympus BA570–620.

**Detection of protein labeling by SDS-PAGE.** BL-tag (20 μM) was added to a solution of probes (30 μM) in 100 mM HEPES buffer (pH 7.4) at 25°C. After 30 min, the labeled protein was denatured in 2× SDS gel loading buffer (100 mM Tris-HCl buffer (pH 6.8), 2.5% SDS, 20% glycerol, and 10% mercaptoethanol) and resolved on a 15% SDS-polyacrylamide gel. Fluorescent images of the gels were captured using a digital camera (Nikon COOLPIX P6000). The gels were stained with Coomassie Brilliant Blue prior to capturing the images.

**Kinetic study of BL-tag labeling with RB, RB2, or RB4 using fluorescence polarization.** The purified BL-tag (100 nM) was added to a solution of **RB**, **RB2**, or **RB4** (2.5–20 nM) in 100 mM HEPES buffer (pH 7.4) at 25°C. Fluorescence polarization ($\lambda_{ex}$ = 530 nm, $\lambda_{em}$ = 575 nm) was detected using a plate reader (Infinite M1000; TECAN). Data were fitted to the equation $v_0 = k\cdot[\text{BL-tag}]_0\cdot[\text{Probe}]_0$, where $v_0$ is the initial reaction rate and $k$ is the bimolecular kinetic constant.

**Cell culture.** HEK293T cells were cultured in high-glucose Dulbecco's modified Eagle medium (DMEM) + Gluta Max-I (Invitrogen) supplemented with 10% fetal bovine serum (FBS; Gibco), penicillin (100 U/mL), and streptomycin (100 µg/mL) (Invitrogen). Cells were incubated at 37°C in a humidified atmosphere of 5% $CO_2$ in air. A subculture was performed every 2–3 days from subconfluent (<80%) cultures using a trypsin-ethylenediamine tetraacetic acid solution (Invitrogen). Transfection of plasmids was carried out in a glass-bottomed dish (Matsunami), 24-well plate (Falcon), or 6-well (TPP) plate using Lipofectamine 2000 (Invitrogen) according to a standard protocol.

**Confocal fluorescence microscopy of Cytoplasmic-BL with RB.** HEK293T cells maintained in a poly-L-lysine-coated glass-bottomed dish with DMEM containing 10% FBS at 37°C under 5% $CO_2$ were transfected with the pcDNA3.1(+)-Cytoplasmic-BL plasmid using Lipofectamine 2000. After 5 h, the culture medium was replaced with DMEM, and the cells were incubated at 37°C for 24 h. Next, the cells were washed three times with Hank's balanced salt solution (HBSS; Invitrogen) and incubated with 100 nM **RB** in DMEM for 30 min in a $CO_2$ incubator. The cells were then washed three times with HBSS and fluorescence microscopic images were captured using appropriate filter sets. Labeled cells were observed soon after the washing step or 7 h after the washing procedure.

**Confocal fluorescence microscopy of Cytoplasmic-BL with RB2 and RB4.** HEK293T cells maintained in a poly-L-lysine-coated glass-bottomed dish with DMEM containing 10% FBS at 37°C under 5% $CO_2$ were transfected with the pcDNA3.1(+)-Cytoplasmic-BL plasmid using Lipofectamine 2000. After 5 h, the culture medium was replaced with DMEM and the cells were incubated at 37°C for 24 h. Next, the cells were washed three times with HBSS and incubated with 200 nM **RB2** or 1 µM **RB4** in DMEM for 30 min in a $CO_2$ incubator. The cells were then washed three times with HBSS and fluorescence microscopic images were captured using appropriate filter sets. Labeled cells were observed soon after the washing step.

**Analysis of fluorescence images.** Labeled cell images with **RB**, **RB2**, and **RB4** were acquired according to the procedure described above over a pixel area of 256 × 256, where cells were confluently cultured; areas were selected at random from acquired fluorescence images. The average fluorescence intensity of different colors per pixel was computed from the selected area using ImageJ software.

**Comparing cell permeability of synthesized probes.** HEK293T cells maintained in glass-bottomed dishes were transfected with the pcDNA3.1 (+)-BL-NLS or the pKmcl-BL-GPI plasmid as described above. After 5 h, the culture medium was replaced with DMEM and the cells were incubated at 37°C for 24 h. Next, the cells were washed

three times with HBSS and incubated with **RB**, **RB2**, or **RB4** (1 μM, 500 nM, 200 nM, or 100 nM) in DMEM for 30 min in a $CO_2$ incubator. The cells were then washed three times with HBSS and microscopic images were acquired. The labeled cells were observed soon after the washing step. The fluorescence intensity of labeled nuclear proteins was analyzed using ImageJ software. The average of fluorescence intensity for 10 cells in each independent experiment was calculated.

**Confocal fluorescence microscopy of $Lyn_{11}$-BL with RB2.** HEK293T cells maintained in a glass-bottomed dish containing DMEM and 10% FBS at 37°C under 5% $CO_2$ were transfected with pcDNA3.1 (+)-$Lyn_{11}$-BL as described above. After 5 h, the culture medium was replaced with DMEM and the cells were incubated at 37°C for 24 h. Next, the cells were washed three times with HBSS and incubated with 200 nM **RB2** for 30 min in a $CO_2$ incubator. The cells were then washed three times with HBSS and microscopic images were acquired. Fluorescence images of the cells in HBSS were captured using appropriate filter sets. Labeled cells were observed soon after the washing step.

## References


1. S. Watanabe, S. Mizukami, Y. Akimoto, Y. Hori, K. Kikuchi, *Chem. Eur. J.* **2011**, *17*, 8342–8349.
2. M. Bejia, C.A.M. Afonso, J.M.G. Martinho, *Chem. Soc. Rev.* **2009**, *38*, 2410–2433.
3. (a) L.M. Wysocki, L.D. Lavis, *Curr. Opin. Chem. Biol.* **2011**, *15*, 752–759. (b) T. Terai, T. Nagano, *Pflug. Arch. –Eur. J. Phy.* **2013**, *465*, 347–359. (c) X. Chen, T. Pradhan, F. Wang, J.S. Kim, J. Yoon, *Chem. Rev.* **2012**, *112*, 1910–1956.
4. (a) K.M. Dean, Y. Qin, A.E. Palmer, *Biochim. Biophys. Acta*. **2012**, *1823*, 1406–1415. (b) L.V. Johnson, M.L. Walsh, L.B. Chen, *Proc. Natl. Acad. Sci. U. S. A.* **1980**, *77*, 990–994.
5. R.Y. Tsien, *Nature* **1981**, *290*, 527–528.
6. M. Kamiya, K. Johnsson, *Anal. Chem.* **2010**, *82*, 6472–6479.
7. (a) G.V. Los, L.P. Encell, M.G. McDougall, D.D. Hartzell, N. Karassina, C. Zimprich, M.G. Wood, R. Learish, R.F. Ohana, M. Urh, D. Simpson, J. Mendez, K. Zimmerman, P. Otto, G. Vidugiris, J. Zhu, A. Darzins, D.H. Klaubert, R.F. Bulleit, K.V. Wood, *ACS Chem. Biol.* **2008**, *3*, 373–382. (b) K. Takemoto, T. Matsuda, M. McDougall, D.H. Klaubert, A. Hasegawa, G.V. Los, K.V. Wood, A. Miyawaki, T. Nagai, *ACS Chem. Biol.* **2011**, *6*, 401–406. (c) E. Martincova, L. Voleman, V. Najdrova, M.D. Napoli, S. Eshar, M. Gualdron, C.S. Hopp, D.E. Sanin, D.L. Tembo,

D.V. Tyne, D. Walker, M. Marcinčiková, J. Tachezy, P. Doležal, *PLoS ONE* **2012**, *7*, e36314.
8. D. Kalderon, B.L. Roberts, W.D. Richardson, A.E. Smith, *Cell* **1984**, *39*, 499–509.
9. P.T. Englund, S.L. Hajduk, J.C. Martini, *Ann. Rev. Biochem.* **1982**, *51***,** 695–726.
10. Y. Nishikawa, K. Hiraki, *Analytical Methods of Fluorescence and Phosphorescence*, Kyoritsu Publishing Company, Tokyo, **1984**.

## **Section 2.2.** Analysis of Immune Systems by Single-Molecule Imaging

Single-molecule imaging is a robust method of studying protein function in detail. To perform single-molecule imaging, a total internal reflection fluorescence (TIRF) microscope is utilized.[1] TIRF microscopy has become a widely used technique for single-molecule detection both in vitro and in living cells.[2] The TIRF microscope, which was originally developed to observe the interface between two media with different diffractive indices,[3] uses an electromagnetic field known as the 'evanescent field' to excite fluorophores. As the evanescent field diminishes exponentially with distance from the interface, the excitation depth in the TIRF microscope is limited to a very narrow range, typically 100 to several hundred nanometers. However, using such a narrow excitation depth is the most effective method for overcoming the problem of background noise, which is often the biggest limitation in single-molecule imaging.

In the study described in Section 2.1, a cell-permeable probe was introduced. In this study, the probe was applied for single-molecule imaging using a TIRF microscope.

### Single-Molecule Imaging of $Lyn_{11}$-BL

First, single-molecule imaging of BL-tag anchored to the plasma membrane was performed using **RB2** and **RB4**. $Lyn_{11}$-BL, which is localized at the plasma membrane by fusing BL-tag to a Lyn N-terminus sequence (GCIKSKGKDSA, $Lyn_{11}$)[4], was expressed in HEK293T cells cultured on coverslips. The culture medium was replaced

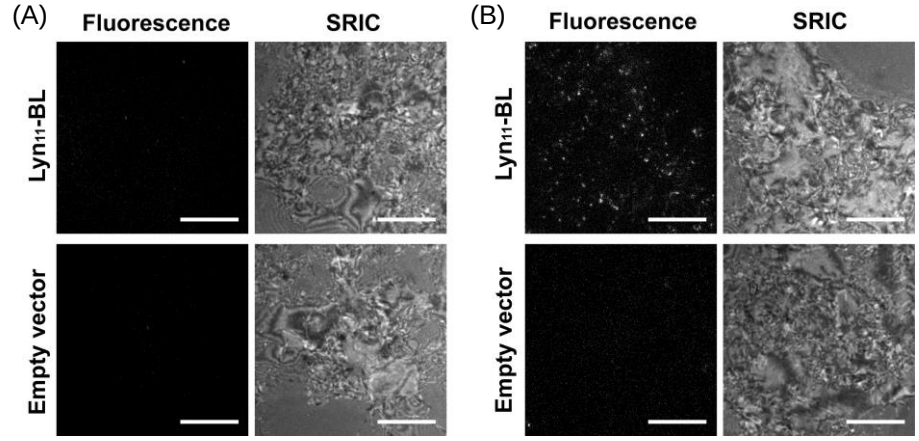


***Figure 2-9.*** Single-molecule fluorescence imaging of $Lyn_{11}$-BL expressed in HEK293T cells. The cells were incubated with (A) 10 nM **RB4** or (B) 5 nM **RB2** for 30 min at 37°C. Excitation at 561 nm, 60× oil-immersion objective lens (60× Oil, NA = 1.49) exposure time: 32.82 ms. Scale bar: 5 μm.

with serum and phenol red-free medium and incubated for 2 h in order to reduce background signals from FBS. Next, the cells were incubated with **RB2** or **RB4** at 37°C for 30 min and washed three times. Finally, single-molecule imaging was performed using a TIRF microscope.

When the cells were incubated with **RB4**, bright spots were not observed from the cells (Figure 2-9A). However, when the cells were incubated with **RB2**, a large number of bright spots were detected from individual proteins (Figure 2-9B). When single-molecule imaging is performed, the probe concentration should be as low as possible in order to reduce background signals derived from non-specific adsorption onto the coverslips of the probe. Moreover, labeling efficiency should be as low as possible. If the labeling efficiency is high, individual bright spots cannot be recognized, making analysis difficult. Therefore, **RB2** is more suitable for performing single-molecule imaging.

**Single-molecule imaging of TLR4-BL**

Single-molecule imaging can be performed using BL-tag system and **RB2**. As a target protein, Toll-like receptor 4 (TLR4)[5] was selected and applied to single-molecule imaging. TLR4 recognizes lipopolysaccharide (LPS) from gram-negative bacteria.[6] This receptor is expressed on many cell types, including macrophages and dendritic cells, and plays a fundamental role in pathogen recognition and innate immunity activation. Normally, TLR4 forms complex with MD-2 in living cells.[7]

Single-molecule imaging of TLR4 was performed. BL-tag was fused to the C-terminus of TLR4 (TLR4-BL) and expressed in HEK293T cells. When TLR4-fused

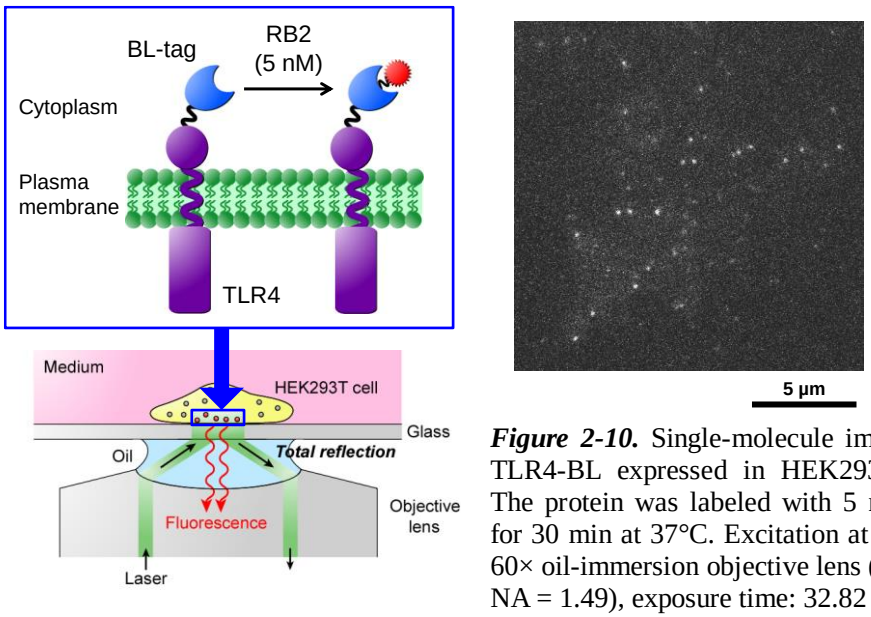


***Figure 2-10.*** Single-molecule imaging of TLR4-BL expressed in HEK293T cells. The protein was labeled with 5 nM **RB2** for 30 min at 37°C. Excitation at 561 nm. 60× oil-immersion objective lens (60× Oil, NA = 1.49), exposure time: 32.82 ms.

proteins were expressed in the cells, MD-2 was expressed at the same time. Next, the culture medium was replaced with fresh serum- and phenol red-free medium and the cells were incubated for 2 h. **RB2** was added to the cells, incubated for 30 min at 37 °C, and washed three times. Single-molecule imaging using a TIRF microscope was then performed. Many bright spots were detected, indicating that single-molecule imaging of TLR4 with BL-tag system was successful (Figure 2-10).

Next, the response of TLR4 to LPS was analyzed by single-molecule imaging. TLR4-BL and MD-2 was expressed in HEK293T cells and labeled with **RB2**. The cells were stimulated by LPS (10 μg/mL) for 15 min and single-molecule imaging was performed using a TIRF microscope. The results were computationally analyzed. A displacement histogram check (DHC) and short-range diffusion (SRD) analysis were performed.[8] DHC analysis involves construction of a histogram of displacement for a particular lag time. SRD analysis constructs the histogram showing diffusion coefficients of individual bright spots. The number of slow-moving proteins increased in response to LPS stimulation according to DHC and SRD analysis (Figure 2-11). This result was likely observed because of the protein-protein interaction between TLR4 and its adaptor protein induced by LPS stimulation.

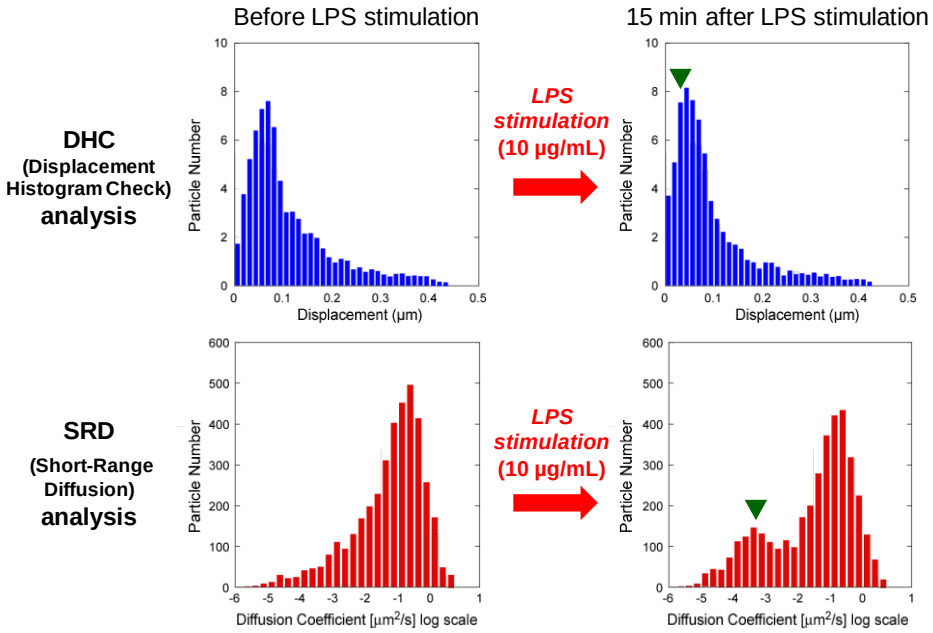


***Figure 2-11.*** DHC analysis and SRD analysis of single-molecule imaging results. TLR4-BL labeled by **RB2** was stimulated with 10 μg/mL LPS. The histogram indicates the result before (left) and 15 min after (right) LPS stimulation.

## Multicolor single-molecule imaging of TLR4 and TIRAP

Following engagement by the ligand LPS, TLR4 triggers specific signaling outcomes by recruiting various combinations of adaptor proteins, which then relay signals to specific downstream signaling molecules.[9] TLR4 signaling pathways can be largely categorized by their use of two main adaptor proteins: myeloid differentiation primary response protein 88 (MyD88) and TIR domain-containing adaptor protein inducing IFNβ (TRIF). In the MyD88-dependent pathway, TLR4 activated at the plasma membrane recruits MyD88 through the TIR domain-containing adaptor protein (TIRAP), and downstream signaling is activated to induce pro-inflammatory cytokines.[10]

To analyze the interaction between TLR4 and its adaptor protein, immunoprecipitation is often utilized. However, live imaging of protein-protein interactions is impossible using this method. Therefore, single-molecule imaging was applied to analyze LPS-induced protein-protein interactions between TLR4 and TIRAP.

Multicolor single-molecule imaging was performed to analyze the interaction between TLR4 and TIRAP. The commercial HaloTag system[11] was used in combination with BL-tag system. HaloTag system is based on engineered haloalkane dehalogenase and is commercially available. The native enzyme is a monomeric protein (33 kDa) that cleaves carbon-halogen bonds in aliphatic halogenated compounds. Upon nucleophilic

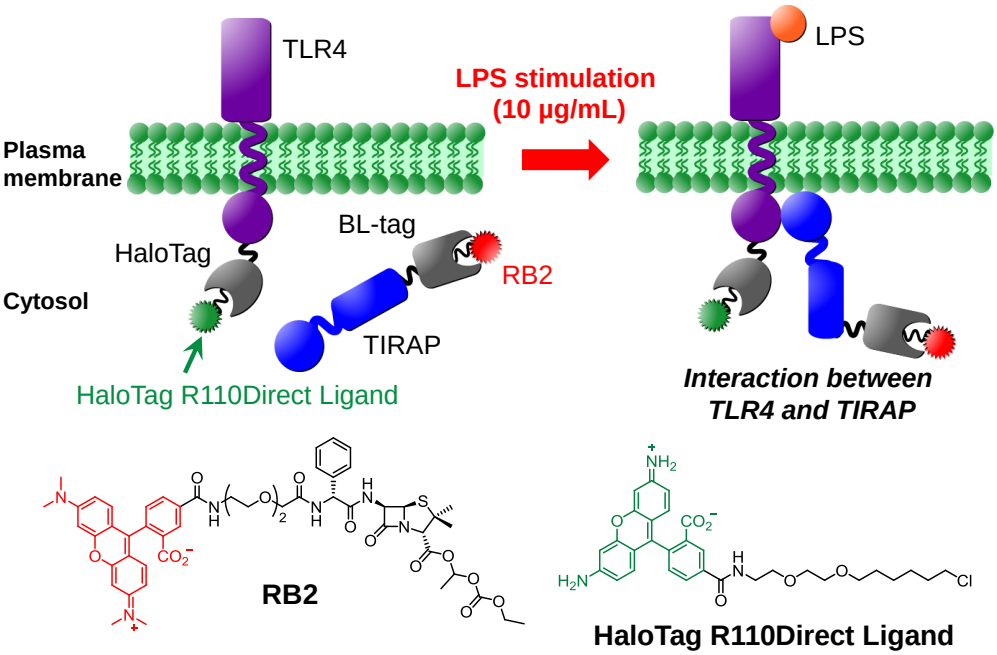


***Figure 2-12.*** LPS stimulation of TLR4-Halo and BL-TIRAP. TLR4-Halo and BL-TIRAP were coexpressed in HEK293T cells and labeled by HaloTag R110Direct Ligand and **RB2**. The proteins were stimulated by 10 μg/mL of LPS.

attack by chloroalkane to Asp106 in the enzyme, an ester bond is formed between HaloTag ligand and the protein. HaloTag contains a critical mutation in its catalytic triad so that the ester bond formed between HaloTag and HaloTag ligand cannot be further hydrolyzed.

BL-tag was fused to the N-terminus of TIRAP (BL-TIRAP), and HaloTag was fused to C-terminus of TLR4 (TLR4-Halo) and expressed in HEK293T cells (Figure 2-12). The cells were incubated with **RB2** and HaloTag R110Direct Ligand for 30 min at 37°C, washed three times, and subjected to confocal fluorescence microscopy (Figure 2-13). Differences in fluorescence images between pre-LPS stimulation and 15 min after LPS stimulation were not observed. Therefore, it was not possible to analyze the protein-protein interaction using confocal fluorescence microscopy and the tag proteins.

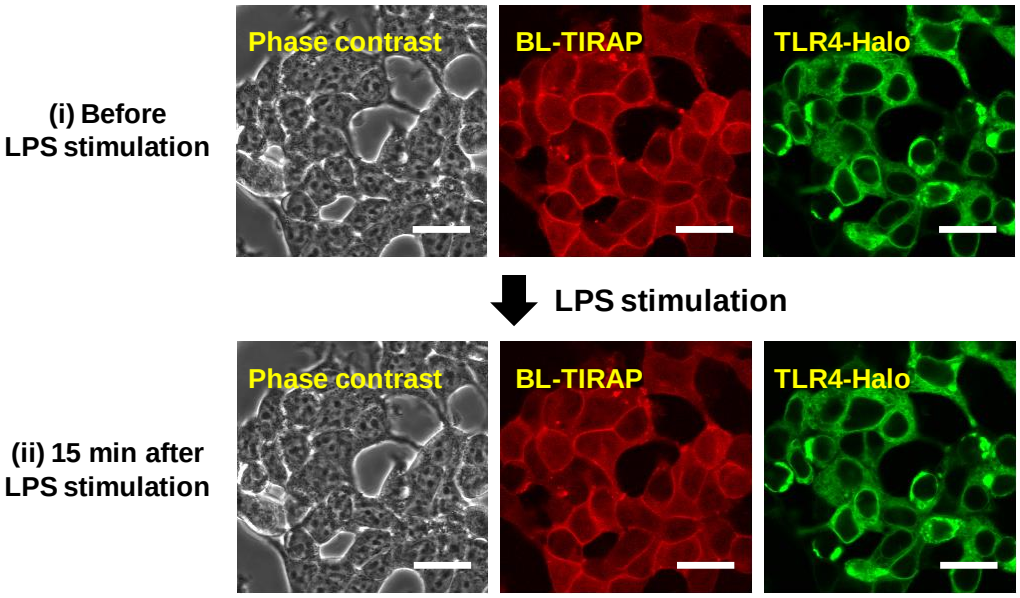


***Figure 2-13.*** Labeling of TLR4-Halo and BL-TIRAP expressed in HEK293T cells with 100 nM HaloTag R110Direct Ligand and 500 nM **RB2** for 30 min at 37°C. HaloTag R110Direct Ligand: excited at 473 nm, detected 490–540 nm. **RB2**: excited at 559 nm, detected 570–670 nm. Scale bar: 20 μm.

Next, multicolor single-molecule imaging of TLR4-Halo and BL-TIRAP was performed (Figure 2-14) and the cells were stimulated with 10 μg/mL LPS. Signals from TLR4 and TIRAP were detected simultaneously and the obtained data were statistically analyzed. The histogram of displacement and diffusion coefficients for individual proteins of interest (POIs) was obtained via DHC and SRD analysis (Figure 2-15 and 2-16). The number of proteins with small displacement and diffusion coefficients was increased following LPS stimulation. This may have occurred because TLR4 interacted with TIRAP, thereby decreasing the motility of the molecule. Moreover, protein-protein interactions can be fully characterized by combining orbital analysis for

each protein. Thus, potential of protein-protein interactions can be analyzed using this system in living cells.

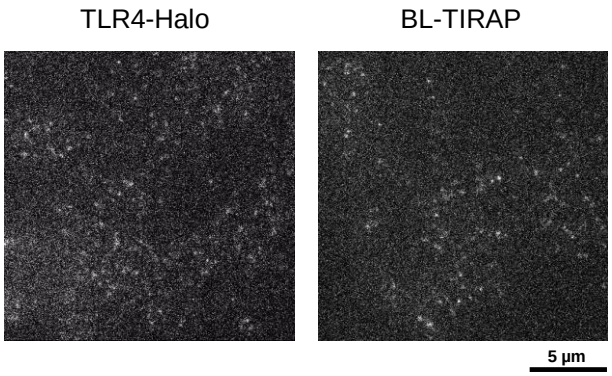


***Figure 2-14.*** Multicolor single-molecule fluorescence imaging of TLR4-Halo and BL-TIRAP expressed in HEK293T cells. The cells were incubated with 0.5 nM HaloTag R110Direct Ligand and 5 nM **RB2** for 30 min at 37°C. Excitation at 488 nm (for HaloTag R110Direct Ligand) or 561 nm (for **RB2**) optically pumped semiconductor laser, 60× oil-immersion objective lens (60× Oil, NA = 1.49) exposure time: 32.82 ms.

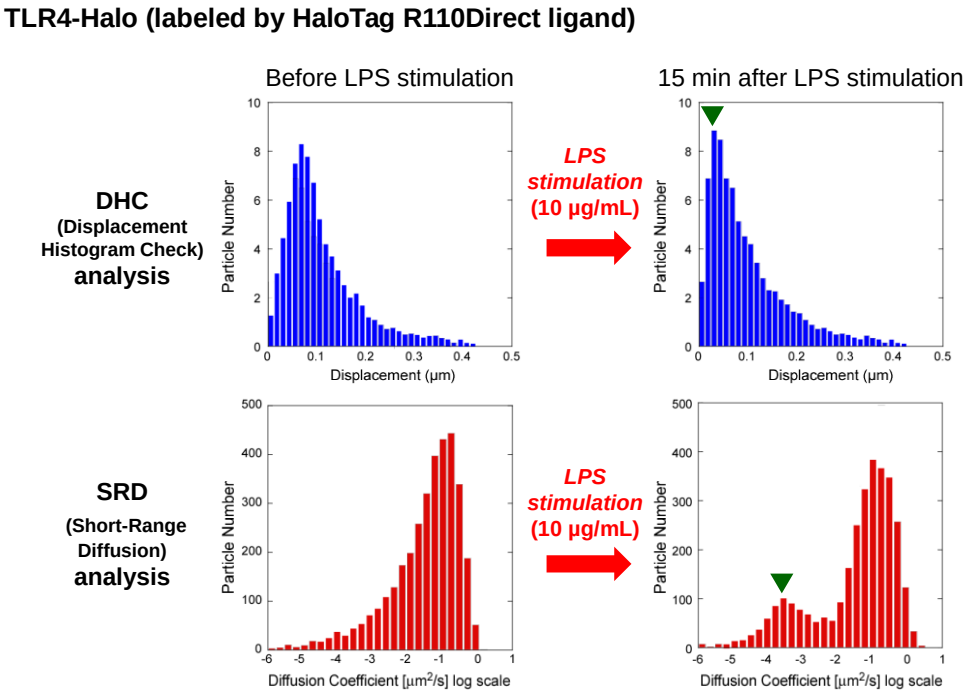


***Figure 2-15.*** DHC and SRD analysis of single-molecule imaging of TLR4-Halo labeled by HaloTag R110Direct Ligand and stimulated with 10 μg/mL LPS. The histogram indicates the results before (left) and 15 min after (right) LPS stimulation.

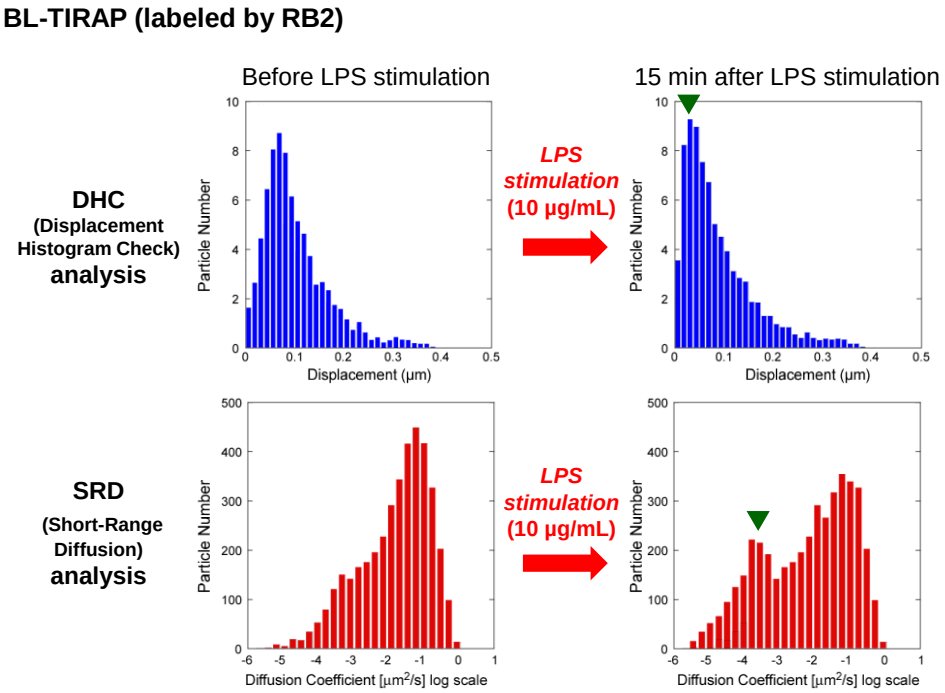


***Figure 2-16.*** DHC and SRD analysis of single-molecule imaging of BL-TIRAP labeled by **RB2** and stimulated with 10 μg/mL LPS. The histogram indicates the results before (left) and 15 min after (right) LPS stimulation.

## Experimental Section

**Materials.** Lipopolysaccharide (LPS) from *Salmonella minnesota* R595 was purchased from Wako Pure Chemical (121-05291). HaloTag R110Direct Ligand was purchased from Promega. Restriction endonucleases and PrimeSTAR® HS DNA polymerase were purchased from Takara Bio, Inc. Ampicillin was purchased from Wako Pure Chemical. Plasmid DNA was isolated using a QIAprep Spin Miniprep kit (Qiagen). Competent high DH5α (TOYOBO) was used as an intermediate host for site-directed mutagenesis experiments. Luria-Bertani (LB) medium was used as the growth medium for all bacterial strains. Bacto Agar (Wako Pure Chemical) was added at a concentration up to 1.0% for preparing solid media. pcDNA3-MD-2, pFC14A-TLR4-Halo and pEF-BOS-BL-TIRAP were a kind gift from Dr. Yutaro Kumagai.

## Experimental Procedures

**Confocal laser scanning fluorescence microscopy.** Confocal fluorescence microscopic images were recorded using a confocal laser scanning microscope

(Olympus; FLUOVIEW FV10i) equipped with a 60× lens. **RB2** and **RB4** were excited at 559 nm. HaloTag R110Direct Ligand was excited at 473 nm. The emission filter sets used were Olympus BA570–620 for **RB2** and **RB4** and BA490–540 for HaloTag R110Direct Ligand.

**Micro coverglass cleaning.** The 25-mm glass coverslips (Matsunami) were extensively cleaned to remove background fluorescence. First, they were sonicated in a solution of 0.1 M KOH for 30 min. Next, they were sonicated in ethanol for 30 min three times. Coverslips were stored in ethanol until use.

**TIRF microscopy.** A TIRF microscope (Nikon, Ti-E) equipped with an EM-CCD camera (Hamamatsu Photonics; ImagEM C9100-13), a 60× oil-immersion objective (Nikon; Apo TIRF 60× oil, NA = 1.49), brightline filter sets (Semrock; LF561-A-000), and a 561 nm optically pumped semiconductor (OPS) laser (COHERENT; Sapphire561) were used. Laser power was 100% and image sequences (300 frames) were acquired with an exposure time of 32.82 ms. Experiments were performed at 37°C.

**Construction of pcDNA3.1(+)-Lyn$_{11}$-BL plasmid.** A DNA fragment of BL containing a termination codon was amplified from the Cytoplasmic-BL plasmid by polymerase chain reaction (PCR) using the following primers containing the Kozak sequence (forward primer: 5′-GTGTGAGGATCCGCCGCCATGAAAAAGACAGCTATCGCGA-3′, subforward primer: 5′-GTGTGAGGATCCGCCG-3′, reverse primer: 5′-CGCGCGGAATTCCAGTTACCAATGCTTAATCA-3′, subreverse primer: 5′-CGCGCGGAATTCCA-3′; Greiner Bio-one). The amplified insert was digested with *BamH*I and *EcoR*I, and ligated in-frame to a similarly digested pcDNA3.1(+) vector. The constructed plasmid was digested with *Hind*III and *BamH*I and ligated in-frame into a similarly digested Lyn$_{11}$ oligo DNA. The Lyn$_{11}$ oligo DNA was amplified from a purchased oligo nucleotide template (5′-AATTAAAAGCTTGCCGCCATGGGATGTATAAAATCAAAAGGGAAAGACAG CGCGGGAGCAGATAGTGCTGGTAGTGCTGGTAG-TGCTGGTGGATCCATCGG A-3′ and 5′-TCCGATGGATCCACCAGCACTACCAGCACTACCAGCACTATCTGCTCCCGC GCTGTCTTTCCCTTTTGATTTTATACATCCCATGGCGGCAAGCTTTTAATT-′; Gene Design, Inc.) using the following primers (forward primer: 5′-AATTAAAAGCTTGCCGC-3′, reverse primer: 5′-AGGCTAGGATCCACCAG-3′).

**Construction of pcDNA3.1(+)-TLR4-BL.** A DNA fragment of TLR4 was amplified from pFC14A-TLR4-Halo by PCR and was digested with *Hind*III and *Nhe*I. The DNA

fragment was ligated to pcDNA3.1(+)-BL which was digested using the same restriction enzymes to yield pcDNA3.1(+)-TLR4-Halo.

**Confocal fluorescence microscopy of TLR4-Halo and BL-TIRAP.** HEK293T cells maintained in a glass-bottomed dish with DMEM containing 10% FBS at 37°C under 5% $CO_2$ were transfected with the plasmids encoding TLR4-Halo, BL-TIRAP and MD-2 as described above. After 5 h, the culture medium was replaced with DMEM and the cells were incubated at 37°C for 24 h. Next, the cells were washed three times with HBSS and incubated with 200 nM **RB2** or 100 nM HaloTag R110Direct Ligand for 30 min in a $CO_2$ incubator. The cells were then washed three times with HBSS and microscopic images were acquired. Fluorescence images of the cells in HBSS were captured using appropriate filter sets. Labeled cells were observed soon after the washing step.

**Single-molecule imaging of $Lyn_{11}$-BL with a TIRF microscope.** HEK293T cells maintained on glass coverslips in a 6-well plate were transfected with $Lyn_{11}$-BL using Lipofectamine 2000. After 5 h, the culture medium was replaced with DMEM and the cells were incubated at 37°C for 24 h. The culture medium was exchanged with Opti-MEM (Gibco) and the cells were incubated at 37°C for 2 h. Next, the cells were washed three times with HBSS and incubated with **RB2** (5 nM) or **RB4** (10 nM) in Opti-MEM for 30 min in a $CO_2$ incubator. The cells were then washed three times with HBSS and single-molecule imaging was performed using a TIRF microscope.

**LPS stimulation of TLR4-BL.** HEK293T cells maintained on glass coverslips in a 6-well plate were co-transfected with TLR4-BL and MD-2 using Lipofectamine 2000. After 5 h, the culture medium was replaced with DMEM and the cells were incubated at 37°C for 24 h. Next, the culture medium was exchanged with Opti-MEM and the cells were incubated at 37°C for 2 h. The cells were then washed three times with HBSS and incubated with **RB2** (5 nM) in Opti-MEM for 30 min in a $CO_2$ incubator. Cells were washed three times with HBSS, after which LPS (10 μg/mL) was added. Single-molecule imaging was performed before and after LPS stimulation every 5 min using a TIRF microscope.

**Multicolor single-molecule imaging of TLR4-Halo and BL-TIRAP.** HEK293T cells maintained on glass coverslips in a 6-well plate were co-transfected with TLR4-Halo, BL-TIRAP, and MD-2 using Lipofectamine 2000. After 5 h, the culture medium was replaced with DMEM, and the cells were incubated at 37°C for 24 h. Next, the culture medium was exchanged with Opti-MEM and the cells were incubated at 37°C for 2 h. The cells were then washed three times with HBSS and incubated with **RB2** (5 nM) and HaloTag R110Direct Ligand (0.5 nM) in Opti-MEM for 30 min in a $CO_2$ incubator. The

cells were washed three times with HBSS, after which Opti-MEM containing LPS (10 μg/mL) was added. Single-molecule imaging was performed before and after LPS stimulation every 5 min using a TIRF microscope.

**Computational analysis.** Particles were detected and tracked using G-count software. Short-range diffusion (SRD) and displacement histogram construction (DHC) analysis were performed using appropriate algorithms implemented in Matlab (The MathWorks).

When SRD analysis was performed, all possible short trajectories were first extracted. Next, mean-squared displacement (MSD) versus lag-time ($\Delta t$) plots for each short trajectory were made. The squared displacement, $\Delta r^2$, during the lag-time, $\Delta t$, was obtained using the following equation:

$$\Delta r^2(\Delta t, t) = (X(t+\Delta t) - X(t))^2 + (Y(t+\Delta t) - Y(t))^2, \Delta t = nt_{\text{intvl}} \quad (1)$$

where *X(t)*, *X(t)*, and *Y(t)* are the X–Y positions of a single molecule at time point *t*. The time interval $t_{\text{intvl}}$ represents the interval for data acquisition, while *n* is a natural number. MSDs for each $\Delta t$ were obtained by averaging the squared displacements, $\Delta r^2$ ($\Delta t$, *t*). Next, obtained data were fitted to the MSD-$\Delta t$ plots using the following linear function:

$$MSD(\Delta t) = 4D\Delta t + a$$

where *D* is the diffusion coefficient and *a* is a constant representing the positioning error of the measurement system. The slopes of the first 4 data points in the MSD plots were used to obtain SRD; finally, a histogram of the SRD was created.

When DHC analysis was performed, the data set of displacements with various lag-times ($\Delta t$) was constructed. Displacements ($\Delta r$) were obtained using equation (1). Next, the histogram of $\Delta r$ for a particular lag time, $\Delta t$, was constructed.

## References


1. T. Funatsu, Y. Harada, M. Tokunaga, K. Saito, T. Yanagida, *Nature* **1995**, *374*, 555–559.
2. (a) A. Ishijima, T. Yanagida, *Trends Biochem. Sci.* **2001**, *26*, 438–444. (b) Y. Sako, T. Uyemura, *Cell Struct. Funct.* **2002**, *27*, 205–213.
3. D. Axelrod, T.P. Burghardt, N.L. Thompson, *Ann. Rev. Biophys. Bioeng.* **1984**, *13*,

247–268.

4. (a) M.D. Resh, *Cell* **1994**, *76*, 411–413. (b) T. Inoue, W.D. Heo, J.S. Grimley, T.J. Wandless, T. Meyer, *Nat. Methods* **2005**, *2*, 415–418.
5. (a) T. Kondo, T. Kawai, S. Akira, *Trends Immunol.* **2012**, *33*, 449–458. (b) S. Akira, *Curr. Opin. Immunol.* **2003**, *15*, 5–11.
6. (a) N. Ruiz, D. Kahne, T.J. Silhavy, *Nat. Rev. Microbiol.* **2009**, *7*, 677–683. (b) S.I. Miller, R.K. Ernst, M.W. Bader, *Nat. Rev. Microbiol.* **2005**, *3*, 36–46.
7. K.A. Fitzgerald, D.C. Rowe, D.T. Golenbock, *Microb. Infect.* **2004**, *6*, 1361–1367.
8. (a) S. Matsuoka, T. Shibata, M. Ueda, *Biophys, J.* **2009**, *97*, 1115–1124. (b) Y. Miyanaga, S. Matsuoka, M. Ueda, *Methods Mol. Biol.* **2009**, *571*, 417–435.
9. (a) T. Kawai, S. Akira, *Arthritis. Res. Ther.* **2005**, *7*, 12–19. (b) H. Hemmi, S. Akira, *Chem. Immunol. Allergy* **2005**, *86*, 120–135.
10. (a) X. Jiang, Z.J. Chen, *Nat. Rev. Immunol.* **2012**, *12*, 35–48. (b) T. Kawai, S. Akira, *Cell. Death Dis.* **2006**, *13*, 816–825. (c) T. Kawai, S. Akira, *Semin. Immunol.* **2007**, *19*, 24–32.
11. G.V. Los, L.P. Encell, M.G. McDougall, D.D. Hartzell, N. Karassina, C. Zimprich, M.G. Wood, R. Learish, R.F. Ohana, M. Urh, D. Simpson, J. Mendez, K. Zimmerman, P. Otto, G. Vidugiris, J. Zhu, A. Darzins, D.H. Klaubert, R.F. Bulleit, K.V. Wood, *ACS Chem. Biol.* **2008**, *3*, 373–382.

# **Chapter 3.** Control of Protein Function in Living Cells

Chapters 1 and 2 described the development of various protein research tools for imaging proteins of interest (POIs). However, these methods are insufficient for functional studies, making the development of additional research tools necessary for studying POIs in more detail. The author hypothesized that artificial activation of protein function would be possible using BL-tag technology. If protein function can be controlled, signal transduction in living cells can be induced artificially, and novel biological functions may be clarified in detail in the study of signaling pathways.

Signal transduction is often controlled through allostery- and proximity-based mechanisms in biological sytems.[1] In allosteric-based mechanisms, molecules related to cell signaling cause conformational changes in the target proteins to activate or inactivate their functions. By contrast, in the proximity-based mechanism, localization of a signaling molecule is changed and interactions between recipients and another interacting partner or substrate are modulated.[2] This proximity can be controlled and manipulated with chemically induced dimerization (CID), which is a powerful tool for investigating biological phenomena.[3]

The principle of CID is based on controlling protein dimerization using a small functional molecule. The functional molecular probe can bind to two target proteins simultaneously, bringing them into close proximity. Depending on the structure of the dimerizer, CID systems can induce the formation of homo- or heterodimers of target proteins. The first CID system was an FK1012-based system, a synthetic dimerizer.[4] The molecule can dimerize two FK506-binding proteins (FKBPs), resulting in formation of a homodimer. Subsequently, the natural product rapamycin was discovered and applied in CID systems.[5] Rapamycin mediates the heterodimerization of FKBP and the FKBP-rapamycin-binding (FRB) domain of the mammalian target of rapamycin (mTOR). By fusing target proteins to dimerization domains, the CID system can be applied to control a wide range of cellular events.[6] Although the system is highly useful because of its high affinity, a cross-reaction with the nutrient sensor mTOR complex 1 (TORC1) is detected.[7] Thus, C16-derivatized rapalogs have been designed to interact only with mutated FRB domains, which do not react with endogenous mTOR.[8] Utilizing rapamycin and rapamycin derivatives, activation of various protein functions was achieved by translocation of target proteins to the plasma membrane or to an organelle.[9]

Recently, a new CID system was developed based on gibberellic acid acetoxymethyl

ester ($GA_3AM$).[10] Gibberellic acid is a plant hormone that regulates various aspects of plant growth and development. This molecule binds to gibberellinin-sensitive dwarf 1 (GID1), causing conformational changes. This complex then binds to another protein known as gibberellin-insensitive (GAI). Dimerization with $GA_3AM$ is orthogonal to the existing rapamycin-based CID system; therefore, two different types of POIs can be activated simultaneously using this system.[11]

Various small molecule-based dimerizers have been developed that successfully control protein function. However, modifying these dimerizers is difficult because they are structurally complicated natural products, and the design flexibility of the molecule is low. Therefore, it is necessary to develop alternative dimerization strategies.

## References


1. D.J. Austin, G.R. Crabtree, S.L. Schreiber, *Chem. Biol.* **1994**, *1*, 131–136.
2. P.J. Belshaw, S.N. Ho, G.R. Crabtree, S.L. Schreiber, *Proc. Natl. Acad. Sci. U. S. A.* **1996**, *93*, 4604–4607.
3. (a) A. Fegan, B. White, J. C. Carlson, C. R. Wagner, *Chem. Rev.* **2010**, *110*, 3315–3336. (b) M. Putyrski, C. Schultz, *FEBS Lett.* **2012**, *586*, 2097–2105. (c) T.W. Corson, N. Aberle, C.M. Crews, *ACS Chem. Biol.* **2008**, *3*, 677–692.
4. D.M. Spencer, T.J. Wandless, S.L. Schreiber, G.R. Crabtree, *Science* **1993**, *262*, 1019–1024.
5. (a) E.J. Brown, M.W. Albers, T.B. Shin, K. Ichikawa, C.T. Keith, W.S. Lane, S.L. Schreiber, *Nature* **1994**, *369*, 756–758. (b) V.M. Rivera, T. Clackson, S. Natesan, R. Pollock, J.F. Amara, T. Keenan, S.R. Magari, T. Phillips, N.L. Courage, F. Cerasoli, Jr., D.A. Holt, M. Gilman, *Nat. Med.* **1996**, *2*, 1028–1032. (c) D.M. Sabatini, H. Erdjument-Bromage, M. Lui, P. Tempst, S.H. Snyder, *Cell* **1994**, *78*, 35–43. (d) G.R. Crabtree, S.L. Schreiber, *Trends Biochem. Sci.* **1996**, *21*, 418–422.
6. A. Fegan, B. White, J.C. Carlson, C.R. Wagner, *Chem. Rev.* **2010**, *110*, 3315–3336.
7. (a) E.J. Brown, M.W. Albers, T.B. Shin, K. Ichikawa, C.T. Keith, W.S. Lane, S.L. Schreiber, *Nature* **1994,** *369*, 756–758. (b) J. Choi, J. Chen, S.L. Schreiber, J. Clardy, *Science* **1996**, *273*, 239–242.
8. (a) S.D. Liberles, S.T. Diver, D.J. Austin, S.L. Schreiber, *Proc. Natl. Acad. Sci. U. S. A.* **1997**, *94*, 7825–7830. (b) S.R. Edwards, T.J. Wandless, *J. Biol. Chem.* **2007**, *282*, 13395–13401.
9. (a) T. Inoue, W.D. Heo, J.S. Grimley, T.J. Wandless, T. Meyer, *Nat. Methods*, **2005**, *2*, 415–418. (b) T. Komatsu, I. Kukelyansky, J.M. McCaffery, T. Ueno, L.C. Varela,

T. Inoue, *Nat. Methods* **2010**, *7*, 206–208. (c) P. Varnai, B. Thyagarajan, T. Rohacs, T. Balla, *J. Cell Biol.* **2006**, *175*, 377–382. (d) N. Fili, V. Calleja, R. Woscholski, P.J. Parker, B. Larijani, *Proc. Natl. Acad. Sci. U. S. A.* **2006**, *103*, 15473–15478.

10. T. Miyamoto, R. DeRose, A. Suarez, T. Ueno, M. Chen, T.-P. Sun, M.J. Wolfgang, C. Mukherjee, D.J. Meyers, T. Inoue, *Nat. Chem. Biol.* **2012**, *8*, 465–470.
11. S.C. Phua, C. Pohlmeyer, T. Inoue, *ACS Chem. Biol.* **2012**, *7*, 1950–1955.

## **Section 3.1.** Protein Dimerization Induced by Protein Labeling Systems

The author focused on a protein labeling system with the goal of developing a new CID system. Chapters 1 and 2 described the successful modification of POIs with functional molecules. Labeling probes were composed of one functional molecule such as a fluorescent dye and biotin, as well as one β-lactam molecule, BL-tag ligand. If the molecule possesses two β-lactam molecules, two BL-tag proteins could be tethered and should form a protein homodimer. Moreover, protein heterodimerization can be induced by using a BL-tag and another reported protein labeling system such as HaloTag,[1] SNAP-tag,[2] or CLIP-tag.[3] These protein tags and their ligands form covalent bonds. The labeling reaction is highly specific, occurs rapidly under physiological conditions, and is essentially irreversible.

Previously, a dimerizer based on the SNAP-tag system was reported and protein homodimerization in living cells was shown to be successful.[4] Subsequently, a protein heterodimerization system based on the SNAP-tag and CLIP-tag system was reported.[5] The dimerizer contains both SNAP- and CLIP-tag ligands, and detection of protein-protein interactions in the cell lysate was successful. Another group reported a homodimerizer based on FlAsH.[6] This molecule was applied for detection of protein-protein interactions in living cells.[7] While some dimerizers based on a protein labeling system have been reported, the control of target proteins in living cells has not yet been achieved.

**Design and synthesis of dimerizers based on a protein labeling system**

First, new dimerizers were designed based on protein labeling systems. A homodimerizer should contain two BL-tag substrates. Moreover, a linker should be introduced between the ligands in order to decrease steric hindrance between BL-tag proteins. HaloTag system was selected as the counterpart of BL-tag and a heterodimerizer was designed. The molecule was composed of a BL-tag ligand, HaloTag ligand, and linker. Upon addition of the dimerizer to cells expressing BL-tag- and HaloTag-fused proteins, dimerization is expected occur (Scheme 3-1). Next, two dimerizers, **BBD** and **BHD**, were designed and synthesized according to Scheme 3-2 and 3-3.

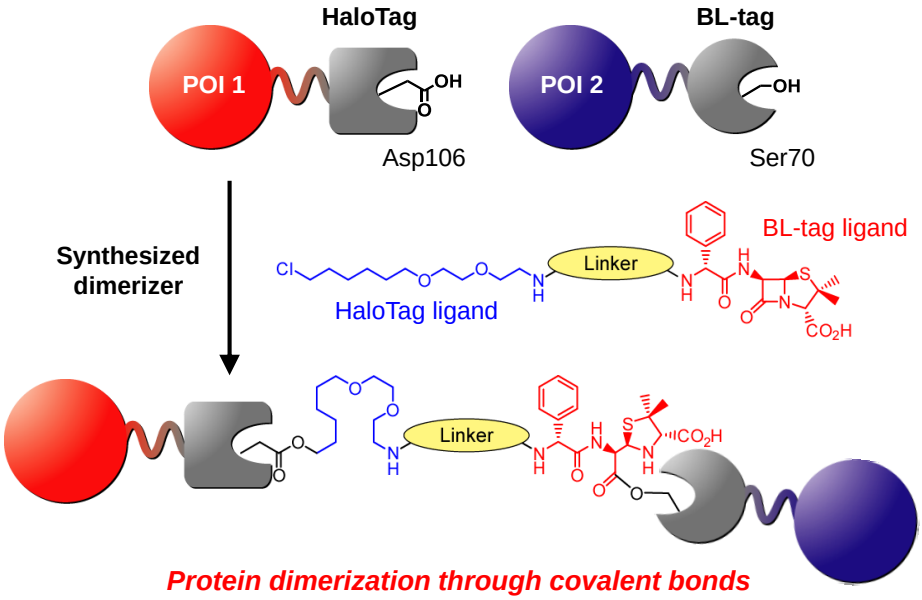


***Scheme 3-1.*** Covalent dimerization of two proteins based on protein labeling system. (A) General scheme for the dimerization of target proteins using dimerizers. (B) Structures of synthesized dimerizers, **BBD** and **BHD**.

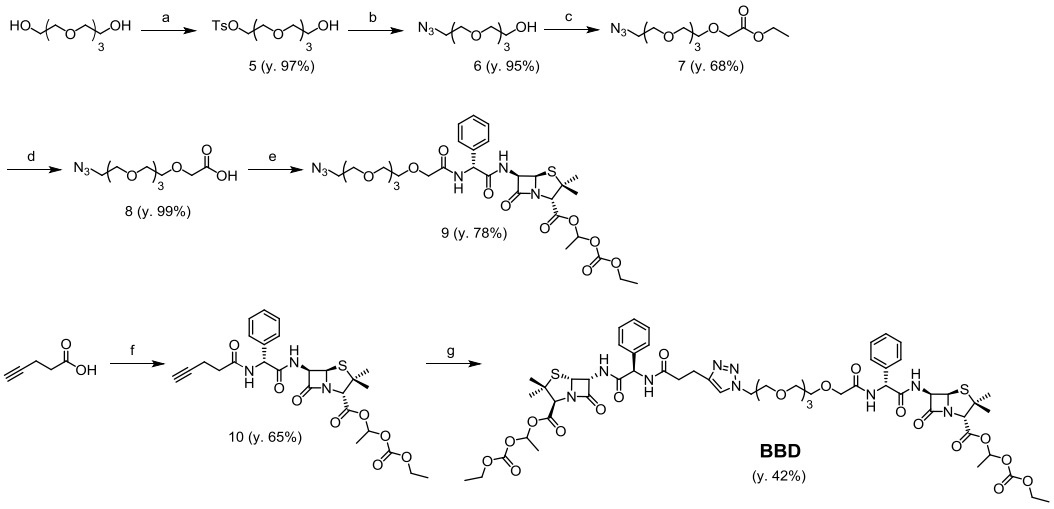


***Scheme 3-2.*** Synthetic scheme of **BBD**. (a) TsCl, NaOH, $CH_2Cl_2$; (b) $NaN_3$, DMF, 80 °C; (c) Ethyl bromoacetate, NaH, DMF; (d) NaOH, MeOH; (e) bacampicillin·HCl, WSCD·HCl, HOBt, TEA, DMF; (f) bacampicillin·HCl, PyBOP, TEA, DMF; (g) **9**, $CuSO_4$, Sodium ascorbate, DMF/$H_2O$.

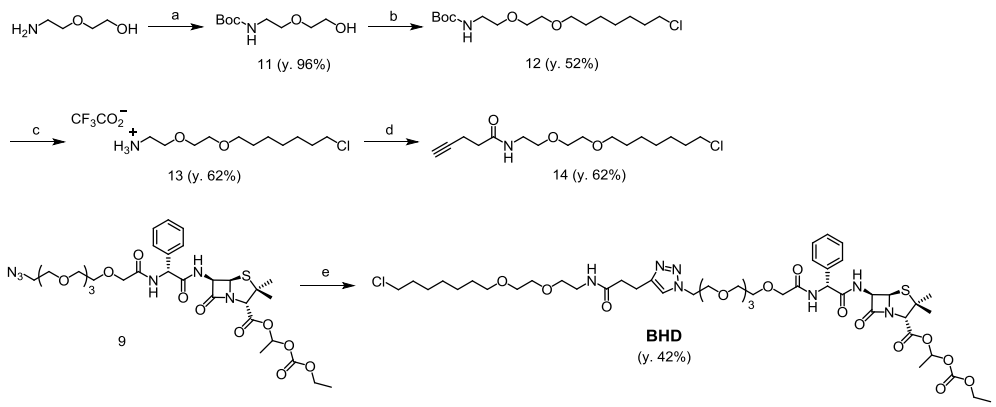


***Scheme 3-3.*** Synthetic scheme of **BHD**. (a) $Boc_2O$, EtOH; (b) NaH, 6-chloro-1-iodohexane, DMF; (c) TFA, $CH_2Cl_2$; (d) 4-pentynoic acid, PyBOP, TEA, DMF; (e) **14**, $CuSO_4$, sodium ascorbate, DMF/$H_2O$.

## Protein dimerization in living cells

Homodimerization of BL-tag-fused proteins was performed with **BBD** in living cells. BL-tag protein was expressed in the cytosol (Cytoplasmic-BL), nuclei (BL-NLS), or on the cell surface (BL-GPI) of HEK293T cells. The cells were incubated with 500 nM **BBD** for 3 h, washed three times, and lysed in sodium dodecyl sulfate (SDS) sample buffer. The cell lysate was analyzed by western blotting. BL-tag proteins were detected by anti-β-lactamase antibody (Figure 3-1). The protein homodimer of BL-tag-fused proteins was detected for each case. Monomers of BL-tag protein were detected simultaneously; therefore, homodimerization of all expressed proteins was not achieved. **BHD** can permeate cells and dimerizes target BL-tag proteins expressed in living cells.

Next, heterodimerization of BL-tag- and HaloTag-fused-proteins were performed using **BHD** in living cells. BL-tag-fused- and HaloTag-fused-proteins were expressed in

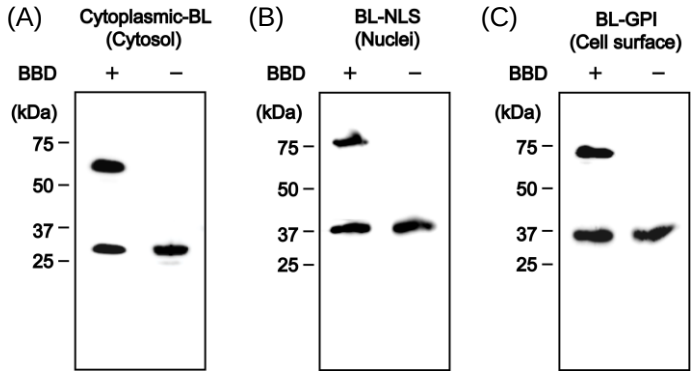


***Figure 3-1.*** Homodimerization of BL-tag fusion proteins in HEK293T cells using **BBD**. (A) Cytoplasmic-BL, (B) BL-NLS or (C) $Lyn_{11}$-BL was expressed in HEK293T cells and treated with 500 nM **BBD** for 3 h at 37°C. Samples were analyzed by Western blot. Primary antibody was anti-β-lactamase antibody. Secondary antibody was HRP-conjugated anti rabbit IgG.

HEK293T cells. (i) BL-tag (Cytosol) and HaloTag (Cytosol), (ii) $Lyn_{11}$-BL (plasma membrane) and Halo-EGFP (Cytosol), and (iii) BL-NLS (Nuclei) and Halo-EGFP (Cytosol) were coexpressed in living HEK293T cells. These cells were incubated with 500 nM **BHD** for 3 h, washed three times, and lysed with SDS sample buffer. The cell lysate was analyzed by western blotting. The proteins were detected by anti-β-lactamase and anti-HaloTag antibodies (Figure 3-2). Protein heterodimers were detected in cells treated with **BHD**. **BHD** can dimerize two proteins when the proteins are expressed in the same or different cell compartments.

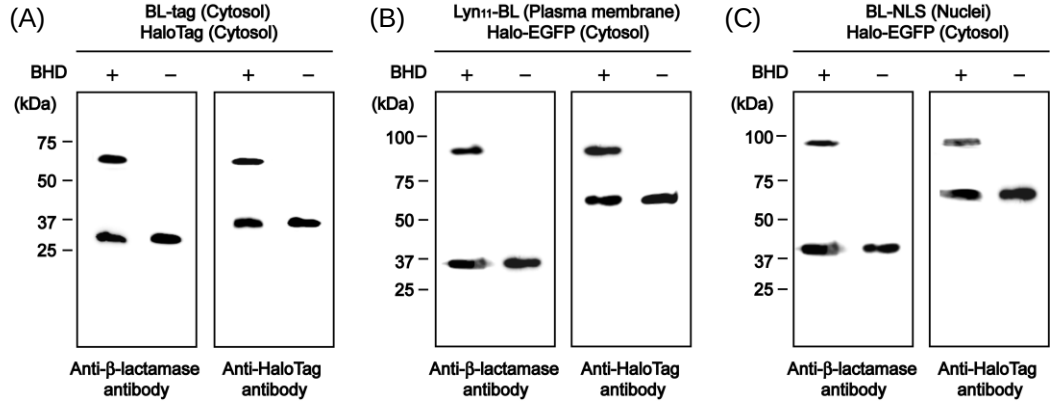


***Figure 3-2.*** Heterodimerization of BL-tag and HaloTag fusion proteins in HEK293T cells using **BHD**. (A) BL-tag and HaloTag, (B) $Lyn_{11}$-BL and Halo-EGFP, or (C) BL-NLS and Halo-EGFP were expressed in HEK293T cells and treated with 500 nM **BHD** for 3 h at 37°C. Samples were analyzed by western blotting. Primary antibody was anti-β-lactamase or anti-HaloTag antibody. Secondary antibody was HRP-conjugated anti rabbit IgG.

**Intercellular protein heterodimerization**

Intercellular protein heterodimerization was performed. HEK293T cells expressing BL-GPI or Halo-GPI were prepared and the cells were mixed. First, the cells were incubated with **RA**[8] and HaloTag R110Direct Ligand, washed three times, and analyzed by confocal fluorescence microscopy (Figure 3-3). Both the fluorescence of **RA** and HaloTag R110Direct Ligand was detected; some of the BL-GPI- and Halo-GPI-expressing cells were located next to each other.

Next, **BHD** was added to the culture dish containing cells expressing BL-GPI and Halo-GPI and incubated for 3 h. The cells were then washed three times and lysed with SDS sample buffer. The cell lysate was analyzed by western blotting and the proteins were detected by anti-β-lactamase or anti-HaloTag antibody (Figure 3-4). When both BL-GPI- and Halo-GPI-expressing cells were present in the same culture dish, protein heterodimers were detected. The expressed BL-GPI was cross-linked with Halo-GPI

expressed in adjoining cells. Based on this result, it is expected that this system can be applied in the detection of cell-cell interactions.

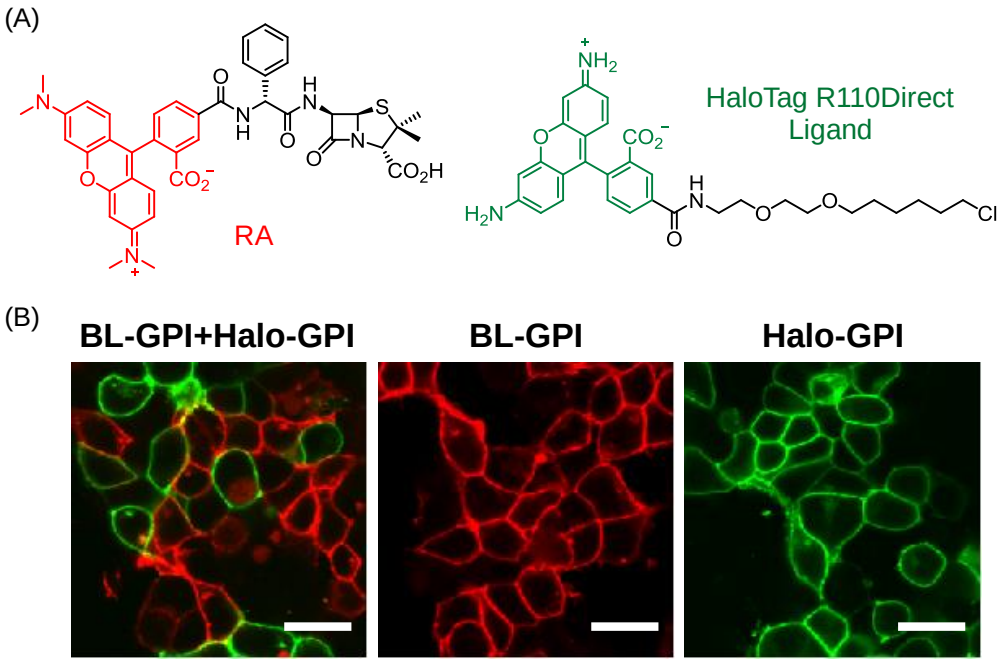


***Figure 3-3.*** (A) Structures of **RA** and HaloTag R110Direct Ligand. (B) Labeling of BL-GPI or Halo-GPI expressed in HEK293T cells. BL-GPI was labeled with **RA** (100 nM) and Halo-GPI was labeled with HaloTag R110Direct Ligand (100 nM) for 30 min at 37°C. HEK293T cells were cotransfected with a plasmid encoding BL-GPI and Halo-GPI. **RA**: excited at 559 nm; detected, 570–670 nm. HaloTag R110Direct Ligand: excited at 473 nm; detected, 490–540 nm. Scale bar 20 µm.

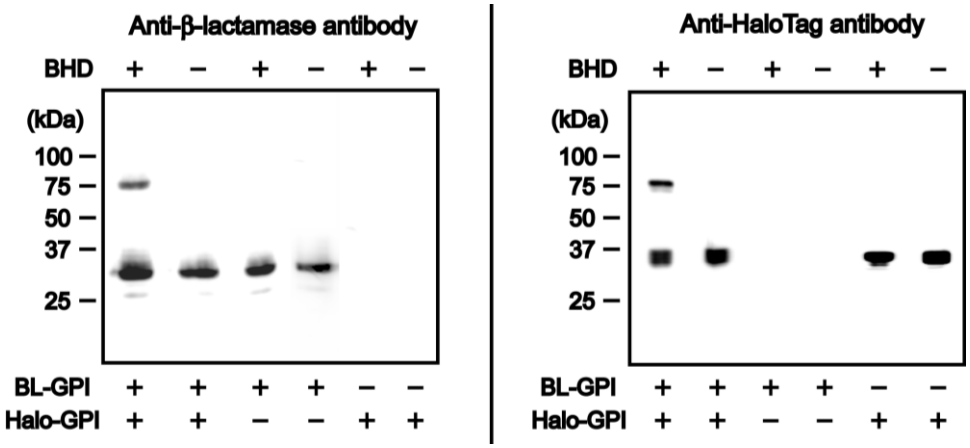


***Figure 3-4.*** **.** Intercellular heterodimerization of BL-GPI and Halo-GPI in HEK293T cells using **BHD**. BL-GPI and Halo-GPI were expressed in HEK293T cells and treated with 500 nM **BHD** for 3 h at 37°C. Samples were analyzed by western blotting. Primary antibody was anti-β-lactamase or anti-HaloTag antibody. Secondary antibody was HRP-conjugated anti rabbit IgG.

## Experimental Section

**Materials.** General chemicals for organic synthesis were of the highest grade available and were supplied by Tokyo Chemical Industries, Wako Pure Chemical, and Sigma-Aldrich. Chemicals were used without further purification. Bacampicillin hydrochloride was a kind gift from Nichi-Iko Phamaceutical Co. Ltd. Anti-β-lactamase antibody was purchased from Abcam (ab12251). Anti-HaloTag antibody was purchased from Promega (G9281). Horseradish peroxidase (HRP)-linked secondary antibody was purchased from GE Healthcare (anti-rabbit NA934, anti-mouse NA931). The pcDNA 3.1(+) vector was purchased from Invitrogen (21083-027). Restriction endonucleases and PrimeSTAR® HS DNA polymerase were purchased from Takara Bio, Inc. Plasmid DNA was isolated using a QIAprep Spin Miniprep kit (Qiagen). All labeling probes were dissolved in dimethyl sulfoxide (DMSO; biochemical grade; Wako Pure Chemical) to facilitate solubilization in aqueous solvents. Silica gel column chromatography was performed using BW-300 (Fuji Silysia Chemical, Ltd.). pkmcl-BL-GPI was a kind gift from Dr. Atsushi Miyawaki.

**Instruments.** NMR spectra were recorded on a JEOL JNM-AL400 instrument at 400 MHz for $^{1}H$ and at 100.4 MHz for $^{13}C$ nuclear magnetic resonance (NMR) using tetramethylsilane as an internal standard. Mass spectra were measured on a JEOL JMS-700 mass spectrometer for FAB and on a Waters LCT-Premier XE mass spectrometer for electrospray ionization.

## Synthesis of Compounds

**Synthesis of 10.** A solution of 4-pentynoic acid (14.7 mg, 0.150 mmol) was dissolved in anhydrous dimethylformamide (DMF; 2 mL), and then PyBOP (117 mg, 0.225 mmol) and TEA (30.2 mg, 0.298 mmol) were added under Ar. After 30 min of stirring at room temperature, bacampicillin hydrochloride (50 mg, 0.0998 mmol) was added and the reaction was continued for 8 h. The organic solvent was removed by evaporation and the residue was diluted with ethyl acetate and washed with 10% citric acid aq., sat. $NaHCO_3$ aq. and water. The organic layer was dried with brine and $Na_2SO_4$ and removed by evaporation. The residue was purified by flash column chromatography to yield compound **10** (53.2 mg, 0.0975 mmol, y. 65%). $^{1}H$ NMR (400 MHz, $CDCl_3$) $\delta$ 7.37 (d, 1H, 7.5 Hz), 7.31 (d, 1H, $J$ = 8.0 Hz), 7.14–7.04 (m, 5H), 6.77 (q, 1H, $J$ = 6.0 Hz), 5.69 (d, 1H, $J$ = 8.0 Hz), 5.61 (dd, 1H, $J$ = 7.5 Hz, 4.2 Hz), 5.42 (d, 1H, $J$ = 4.2 Hz), 4.34 (s, 1H), 4.23 (q, 2H, $J$ = 7.1 Hz), 2.03 (s, 1H), 2.57–2.47 (m, 4H), 1.57–1.46 (m,

9H), 1.27 (t, 3H, *J* = 7.1 Hz); $^{13}$C NMR (100 MHz, $CDCl_3$) $\delta$ 174.4, 173.9, 172.0, 168.1, 160.3, 134.9, 129.7, 129.2, 128.0, 97.3, 82.7, 78.8, 71.0, 68.9, 65.6, 64.4, 60.1, 60.0, 31.9, 30.2, 29.7, 18.3, 14.2; HRMS ($FAB^+$) *m/z*: 546.1982 (Calcd for $[M+H]^+$ 546.1904).

**Synthesis of BBD.** Compounds **9** (7.0 mg, 9.67 µM) and **10** (5.8 mg, 10.6 µM) were dissolved in a solvent mixture consisting of DMF (1.6 mL) and water (0.4 mL), and then sodium ascorbate (1.92 mg, 9.69 µmol) and $CuSO_4$ (1.55 mg, 9.71 µM) were added. The reaction was continued for 3 h at room temperature and the solvent was removed by evaporation. The product was purified by flash column chromatography to yield **BBD** (5.16 mg, 4.06 µmol, y. 42%). $^1$H NMR (400 MHz, $CDCL_3$) $\delta$ 7.96 (d, 1H, *J* = 7.6 Hz), 7.55 (s, 1H), 7.42–7.38 (m, 3H), 7.35–7.30 (m, 10H), 6.80–6.76 (m, 2H), 5.72 (dd, 1H, *J* = 7.8 Hz, 4.7 Hz), 5.62 (m, 2H), 5.48–5.41 (m, 2H), 4.42 (s, 1H), 4.34 (s, 1H), 4.28–4.18 (m, 5H), 3.80–3.54 (m, 16H), 3.50 (s, 2H), 3.04 (t, 2H, *J* = 5.2 Hz), 2.66 (t, 2H, *J* = 5.2 Hz), 1.58–1.51 (m, 18H), 1.36–1.30 (m, 6H); HRMS ($FAB^+$) *m/z*: 1270.4658 (Calcd for $[M+H]^+$ 1270.4642).

**Synthesis of 11.** A solution of 2-(2-aminoethoxy)ethanol (1.06 g, 10.0 mmol) was dissolved in anhydrous EtOH (20 mL), and then $Boc_2O$ (2.42 g, 11.1 mmol) was added at 0°C under Ar. After stirring at room temperature for 2 h, the reaction mixture was diluted with $CH_2Cl_2$ and washed with water. The organic solvent was dried with brine and $Na_2SO_4$. The organic solvent was removed by evaporation to yield compound **11** (1.97 g, 9.6 mmol, 96%). $^1$H NMR (400 MHz, $CDCl_3$) $\delta$ 5.07 (br, 1H), 3.74(m, 2H), 3.60 (m, 4H), 3.33 (m, 2H), 2.69 (s, 1H), 1.45 (s, 9H); $^{13}$C NMR (100 MHz, $CDCl_3$) $\delta$ 161.1, 77.5, 70.5, 70.0, 62.3, 41.5, 28.0; HRMS ($FAB^+$) *m/z*: 203.1321 (Calcd for $[M+H]^+$ 206.1386).

**Synthesis of 12.** Compound **11** (1.00 g, 4.87 mmol) was dissolved in tetrahydrofuran (THF; 10 mL) and DMF (5 mL) and then NaH (234 mg, 9.74 mmol) was added at 0°C. After stirring at 0°C for 30 min, 6-chloro-1-iodohexane (1.8 g, 7.3 mmol) was added drop-wise. The reaction mixture was stirred overnight and quenched with methanol and ice water. The mixture was extracted with ethyl acetate and washed with water. The organic layer was dried with brine and $Na_2SO_4$. The organic solvent was removed by evaporation and the product was purified by flash column chromatography to yield compound **12** (818 mg, 2.53 mmol, 52%). $^1$H NMR (400 MHz, $CDCl_3$) $\delta$ 5.06 (br, 1H), 3.62 (m, 2H), 3.55 (m, 6H), 3.47 (m, 2H), 3.33 (m, 2H), 1.78 (m, 2H), 1.62 (m, 2H), 1.55–1.32 (m, 4H), 1.43 (s, 9H); $^{13}$C NMR (400 MHz, $CDCl_3$) $\delta$ 161.5, 80.1, 71.0, 70.8, 70.6, 70.3, 70.1, 30.8, 45.6, 30.7, 28.7, 27.5, 25.1; HRMS ($FAB^+$) *m/z*: 324.1985 (Calcd for $[M+H]^+$ 324.1936).

**Synthesis of 13.** Compound **12** (300 mg, 0.928 mmol) was dissolved in 8 mL of $CH_2Cl_2$ and then TFA (822 µL) was added at 0°C. After stirring for 1 h, the solvent was removed and the residue was treated with $K_2CO_3$ (640 mg, 4.63 mmol) in MeOH (10 mL). The mixture was filtered and the filtrate was concentrated to yield compound **13** (128 mg, 0.575 mmol, 62%). $^1$H NMR (400 MHz, $CDCl_3$) $\delta$ 3.85–3.80 (m, 2H), 3.50–3.43 (m, 8H), 2.95–2.92 (m, 2H), 1.78–1.76 (m, 2H), 1.60–1.57 (m, 2H), 1.53–1.30 (m, 4H); $^{13}$C NMR (100 MHz, $CDCl_3$) $\delta$ 72.3, 71.2, 70.2, 67.2, 44.8, 40.0, 33.8, 30.1, 26.9, 25.5; HRMS (FAB$^+$) *m/z*: 224.1411 (Calcd for $[M+H]^+$ 224.1435).

**Synthesis of 14.** A solution of 4-pentynoic acid (81.3 mg, 0.829 mmol) was dissolved in anhydrous DMF (1 mL) and then PyBOP (647 mg, 1.25 mmol) and anhydrous TEA (207 mg, 2.05 mmol) were added under Ar. After 30 min of stirring at room temperature, compound **13** (124.12 mg, 0.554 mmol) was added and the reaction was continued for 6 h. The organic solvent was removed by evaporation and the residue was diluted with ethyl acetate and washed with 10% citric acid aq., sat. $NaHCO_3$ aq., water, and brine. The organic layer was dried with brine and $Na_2SO_4$ and concentrated by evaporation. The residue was purified by flash column chromatography to yield compound **14** (104.1 mg, 0.343 mmol, y. 62%). $^1$H NMR (400 MHz, $CDCl_3$) $\delta$ 5.10 (br, 1H), 3.65–3.63 (m, 2H), 3.53–3.48 (m, 6H), 3.43–3.42 (m, 2H), 3.35–3.33 (m, 2H), 2.79 (t, 1H, $J$ = 7.9 Hz), 2.39–2.37 (m, 2H), 2.35–2.34 (m, 2H), 1.75–1.72 (m, 2H), 1.65–1.64 (m, 2H), 1.54–1.32 (m, 4H); $^{13}$C NMR (100 MHz, $CDCl_3$) $\delta$ 173.3, 83.8, 71.7, 71.4, 70.9, 70.5, 69.5, 44.7, 41.3, 32.7, 31.2, 29.8, 26.7, 25.1, 18.5; HRMS (FAB$^+$) *m/z*: 304.1601 (Calcd for $[M+H]^+$ 304.1674).

**Synthesis of BHD.** Compounds **9** (30.5 mg, 42.1 µmol) and **14** (11.6 mg, 38.3 µmol) were dissolved in a solvent mixture consisting of DMF (1.6 mL) and water (0.4 mL) and then sodium ascorbate (7.58 mg, 38.3 µmol) and $CuSO_4$ (6.11 mg, 38.3 µmol) were added. The reaction was continued for 3 h at room temperature and the organic solvent was removed by evaporation. The residue was purified by flash column chromatography to yield **BHD** (16.2 mg, 15.8 µmol, 42%). $^1$H NMR (400 MHz, $CDCl_3$) $\delta$ 7.75 (s, 1H), 7.48–7.21 (m, 5H), 6.77 (q, 1H, $J$ = 5.1 Hz), 5.63(d, 1H, $J$ = 6.4 Hz), 5.56 (dd, 1H, $J$ = 3.8 Hz, 7.1 Hz), 5.44 (d, 1H, $J$ = 4.0 Hz), 4.72 (s, 1H), 4.36 (s, 1H), 4.26 (q, 2H, $J$ = 6.3 Hz), 3.86–3.62 (m, 14H), 3.54–3.33 (m, 8H), 2.41–2.31 (m, 4H), 1.72–1.65 (m, 4H), 1.56–1.35 (m, 15H), 1.25 (t, 3H, $J$=6.3); $^{13}$C NMR (100 MHz, $CDCl_3$) 174.5, 173.1, 172.0, 169.4, 168.6, 156.1, 134.0, 131.2, 129.1, 128.7, 127.5, 123.0, 97.6, 76.2, 72.1, 71.4, 71.3, 70.4, 70.3, 70.1, 69.8, 69.6, 69.3, 69.2. 65.7, 64.4, 61.0, 60.1, 53.3, 44.2, 41.1, 34.9, 31.8, 30.1, 29.7, 27.0, 26.9, 25.2, 18.4, 12.9; HRMS (FAB$^+$) *m/z*: 1025.4428 (Calcd for $[M+H]^+$ 1028.4411).

**Synthesis of RA.** The synthesis of this compound is described elsewhere.[8]

## Experimental Procedures

**Construction of the pcDNA3.1(+)-BL-tag, pcDNA3.1(+)-BL-EGFP and pcDNA3.1(+)-BL-NLS plasmids.** The plasmids were constructed as previously described.[9]

**Construction of pcDNA3.1(+)-HaloTag plasmid.** A DNA fragment of HaloTag was amplified from pFC14A-HaloTag by polymerase chain reaction (PCR) and digested with *Hind*III and *Nhe*I. The DNA fragment was ligated to pcDNA3.1(+), which was digested with the same restriction enzymes, to yield pcDNA3.1(+)-HaloTag.

**Construction of pcDNA3.1(+)-Halo-EGFP.** A DNA fragment of HaloTag was amplified from pFC14A-HaloTag by PCR and was digested with *Hind*III and *Nhe*I. The DNA fragment was ligated to pcDNA3.1(+)-BL-EGFP, which was digested with the same restriction enzymes, to yield pcDNA3.1(+)-Halo-EGFP.

**Construction of pkmcl-Halo-GPI.** A DNA fragment of HaloTag was amplified from pFC14A-HaloTag by PCR and was digested with *Eco*RI and *Hind*III. The DNA fragment was ligated to pkmcl-BL-GPI, which was digested with the same restriction enzymes, to yield pkmcl-Halo-GPI.

**Protein homodimerization in living cells with BBD.** HEK293T cells maintained in a 24-well plate with Dulbecco's modified Eagle medium (DMEM; Invitrogen) containing 10% fetal bovine serum (FBS) at 37°C under 5% $CO_2$ were transfected with a plasmid encoding Cytoplasmic-BL, BL-NLS, or BL-GPI, using Lipofectamine 2000 (Invitrogen). After 5 h, the culture medium was replaced with DMEM and the cells were incubated at 37°C for 20 h. Next, the cells were washed with phosphate-buffered saline (PBS) and incubated with **BBD** (500 nM) for 3 h at 37°C. The cells were washed with PBS three times and were lysed with 250 μL of 1× sodium dodecyl sulfate (SDS) sample buffer (50 mM Tris-HCl buffer (pH 6.8), 1.3% SDS, 10% glycerol, and 200 mM dithiothreitol). After scraping, the lysates were boiled at 95°C for 3 min. Subsequently, samples were electrophoresed on a 12% SDS-polyacrylamide gel and transferred to polyvinylidene fluoride (PVDF) membranes for western blot analysis. The membranes were blocked by 1 h incubation with Tris-buffered saline with Tween 20 (TBST) buffer (0.01% Tween 20, 138 mM NaCl, 20 mM Tris, pH 7.6) containing 2% skim milk at room temperature. Next, anti-β-lactamase (1:100 dilution) antibody was added to the membrane. After incubation for 14 h at 4°C with shaking, the membrane was washed three times with TBST buffer, incubated with HRP-linked secondary antibody

(anti-mouse;1:10,000 dilution), washed three times with TBST buffer, and visualized using ECL Prime Western Blotting Detection Reagent (GE Healthcare; RPN2232).

**Protein heterodimerization in living cells with BHD.** HEK293T cells maintained in a 24-well plate with DMEM containing 10% FBS at 37°C under 5% $CO_2$ were transfected with a pair of plasmids encoding BL-tag and HaloTag, $Lyn_{11}$-BL and Halo-EGFP, or BL-NLS and Halo-EGFP using Lipofectamine 2000. After 5 h, the culture medium was replaced with DMEM and the cells were incubated at 37°C for 20 h. Next, the cells were washed with PBS and incubated with **BHD** (500 nM) for 3 h at 37°C. The cells were washed with PBS three times and were lysed with 250 µL of 1× SDS sample buffer. After scraping, the lysates were boiled at 95°C for 3 min. Subsequently, samples were electrophoresed on a 12% SDS-polyacrylamide gel and transferred to PVDF membranes for western blot analysis. The membranes were blocked by 1 h incubation with TBST buffer containing 2% skim milk at room temperature. Anti-β-lactamase (1:100 dilution) or anti-HaloTag (1:1000 dilution) antibody was added to each membrane. After incubation for 14 h at 4°C with shaking, the membrane was washed three times with TBST buffer, incubated with HRP-linked secondary antibody (anti-mouse; 1:10,000 dilution), anti-rabbit (1:20,000 dilution), washed three times with TBST buffer, and visualized using ECL Prime Western Blotting Detection Reagent.

**Intercellular protein dimerization with BHD.** HEK293T cells maintained in 60-mm culture dishes with DMEM containing 10% FBS at 37°C under 5% $CO_2$ were transfected with a plasmid encoding BL-GPI or Halo-GPI using Lipofectamine 2000. After 5 h, the cells were washed once with PBS and scratched by trypsin/ethylenediamine tetraacetic acid. Cells transfected with BL-GPI and Halo-GPI were mixed at ratios of 1:1 and maintained in DMEM for 20 h at 37°C. Next, the cells were washed with PBS and incubated with **BHD** (500 nM) for 3 h at 37°C. The cells were washed with PBS three times and were lysed with 250 µL of 1× SDS sample buffer. After scraping, the lysates were boiled at 95°C for 3 min. Subsequently, samples were electrophoresed on a 12% SDS-polyacrylamide gel and transferred to PVDF membranes for western blot analysis. The membranes were blocked by 1 h incubation with TBST buffer containing 2% skim milk at room temperature. Next, anti-β-lactamase (1:100 dilution) or anti-HaloTag (1:1000 dilution) antibody was added to each membrane. After incubation for 14 h at 4°C with shaking, the membrane was washed three times with TBST buffer, incubated with HRP-linked secondary antibody (anti-mouse; 1:10,000 dilution), anti-rabbit (1:20,000 dilution), washed three times with TBST buffer, and visualized using ECL Prime Western Blotting Detection Reagent.

## References


1. G.V. Los, L.P. Encell, M.G. McDougall, D.D. Hartzell, N. Karassina, C. Zimprich, M.G. Wood, R. Learish, R.F. Ohana, M. Urh, D. Simpson, J. Mendez, K. Zimmerman, P. Otto, G. Vidugiris, J. Zhu, A. Darzins, D.H. Klaubert, R.F. Bulleit, K.V. Wood, *ACS Chem. Biol.* **2008**, *3*, 373–382.
2. A. Keppler, S. Gendreizig, H. Pick, H. Vogel, K. Johnsson, *Nat. Biotechnol.* **2003**, *21*, 86–89.
3. A. Gautier, A. Juillerat, C. Heinis, I.R. Corrêa Jr., M. Kindermann, F. Beaufils, K. Johnsson, *Chem. Biol.* **2008**, *15*, 128–136.
4. G. Lemercier, S. Gendreizig, M. Kindermann, K. Johnsson, *Angew. Chem. Int. Ed.* **2007**, *46*, 4281–4284.
5. A. Gautier, E. Nakata, G. Lukinavičius, K.T. Tan, K. Johnsson, *J. Am. Chem. Soc.* **2009**, *131*, 17954–17962.
6. B.A. Griffin, S.R. Adams, R.Y. Tsien, *Science* **1998**, *281*, 269–272.
7. A. Rutkowska, C.H. Haering, C. Shultz, *Angew. Chem. Int. Ed.* **2011**, *50*, 1–5.
8. S. Watanabe, S. Mizukami, Y. Hori, K. Kikuchi, *Bioconjugate Chem.* **2010**, *21*, 2320–2326.
9. S. Watanabe, S. Mizukami, Y. Akimoto, Y. Hori, K. Kikuchi, *Chem. Eur. J.* **2011**, *17*, 8342–8349.

## **Section 3.2.** Activation of Epidermal Growth Factor Receptor (EGFR)

As described in Section 3.1, the induction of protein dimerization with protein labeling systems and synthetic dimerizers was successful in living cells. In this section, activation of target protein and induction of signal transduction by protein dimerization is described.

Epidermal growth factor receptor (EGFR) was selected as a target protein. EGFR is a cell-surface receptor of members of the epidermal growth factor family (EGF-family).[1] EGFR regulates proliferation, motility, and growth in living cells.[2] The protein is activated by binding of its ligands such as epidermal growth factor (EGF). Upon activation by the ligands, EGFR forms an active homodimer and its intrinsic intracellular protein-tyrosine kinase activity is stimulated.[3] As a result, phosphorylation of several tyrosine (Y) residues at the C-terminal domain of EGFR occurs.[4] This phosphorylation activates downstream cell signaling by some other proteins whose tyrosine residue is phosphorylated.[5] This signaling modulates phenotypes such as cell proliferation[6] and membrane ruffling,[7] which are critical for cell motility. EGFR is activated by the formation of a homodimer; therefore, activation can be manipulated using BL-tag dimerizer system.

**Homodimerization of BL-EGFR**

First, induction of EGFR homodimerization was performed with **BBD** in living cells. BL-tag was fused to the N-terminus of EGFR (BL-EGFR) and expressed in CHO-K1 cells. CHO-K1 cells are suitable for studying EGFR function because of their low intrinsic expression of wtEGFR.[8] The cells were treated with **BBD** (20, 10, 5, 1, 0.5 μM), washed three times, and lysed with SDS sample buffer. The cell lysate was

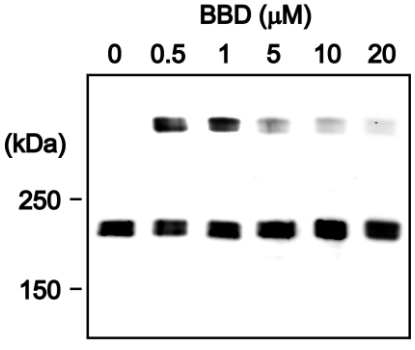


***Figure 3-5.*** Homodimerization of BL-tag-fused EGFR (BL-EGFR) in CHO-K1 cells using **BBD**. BL-EGFR was expressed in CHO-K1 cells and treated with 20, 10, 5, 1, 0.5 μM **BBD** for 1 h at 37°C. Samples were analyzed by western blot. Primary antibody was anti-EGFR antibody. Secondary antibody was HRP-conjugated anti-mouse IgG.

analyzed by western blotting and the protein was detected by anti-EGFR antibody (Figure 3-5). As a result, the EGFR homodimer was detected when the cells were treated with **BBD** (1 μM and 0.5 μM). When the cells were treated with higher concentrations of **BBD** (20, 10, 5 μM), the signal intensity of the homodimer was weak. This is because excess dimerizer decreases the crosslinking efficiency.

**Activation of EGFR by BBD**

When EGFR binds to its ligand, EGF, dimerization of the protein is induced followed by autophosphorylation of several tyrosine (Y) residues in the C-terminal domain of EGFR. This activates downstream signaling pathways, including the Ras/Raf/mitogen-activated protein kinase pathway, phosphatidylinositol 3-kinase (PI3K)/Akt pathway, and signal transduction and activator of transcription (STAT).[9] The author examined whether EGFR can be activated by dimerization from **BBD**.

BL-EGFR was expressed in CHO-K1 cells and the cells were incubated with **BBD** at 37°C for 30 min. Next, the cells were washed three times and lysed with SDS sample buffer. The cell lysate was analyzed by western blotting and detected by anti-EGFR antibody (Figure 3-6A). Moreover, phosphorylation of EGFR tyrosine 1197 (Y1197) was analyzed as an indicator of autophosphorylation. The phosphorylated protein was detected using a phosphorylated Y1197-specific antibody (pY1197). Stimulation of EGFR with **BBD** resulted in increased phosphorylation of Y1197 (Figure 3-6B). An increase of phosphorylation was detected only from cells containing dimerized EGFR.

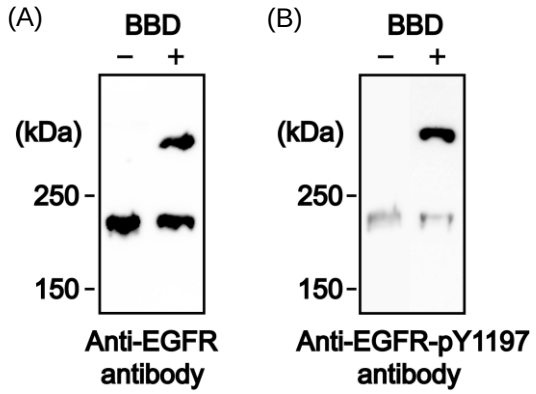


***Figure 3-6*** Homodimerization of BL-EGFR and induction of phosphorylation in CHO-K1 cells using **BBD**. BL-EGFR was expressed in CHO-K1 cells and treated with **BBD** (500 nM) for 30 min at 37°C. The samples were analyzed by western blotting. The proteins were detected by (A) anti-EGFR or (B) anti-EGFR-pY1197 antibody.

**Induction of EGFR internalization by BBD**

Ligand binding to EGFR is known to induce rapid internalization of the protein.[10] The event induced by ligand binding likely contributes to the regulation of ligand-induced EGFR internalization. These events include receptor dimerization, activation of intrinsic tyrosine kinase activity, and autophosphorylation of several

tyrosine residues. The author examined whether internalization of EGFR was induced by dimerization with **BBD**. BL-EGFR was expressed in CHO-K1 cells and incubated with **BBD** for 30 min at 37°C. Next, the cells were fixed and permeabilized, and EGFR was visualized using anti-EGFR antibody followed by fluorescein isiothiocyanate (FITC)-conjugated secondary antibody. The cells were observed using a confocal laser scanning microscope (Figure 3-7).

Fluorescence was detected only from the plasma membrane before stimulation with **BBD**. When the cells were incubated with **BBD**, several fluorescent vesicles were detected inside of cells and internalization of EGFR was detected. EGFR can be activated using BL-tag system and synthesized dimerizer **BBD**.

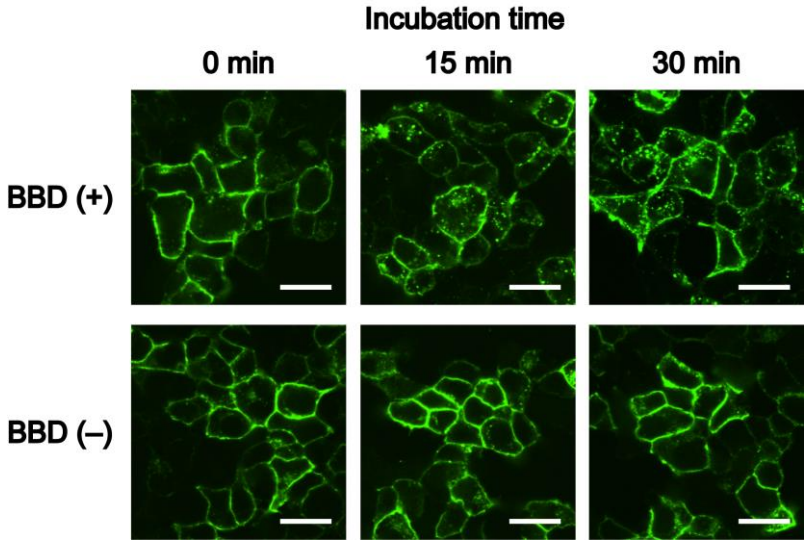


***Figure 3-7***. EGFR internalization after **BBD**-induced dimerization. BL-EGFR was expressed in CHO-K1 cells and treated with **BBD** (500 nM) for 30 min at 37°C. Localization of BL-EGFR was detected by immunostaining with anti-EGFR antibody. Scale bar: 20 μm.

### Induction of lamellipodia formation by BBD

Stimulation of EGFR by EGF leads to actin reorganization and the formation of lamellipodia, which are sheet-like plasma membrane protrusions formed by branched actin networks.[11] Therefore, the author examined whether lamellipodia formation was induced by dimerizing BL-EGFR and activating signal transduction by **BBD**. BL-EGFR was expressed in CHO-K1 cells and incubated with **BBD** for 30 min at 37°C. Next, F-actin was stained with TRITC-conjugated phalloidin, which binds F-actin and prevents its depolymerization and poisoning of the cell.[12] These events were evaluated using confocal fluorescence microscopy (Figure 3-8).

Lamellipodia formation was detected in cells expressing BL-EGFR when they were

stimulated with **BBD**. No significant lamellipodia formation was observed when the cells were not treated with **BBD**. This result indicates that dimerization of BL-EGFR by **BBD** activates EGFR and subsequent downstream cell signaling activation.

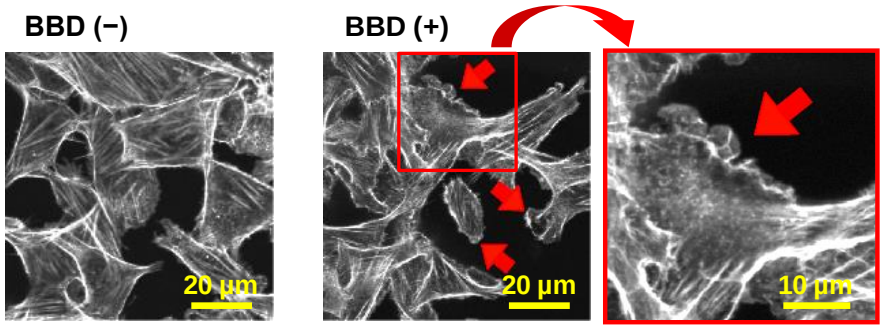


***Figure 3-8.*** Lamellipodia formations in BL-EGFR-expressing CHO-K1 cells induced by the treatment of **BBD** (500 nM) for 30 min at 37°C. F-actin was stained with TRITC-phalloidin. Arrows show representative lamellipodia.

## Cell migration assay in CHO-K1 cells

Activation of EGFR stimulates cell migration through the PI3K/Akt and STAT pathways.[13] The author examined whether cell migration and proliferation are induced by activation of EGFR with **BBD**. BL-EGFR was expressed in CHO-K1 cells and incubated in a culture dish, then partially scraped using a pipette tip. The cells were incubated with **BBD** for 24 h and then the culture medium containing **BBD** was changed. The cells were incubated for a further 24 h and cell migration was observed using confocal laser scanning microscopy (Figure 3-9).

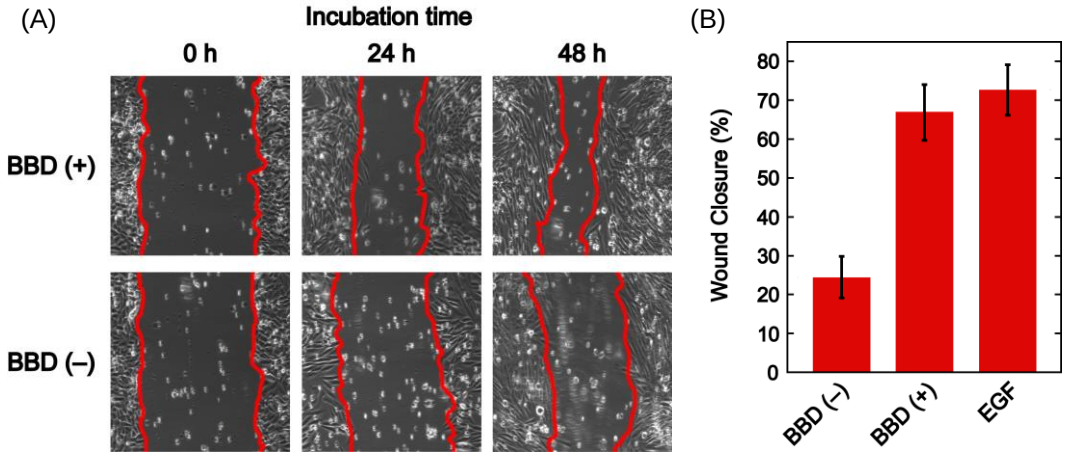


***Figure 3-9.*** (A) Migration of BL-EGFR-expressing CHO-K1 cells treated with 500 nM **BBD** for 48 h at 37°C, observed using an FV-10i confocal laser scanning microscope. (B) Average wound closure area of BL-EGFR-expressing CHO-K1 cells treated with **BBD** (500 nM) or EGF (100 ng/mL) for 48 h at 37°C. Average wound closure area during **BBD** stimulation was calculated using ImageJ software. Data are means ± S.E.M. of triplicate determinations from phase contrast images.

The area of the cells was increased with stimulation of **BBD**. Similar cell migration was observed when cells expressing wtEGFR were stimulated with EGF. Based on these results, the activation of EGFR can be controlled by **BBD**. For example, the system can be applied to the study of EGFR signaling pathways.

## Experimental Section

**Materials.** Anti-EGFR antibody was purchased from Abcam (ab2430); anti-EGFR-pY1197 antibody was purchased from DAKO (M7299). HRP-linked secondary antibody was purchased from GE Healthcare (anti-rabbit NA934, anti-mouse NA931). Fluorescein-conjugated goat anti-rabbit IgG was purchased from Calbiochem (401314). TRITC-conjugated phalloidin was purchased from Molecular Probes (R415). Plasmid DNA was isolated using a QIAprep Spin Miniprep kit (Qiagen). All dimerizers used were dissolved in DMSO (biochemical grade; Wako Pure Chemical) to facilitate solubilization in aqueous solvents.

## Experimental Procedures

**Construction of the pcDNA3.1(+)-BL-EGFR plasmids.** The plasmids were constructed as previously described.[14]

**Confocal laser scanning fluorescence microscopy.** Confocal fluorescence microscopic images were recorded using a confocal laser scanning microscope (Olympus; FLUOVIEW FV10i) equipped with a 60× lens. Fluorescein-conjugated goat anti-rabbit IgG was excited at 473 nm. TRITC-conjugated phalloidin was excited at 559 nm. The emission filter sets used were Olympus BA490–540 for fluorescein-conjugated goat anti-rabbit IgG and BA570–620 for TRITC-conjugated phalloidin.

**Homodimerization of EGFR in living cells with BBD.** CHO-K1 cells maintained in a 24-well plate with F-12 (Invitrogen) containing 10% FBS at 37°C under 5% $CO_2$ were transfected with a plasmid encoding BL-EGFR using Lipofectamine 2000 (Invitrogen). After 5 h, the culture medium was replaced with F-12 and the cells were incubated at 37°C for 20 h. Next, the cells were washed with PBS and incubated with **BBD** (500 nM, 1, 5, 10, or 20 μM) for 1 h at 37°C. The cells were washed with PBS three times and lysed with 250 μL of 1× SDS sample buffer (50 mM Tris-HCl buffer (pH 6.8), 1.3% SDS, 10% glycerol, and 200 mM dithiothreitol). After scraping, the lysates were boiled at 95°C for 3 min. Subsequently, samples were electrophoresed on a 7.5%

SDS-polyacrylamide gel and transferred to PVDF membranes for western blot analysis. The membranes were blocked by 1 h incubation with TBST buffer (0.01% Tween 20, 138 mM NaCl, 20 mM Tris, pH 7.6) containing 2% skim milk at room temperature. Anti-EGFR (1:500 dilution) antibody was added to the membrane. After incubation for 16 h at 4°C with shaking, the membrane was washed three times with TBST buffer, incubated with HRP-linked secondary antibody (anti-rabbit; 1:20,000 dilution), washed three times with TBST buffer, and visualized using ECL Prime Western Blotting Detection Reagent (GE Healthcare; RPN2232).

**Inducing EGFR autophosphorylation by BBD.** CHO-K1 cells maintained in F-12 containing 10% FBS at 37°C under 5% $CO_2$ were transfected with a plasmid encoding BL-EGFR using Lipofectamine 2000 (Invitrogen). After 5 h, the culture medium was replaced with F-12 and the cells were incubated at 37°C for 20 h. Next, the cells were washed with PBS and the culture medium was replaced with F-12 (FBS−) and incubated for 24 h at 37°C. The cells were washed with PBS and incubated with **BBD** (500 nM) for 1 h at 37°C. The cells were washed with PBS three times and lysed with 250 µL of 1× SDS sample buffer. After scraping, the lysates were boiled at 95°C for 3 min. Subsequently, samples were electrophoresed on a 7.5% SDS-polyacrylamide gel and transferred to PVDF membranes for western blot analysis. The membranes were blocked by 1 h incubation with TBST buffer containing 2% skim milk at room temperature. Anti-EGFR (1:500 dilution) or anti-EGFR-pY1197 (1:500 dilution) antibody was added to each membrane. After incubation for 16 h at 4°C with shaking, the membrane was washed three times with TBST buffer, incubated with HRP-linked secondary antibody (anti-rabbit; 1:20,000 dilution), anti-mouse (1:10,000), washed three times with TBST buffer, and visualized using ECL Prime Western Blotting Detection Reagent.

**Induction of EGFR internalization by BBD.** CHO-K1 cells maintained in glass-bottomed dish with F-12 containing 10% FBS at 37°C under 5% $CO_2$ were transfected with a plasmid encoding BL-EGFR using Lipofectamine 2000. After 5 h, the culture medium was replaced with F-12, and the cells were incubated at 37°C for 20 h. Next, the cells were washed with PBS and the culture medium was replaced with F-12 (−) and incubated for 24 h at 37°C. The cells were washed with PBS and incubated with **BBD** (500 nM) for 30 min at 37°C. The cells were then washed three times with PBS, fixed with 4% paraformaldehyde (Wako) at 4°C for 30 min, and treated with 0.5% Triton X-100 (Wako) in PBS at room temperature for 2 min. After three rinses with PBS, the cells were blocked with blocking buffer (PBS containing 3% bovine serum albumin (BSA)) at room temperature for 1 h. Anti-EGFR antibody, followed by

fluorescein-conjugated goat anti-mouse antibody was used to stain BL-EGFR. Microscopic images were acquired using a filter set for fluorescein.

**Induction of lamellipodia formation by BBD.** CHO-K1 cells were transfected with BL-EGFR using Lipofectamine 2000. After 5 h, the culture medium was replaced with F-12 and the cells were incubated at 37°C for 20 h. Next, the cells were washed with F-12 (−) medium and incubated with the medium for 24 h at 37°C. After two washings with F-12 (−) medium, the cells were treated with **BBD** (500 nM) in F-12 (−) medium for 30 min at 37°C under 5% $CO_2$. The cells were then washed three times with PBS, fixed with 4% paraformaldehyde at 4°C for 30 min, and treated with 0.5% Triton X-100 in PBS at room temperature for 2 min. The cellular F-actin was stained with phalloidin-TRITC (4.8 U/mL) for 1 h at room temperature, followed confocal fluorescence microscopy (FV-10i; Olympus) equipped with 60× objective.

**Cell migration assay.** CHO-K1 cells were transfected with BL-EGFR using Lipofectamine 2000. After 5 h, the culture medium was replaced with F-12 and the cells were incubated at 37°C for 20 h. Next, the cells were washed with F-12 (−) medium and incubated for 24 h at 37°C. A scratch wound was made using an MBP® 10 pipette tip (Molecular BioProducts). The cells were treated with **BBD** (500 nM) in F-12 (−) medium for 24 h at 37°C under 5% $CO_2$. The culture medium was then removed and the cells were treated with fresh medium dissolved with **BBD** for 24 h at 37°C under 5% $CO_2$. The cells were observed using an FV10i confocal scanning laser microscope (Olympus) equipped with a 10× objective before and after treatment with **BBD**. Cell migration was analyzed using ImageJ software.

## References


1. (a) R.S. Herbst, *Int. J. Radiation Oncology Biol. Phys.* **2004**, *59*, 21–26. (b) A. Bill, A. Schmitz, B. Albertoni, J.N. Song, L.C. Heukamp, D. Walrafen, F. Thorwirth, P.J. Verveer, S. Zimmer, L. Meffert, A. Schreiber, S. Chatterjee, R.K. Thomas, R.T. Ullrich, T. Lang, M. Famulok, *Cell* **2010**, *143*, 201–211. (c) E.R. Eden, I.J. White, C.E. Futter, *Biochem. Soc. Trans.* **2009**, *37*, 173–177.
2. (a) K.M. Ferguson, M.B. Berger, J.M. Mendrola, H.S. Cho, D.J. Leahy, M.A. Lemmon, *Mol. Cell* **2003**, *11*, 507 – 517. (b) J.P. Dawson, M.B. Berger, C.C. Lin, J. Schlessinger, M.A. Lemmon, K.M. Ferguson, *Mol. Cell. Biol.* **2005**, *25*, 7734–7742. (c) E.R. Eden, I.J. White, C.E. Futter, *Biochem. Soc. Trans.* **2009**, *37*, 173–177.
3. (a) A.W. Burgess, H.S. Cho, C. Eigenbrot, K.M. Ferguson, T.P. Garrett, D.J. Leahy, M.A. Lemmon, M.X. Sliwkowski, C.W. Ward, S. Yokoyama, *Mol. Cell* **2003**, *12*,

541–552. (b) C.M. Warren, R. Landgraf, *Cell. Signalling* **2006**, *18*, 923–933.

4. (a) J. Schlessinger, *Biochemistry*, **1988**, *27*, 3119–3123. (b) A. Ullrich, J. Schlessinger, *Cell* **1990**, *61*, 203–211.
5. (a) T. Pawson, *Nature* **1995**, *373*, 573–580. (b) J. Schlessinger, *Cell* **2000**, *103*, 211–225.
6. (a) G. Carpenter, S. Cohen, *Annu. Rev. Biochem.* **1979**, *48*, 193–216. (b) J. Schlessinger, A.B. Schreiber, A. Levi, I. Lax, T. Libermann, Y. Yarden, *CRC Crit. Rev. Biochem.* **1983**, *14*, 93–111.
7. (a) M. Chinkers, J.A. Mckanna, S. Cohen, *J. Cell Biol.* **1979**, *83*, 260–265. (b) M. Chinkers, J.A. Mckanna, S. Cohen, *J. Cell Biol.* **1981**, *88*, 422–429. (c) T. Kadowaki, S. Koyasu, E. Nishida, H. Sasaki, F. Takaku, I. Yahara, M. Kasuga, *J. Biol. Chem.* **1986**, *261*, 16141–16147.
8. (a) C. Puttikhunt, W. Kasinrerk, S. Srisa-ad, T. Duangchinda, W. Silakate, S. Moonsom, N. Sittisombut, P. Malasit, *J. Virol. Methods* **2003**, *109*, 55–61. (b) J. Yang, Z. Zhang, J. Lin, J. Lu, B. F. Liu, S. Zeng, Q. Luo, *Biochim. Biophys. Acta Mol. Cell Res.* **2007**, *1773*, 400–407.
9. M. Ono, M. Kuwano, *Clin. Cancer. Res.* **2006**, *12*, 7242–7251.
10. (a) Q. Wang, G. Villeneuve, Z. Wang, *EMBO Rep.* **2005**, 6, 942–948. (b) Z. Wang, L. Zhang, T. K. Yeung, X. Chen, *Mol. Biol. Cell* **1999**, *10*, 1621–1636.
11. (a) M. Nogami, M. Yamazaki, H. Watanabe, Y. Okabayashi, Y. Kido, M. Kasuga, T. Sasaki, T. Maehama, Y. Kanaho, *FEBS Lett.* **2003**, *536*, 71–76. (b) R.S. Dise, M.R. Frey, R.H. Whitehead, D.B. Polk, *Am. J. Physiol. Gastrointest. Liver Physiol.* **2008**, *294*, G276–G285.
12. A.M. Lengsfeld, I. Löw, T. Wieland, P. Dancker, W. Hasselbach, *Proc. Nat. Acad. Sci. U. S. A.* **1974**, *71*, 2803–2807.
13. (a) Y. Wang, S. Pennock, X. Chen, Z. Wang, *Mol. Cell. Biol.* **2002**, *22*, 7279–7290. (b) Y. Gan, C. Shi, L. Inge, M. Hibner, J. Balducci, Y. Huang, *Oncogene* **2010**, *29*, 4947–4958. (c) C.D. Andl, T. Mizushima, K. Oyama, M. Bowser, H. Nakagawa, A.K. Rustgi, *Am. J. Physiol. Gastrointest. Liver Physiol.* **2004**, *287*, G1227–G1237.
14. S. Mizukami, S. Watanabe, Y. Hori, K. Kikuchi, *J. Am. Chem. Soc.* **2009**, *131*, 5016–5017.

## **Section 3.3.** Light Regulation of EGFR Activity by Using Photoactivatable Dimerizer

In Section 3.2, induction of cell signaling from EGFR was shown to be successful by dimerization of the protein with the synthesized dimerizer. However, spatiotemporal activation of target proteins is impossible using this method. Spatiotemporal control of target proteins is an essential method for understanding various complex biological phenomena. Such inducible activation of target proteins may be spatially confined to a subcellular level if the dimerizer is activated and forms protein dimers in a small region of cells. Photocaging compounds are useful for releasing small molecules in a spatially and temporally controlled manner using light.[1] A photocaged compound is a small molecule whose activity is suppressed with a photocleavable protecting group known as a caging group. Light irradiation at an appropriate wavelength initiates a photochemical reaction that results in the removal of the caging group from the mother compound, leading to restoration of the original activity. Previously, control of protein function by ultraviolet (UV) light was reported to be successful in living cells using caged rapamycin.[2]

The author introduced a caging group onto BL-tag ligand and inhibited the labeling reaction of BL-tag. The carboxy group of the β-lactam molecule is important for the recognition of β-lactamase[3]; therefore, the labeling reaction of BL-tag may be suppressed by introducing a photocaging group at the carboxy group. Next, the photoactivatable dimerizer was developed using the caged β-lactam molecule and protein dimerization was regulated by light irradiation. Using the newly synthesized dimerizer, activation of EGFR was regulated by UV light irradiation and downstream cell signaling was activated.

**Design and synthesis of caged group-modified β-lactam molecule**

First, suppression of the labeling reaction was examined by introducing a caging group onto the carboxy group of the β-lactam molecule, which is important for recognition of β-lactamase. Two types of caging groups were introduced onto the β-lactam molecule: DEACM ([7-(diethylamino) coumarin-4-yl] methyl) and DMNB (4,5-dimethoxy-2-nitrobenzyl) groups (Scheme 3-4A).[4] Moreover, 6-carboxy-fluorescein was conjugated with the caged β-lactam molecules in order to evaluate whether the labeling reaction is inhibited. Two types of fluorescent probes

modified with a caging group, **FPA-Caged 1** and **2**, were designed (Scheme 3-4B). These caging groups can be removed by UV light irradiation. The molecules were synthesized according to Scheme 3-5.

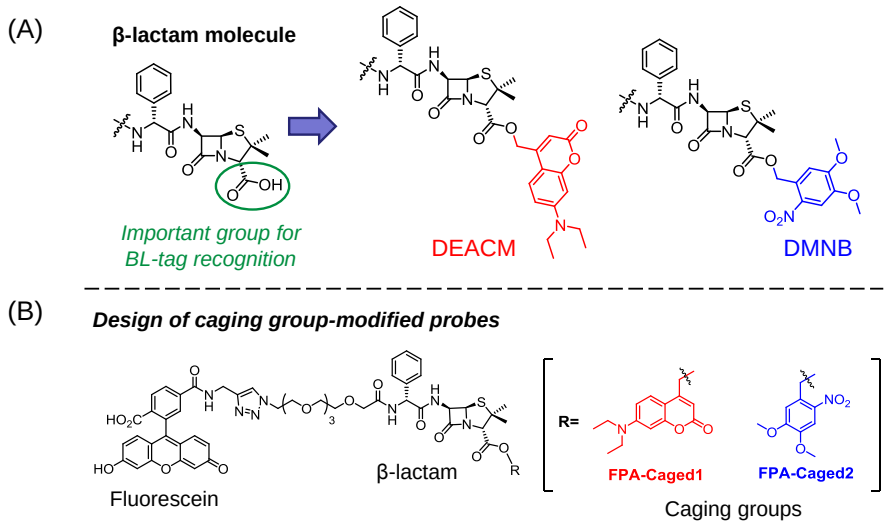


***Scheme 3-4.*** (A) Introduction of caging groups onto β-lactam molecule. (B) Structures of fluorescent probe with β-lactam modified with a caging group.

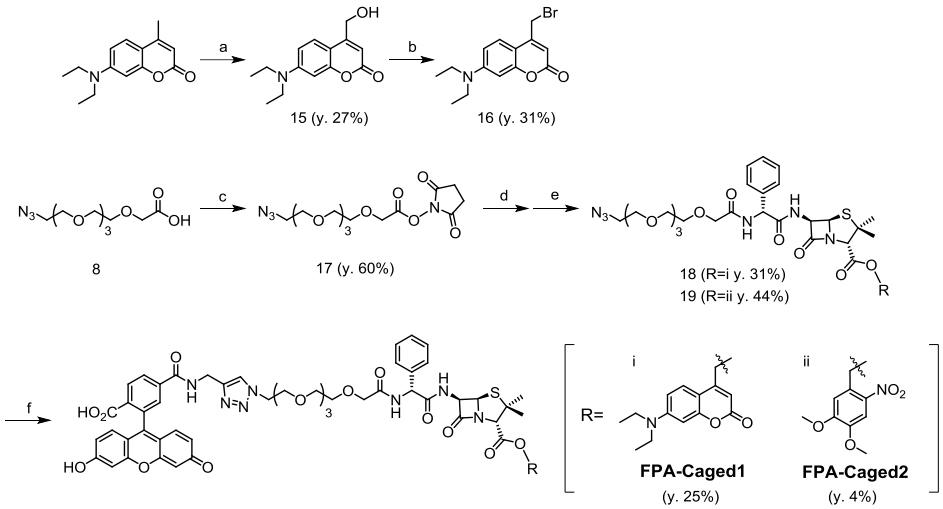


***Scheme 3-5.*** Synthetic scheme of **FPA-Caged 1** and **2**. (a) (i) $SeO_2$, *p*-xylene, (ii) $NaBH_4$, EtOH; (b) $PBr_3$, THF; (c) WSCD·HCl, *N*-hydroxysuccinimide, TEA, DMF; (d) ampicillin, TEA, DMF; (e) **FPA-Caged 1**: 4-bromomethyl-7-diethylaminocoumarin, TEA, DMF; **FPA-Caged 2**: 2,3-dimethoxy 5-nitrobenzene, TEA, DMF; (f) 6-carboxyfluorescein-alkyne, $CuSO_4$, sodium ascorbate, DMF/$H_2O$.

Absorption spectra, emission spectra, and fluorescence quantum efficiency of synthesized probes are shown in Figure 3-10. Based on the results, **FPA-Caged 1** is quenched by introduction of a caging group ($\Phi$ = 0.13). Uncaging of the synthesized probes was monitored with reversed-phase high-performance liquid chromatography (HPLC) (Figure 3-11). **FPA-Caged 1** or **2** was dissolved in HEPES buffer and irradiated

with UV light (365 ± 5 nm). Next, the sample was analyzed by reversed-phase HPLC. Both caging groups were removed by UV irradiation in 600 s. The uncaging reaction for **FPA-Caged 1** was more efficient than that of **FPA-Caged 2**.

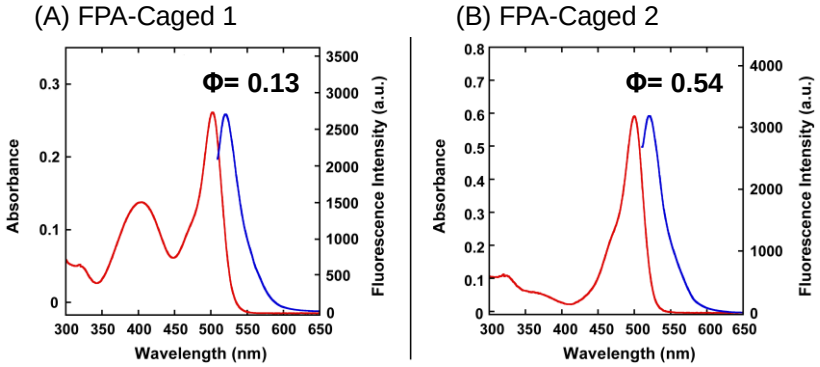


***Figure 3-10.*** Absorption spectra (red lines) and emission spectra (blue lines) of (A) **FPA-Caged 1** and (B) **2** in 100 mM HEPES buffer (pH 7.4). In the absorption measurements, the concentration of probes was 5 μM. In the fluorescence measurements, the concentration of probes was 0.5 μM. Excitation wavelengths were 499 nm. Fluorescence quantum efficiencies of the probes are shown in the graphs.

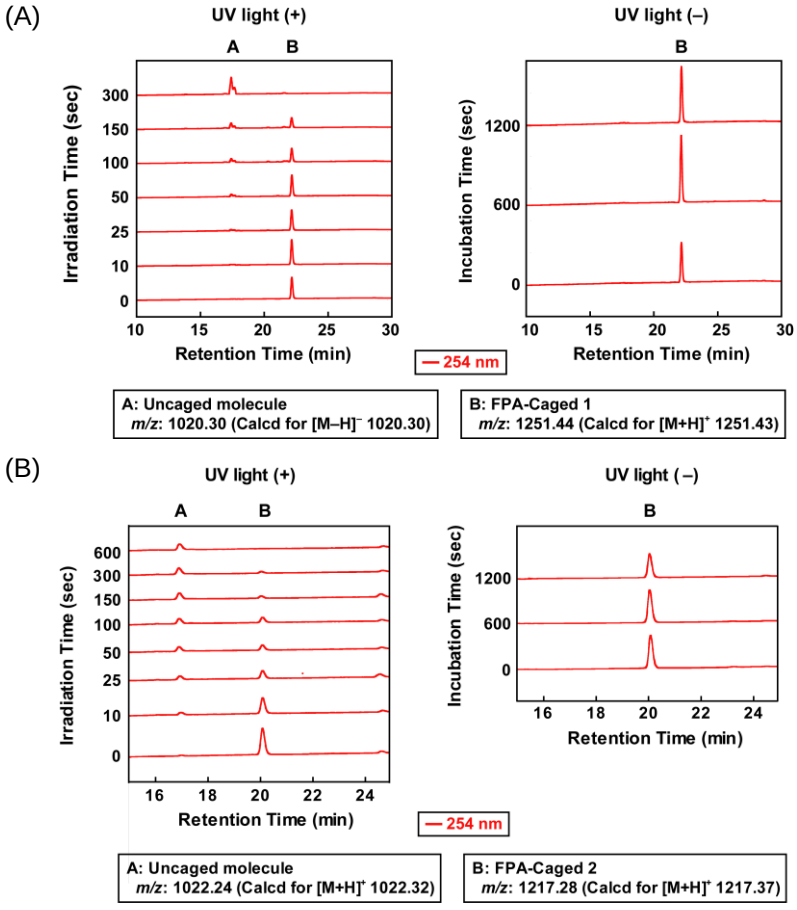


***Figure 3-11.*** Uncaging of (A) **FPA-Caged 1** and (B) **2**. Sample: 50 μM **FPA-Caged 1** or **2** in 100 mM HEPES buffer (pH 7.4). Uncaging light: 365 ± 5 nm. Intensity: 9.3 mW/cm$^2$. HPLC condition: 0.1% formic acid containing $H_2O$ and acetonitrile, 80/20 (v/v) (0 min) → 10/90 (v/v) (25 min), detected at 254 nm.

## SDS-PAGE analysis of FPA-Caged 1 and 2

Whether the labeling reaction of BL-tag is inhibited by introduction of a caging group was examined. The purified BL-tag was mixed with synthesized probes in HEPES buffer (pH 7.4) and was irradiated with UV light for 5 min. The sample was incubated for 30 min at room temperature and then analyzed by SDS-PAGE (Figure 3-12). When **FPA-Caged 1** was incubated with BL-tag, fluorescence was detected from both samples with and without UV light irradiation. Introduction of a DEACM group did not inhibit the labeling reaction of BL-tag. However, a fluorescence band was detected only when **FPA-Caged 2** was irradiated with UV light and incubated with BL-tag.

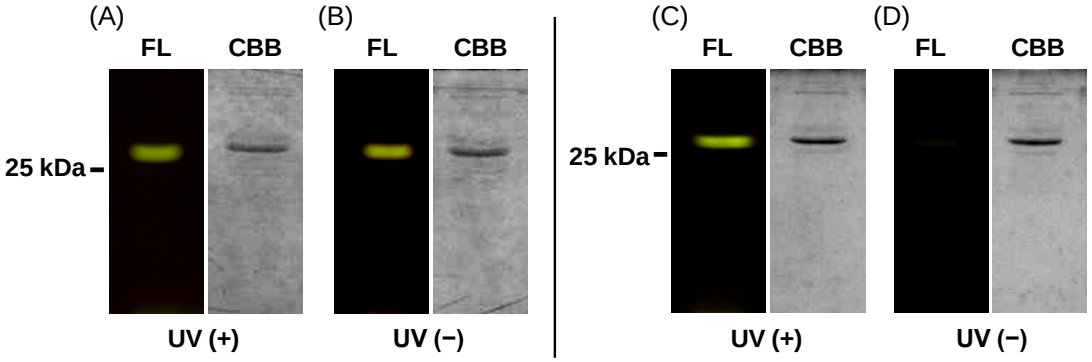


***Figure 3-12.*** SDS-PAGE analysis of labeling reactions of BL-tag with probes, **FPA-Caged 1** (A, B) and **2** (C, D). BL-tag (10 μM) and Probe (15 μM) were incubated at 37°C for 1 h. Fluorescence (left) and Coomassie Brilliant Blue (CBB)-stained (right) gel images of (A, B) BL-tag and **FPA-Caged 1**, (C, D) **FPA-Caged 2** and BL-tag. The samples were irradiated (A, C) with or (B, D) without UV light. Uncaging light: 365 ± 5 nm. Intensity: 9.3 mW/cm$^2$, Time: 5 min.

## Labeling of BL-EGFR expressed in living cells with FPA-Caged 1 and 2

Labeling of cell-surface proteins by **FPA-Caged 1** and **2** was performed in living cells. BL-EGFR was expressed in HEK293T cells and then **FPA-Caged 1** and **2** were irradiated with UV light for 5 min to remove the caging group. Uncaged compounds were incubated with BL-tag-expressing cells at 37°C for 30 min. The cells were washed three times and observed using a confocal fluorescence microscope.

When **FPA-Caged 1** was not irradiated with UV light, strong fluorescence was detected from the plasma membrane of the cells (Figure 3-13A). By contrast, fluorescence was detected only when **FPA-Caged 2** was irradiated with UV light (Figure 3-13B). Based on these results, the DMNB group can efficiently inhibit the labeling reaction of BL-tag. Thus, protein dimerization can be induced by UV light when a DMNB group is introduced onto the dimerizer.

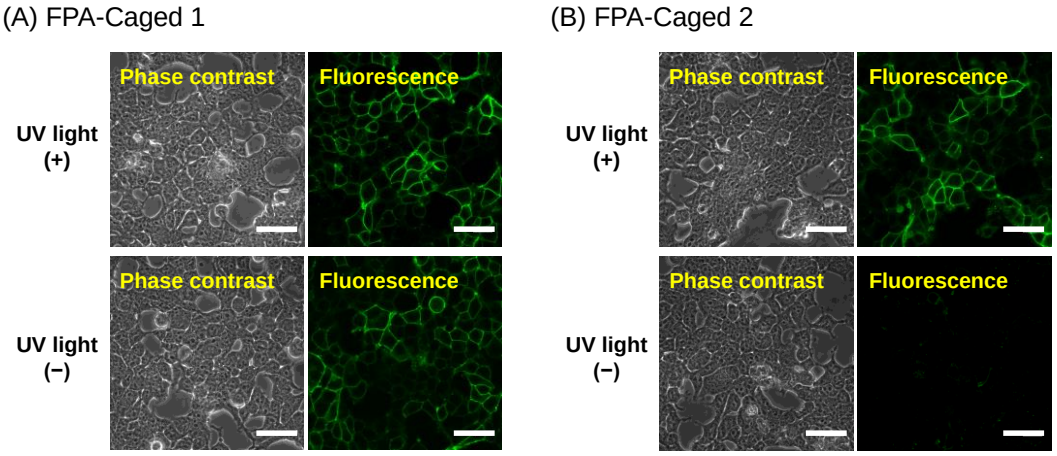


***Figure 3-13.*** Labeling of BL-tag-fused EGFR (BL-EGFR) with (A) **FPA-Caged 1** or (B) **FPA-Caged 2**. The cells were incubated with (A) 100 nM **FPA-Caged 1** or (B) 100 nM **FPA-Caged 2** at 37°C for 30 min with or without uncaging light. For fluorescence microscopic images, the cells were excited at 473 nm and detected at 490–590 nm. Scale bar: 40 μm. Uncaging light: 365 ± 5 nm. Intensity: 9.3 mW/cm$^2$.

## Design and synthesis of CBtBHD

The photoactivatable dimerizer **CBtBHD** was designed and synthesized (Scheme 3-6). This dimerizer has both BL-tag and HaloTag ligands and the carboxy group of the β-lactam molecule is modified with a DMNB group. Moreover, this molecule possesses biotin so that the molecule can be detected by western blotting using streptavidin-conjugated HRP.

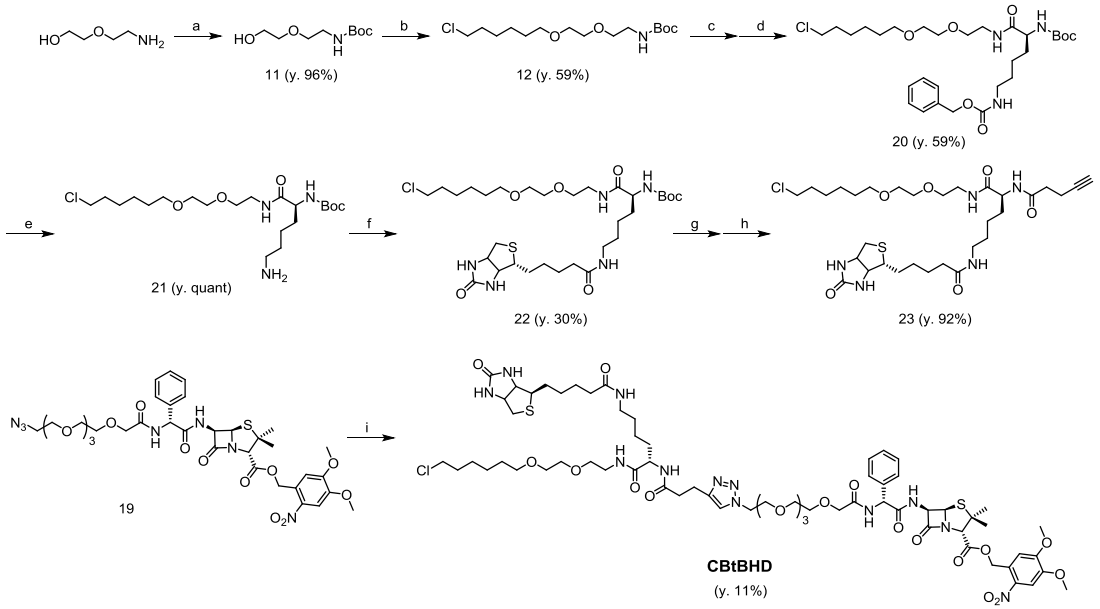


***Scheme 3-6.*** Synthetic scheme of **CBtBHD**. (a) $Boc_2O$, EtOH; (b) NaH, 6-chloro-1-iodohexane, DMF; (c) TFA, $CH_2Cl_2$; (d)Boc-Lys (Z), WSCD·HCl, HOBt, TEA, DMF; (e) $H_2$, Pd/C, MeOH; (f) biotin, WSCD·HCl, HOBt, TEA, DMF; (g) TFA, $CH_2Cl_2$; (h) 4-pentynoic acid, WSCD·HCl, HOBt, DMF; (i) **23**, $CuSO_4$, sodium ascorbate, DMF/$H_2O$.

Uncaging of **CBtBHD** by UV light irradiation was monitored by reversed-phase HPLC. **CBtBHD** (50 µM) was dissolved in HEPES buffer and irradiated with UV light (365 ± 5 nm) for 5 min. Next, the sample was analyzed using reversed-phase HPLC (Figure 3-14). The caging group was removed by UV light irradiation for 600 s.

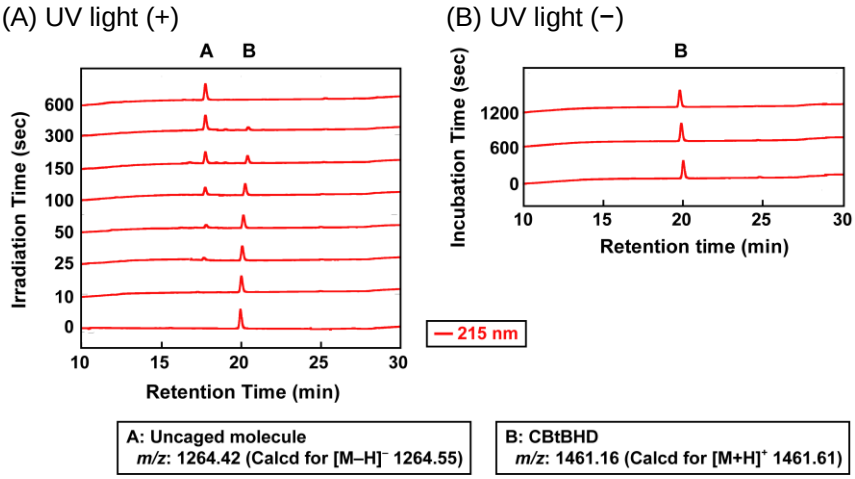


***Figure 3-14.*** Uncaging of **CBtBHD**. The compound was irradiated (A) with or (B) without UV light and analyzed with reversed-phase HPLC. Sample: 50 µM **CBtBHD** in 100 mM HEPES buffer (pH 7.4). Uncaging light: 365 ± 5 nm. Intensity: 9.3 mW/cm$^2$. HPLC condition: 0.1% formic acid containing $H_2O$ and acetonitrile, 80/20 (v/v) (0 min) → 10/90 (v/v) (25 min), detected at 215 nm.

## Induction of protein dimerization by UV light

Induction of protein dimerization was performed by **CBtBHD** and UV light irradiation in living cells. BL-GPI and Halo-GPI were coexpressed in HEK293T cells and **CBtBHD** was added. Next, the cells were irradiated with UV light for 5 min and incubated for 30 min at 37°C. The cells were lysed with SDS sample buffer and the cell lysate was analyzed by western blotting. The protein was detected by anti-β-lactamase antibody, anti-HaloTag antibody, or streptavidin-conjugated HRP (Figure 3-15). When the cells were irradiated with UV light, protein heterodimers were detected by the antibodies. Moreover, when the cells were not irradiated with UV light, a strong HaloTag protein signal was detected by streptavidin-conjugated HRP. This indicates that **CBtBHD** can bind only to HaloTag and that the labeling reaction of BL-tag was inhibited. Thus, induction of protein dimerization with **CBtBHD** can be regulated by UV light irradiation.

However, little dimerization was detected even when the cells were not irradiated with UV light. When **CBtBHD** was added to the cells, weak bands of BL-tag binding to the molecule were detected by streptavidin-conjugated HRP. This was because the

labeling reaction of BL-tag to **CBtBHD** was not completely inhibited. Protein dimerization efficiency was largely increased by UV light irradiation; therefore, the molecule can be applied for light regulation of protein function.

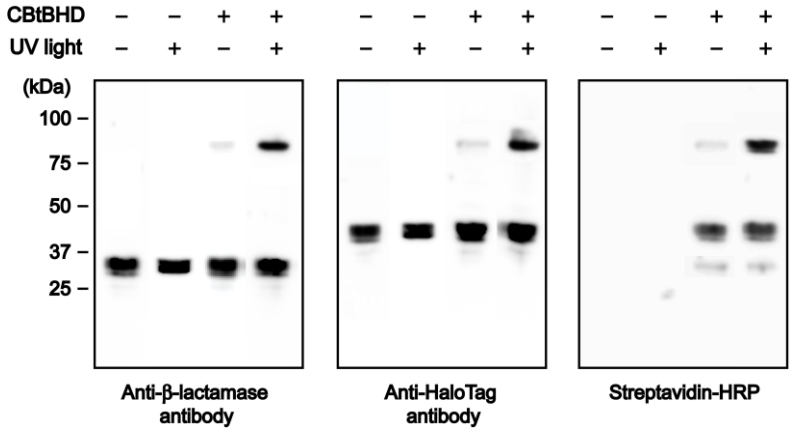


***Figure 3-15.*** Dimerization of BL-GPI and Halo-GPI in HEK293T cells using **CBtBHD** and UV light irradiation. BL-GPI and Halo-GPI were coexpressed in HEK293T cells and treated with 500 nM **CBtBHD** for 30 min at 37°C. Next, the cells were irradiated with UV light followed by incubation for 30 min. Samples were analyzed by western blotting. Primary antibody was anti-β-lactamase, anti-HaloTag antibody, or streptavidin-conjugated HRP. Secondary antibody was HRP-conjugated anti rabbit IgG. UV light: 365 ± 5 nm. Intensity: 9.3 mW/cm$^2$, Time: 5 min.

**EGFR dimerization induced by UV light**

Induction of EGFR dimerization was performed by **CBtBHD** and UV irradiation. BL-EGFR and EGFR fused to the C-terminus of HaloTag (Halo-EGFR) were coexpressed in CHO-K1 cells. Next, **CBtBHD** was added and incubated for 30 min followed by UV irradiation for 5 min. The cells were incubated for 30 min again and lysed with SDS sample buffer. The cell lysate was analyzed by western blotting. The

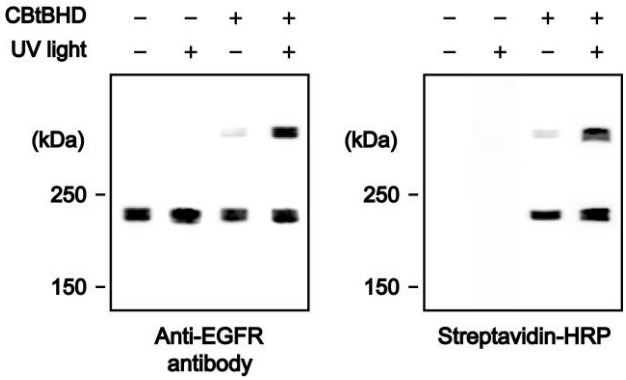


***Figure 3-16.*** Dimerization of BL-EGFR and Halo-EGFR in CHO-K1 cells using **CBtBHD** and UV light irradiation. BL-GPI and Halo-GPI were coexpressed in CHO-K1 cells and treated with 500 nM **CBtBHD** for 30 min at 37°C. Next, the cells were irradiated with UV light followed by incubation for 30 min. Samples were analyzed by western blotting. Primary antibody was anti-EGFR antibody or streptavidin-conjugated HRP. Secondary antibody was HRP-conjugated anti mouse IgG.

proteins were detected with anti-EGFR or streptavidin-conjugated HRP (Figure 3-16). The protein dimer of EGFR was detected when the cells were incubated with **CBtBHD** and irradiated with UV light.

**Activation of EGFR by UV light**

When EGFR binds to its ligand, EGF, dimerization of the protein is induced, followed by autophosphorylation of several tyrosine (Y) residues in the C-terminal domain of EGFR.[5] This activates downstream signaling pathways as described in Section 3.2. Whether EGFR can be activated by **CBtBHD** and UV light irradiation was examined. BL- and Halo-EGFR were coexpressed in CHO-K1 cells and **CBtBHD** was added. The cells were incubated for 30 min followed by UV light irradiation for 5 min. The cells were incubated at 37°C for 30 min again, washed three times, and lysed with SDS sample buffer. The cell lysate was analyzed by western blotting and the protein was detected with anti-EGFR antibody (Figure 3-17A). Furthermore, phosphorylation of EGFR tyrosine 1197 (Y1197) was detected by using a phosphorylated Y1197-specific antibody (anti-EGFR-pY1197) (Figure 3-17B). Phosphorylation of EGFR Y1197 was increased by **CBtBHD** and UV light irradiation. Increased phosphorylation was detected only from dimerized EGFR. A very weak phosphorylation signal was detected when the cells were incubated with the dimerizer without UV light irradiation. In addition, activation of EGFR by the photoactivatable dimerizer and UV light was successful.

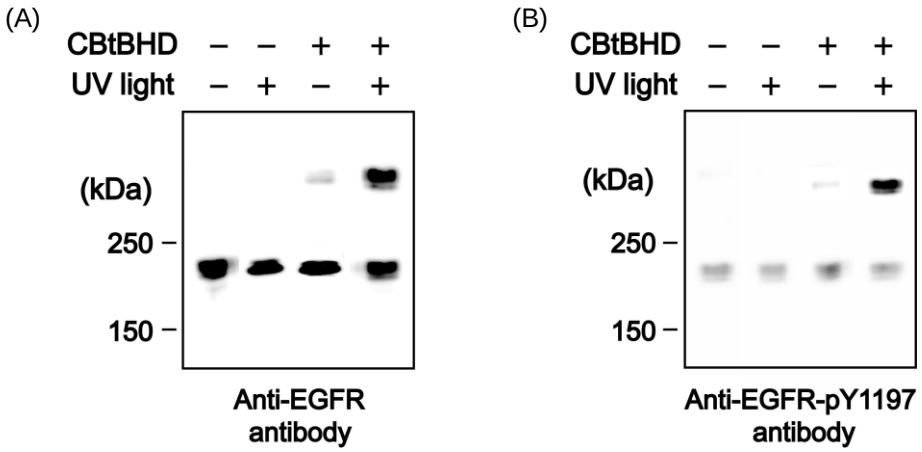


***Figure 3-17***. Dimerization of EGFR and induction of phosphorylation in CHO-K1 cells using **CBtBHD** and UV light irradiation. BL-EGFR and Halo-EGFR were expressed in CHO-K1 cells and treated with **CBtBHD** (500 nM) for 30 min at 37°C. Next, the cells were irradiated (A) with or (B) without UV light, followed by incubation for 30 min. The samples were analyzed by western blotting. Primary antibody was anti-EGFR or anti-EGFR-pY1197 antibody. Secondary antibody was HRP-conjugated anti mouse IgG.

## Induction of EGFR internalization by light

In living cells, ligand binding to EGFR induces rapid internalization of the protein.[6] These events include receptor dimerization, activation of intrinsic tyrosine kinase activity, and autophosphorylation of several tyrosine residues.[5] The author examined whether internalization of EGFR was induced by dimerization with **CBtBHD** and UV light irradiation. BL- and Halo-EGFR was coexpressed in CHO-K1 cells, after which **CBtBHD** was added. The cells were incubated for 30 min followed by UV light irradiation for 5 min. The cells were incubated for 30 min again. The cells were fixed with paraformaldehyde, permeabilized with Triton X-100, and EGFR was visualized using anti-EGFR antibody followed by FITC-conjugated secondary antibody. The cells were observed using confocal laser scanning microscopy (Figure 3-18).

Fluorescence was detected only from the plasma membrane when the cells were not irradiated with UV light. By contrast, many fluorescent vesicles were detected inside of cells, indicating internalization of EGFR when cells were irradiated by UV light.

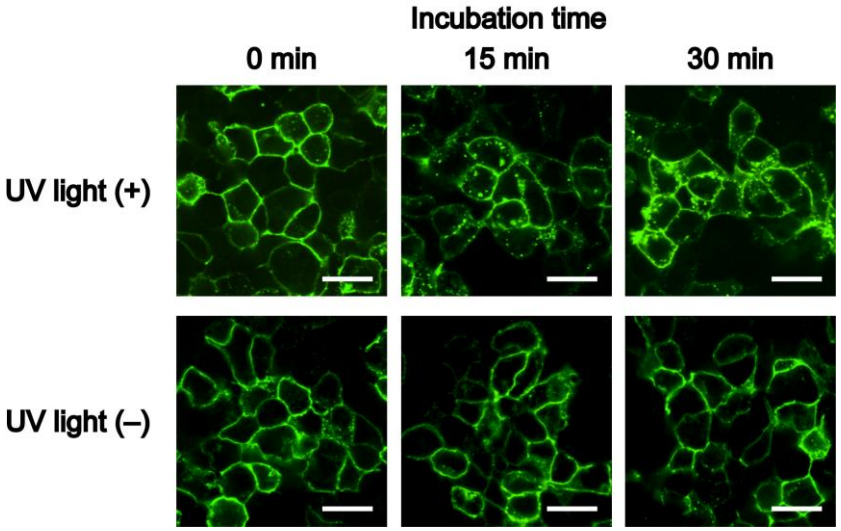


***Figure 3-18***. EGFR internalization after **CBtBHD**-induced dimerization. BL- and Halo-EGFR were coexpressed in CHO-K1 cells and treated with **CBtBHD** (500 nM) for 30 min at 37°C. Next, the cells were irradiated with UV light followed by incubation for 30 min. The localization of EGFR was detected by immunostaining. Primary antibody was anti-EGFR antibody. Secondary antibody was FITC-conjugated anti mouse IgG. Scale bar: 20 μm.

## Induction of lamellipodia formation by UV light irradiation

Stimulation of EGFR by EGF leads to actin reorganization and the formation of lamellipodia, which are sheet-like plasma membrane protrusions formed by branched actin networks.[7] Therefore, the author examined whether lamellipodia formation is induced by dimerizing BL- and Halo-EGFR and activating the signal transduction by

**CBtBHD** and UV light irradiation. BL- and Halo-EGFR were coexpressed in CHO-K1 cells, after which **CBtBHD** was added. Next, the cells were incubated for 30 min followed by UV light irradiation. The cells were incubated for 30 min again, washed three times, fixed with paraformaldehyde, and permeabilized with Triton X-100. Finally, F-actin was stained with TRITC-conjugated phalloidin and analyzed by confocal fluorescence microscopy.

Lamellipodia formation was detected from the cells irradiated with UV light (Figure 3-19). By contrast, no significant lamellipodia formation was observed when the cells were not irradiated with UV light. Thus, downstream cell signaling from EGFR can be activated by UV light irradiation with the photoactivatable dimerizer.

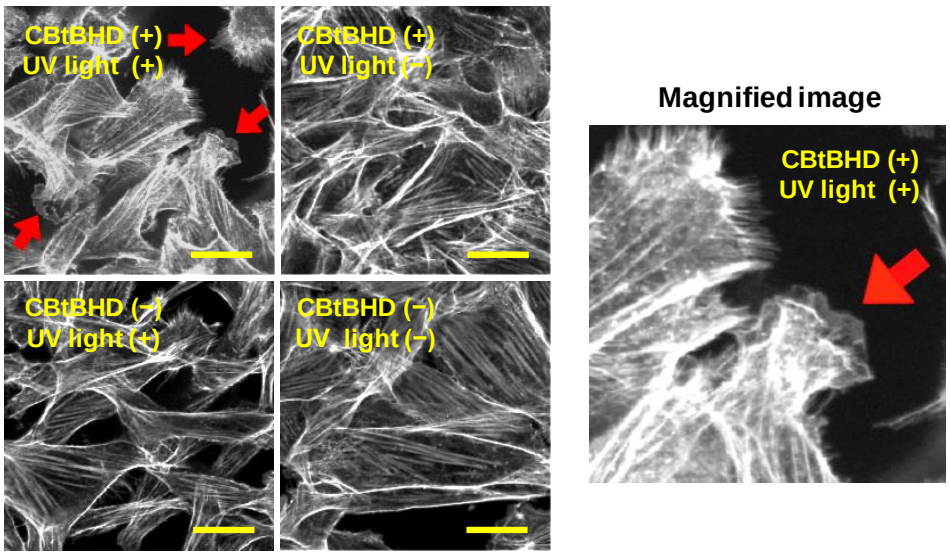


***Figure 3-19***. Lamellipodia formations in BL- and Halo-EGFR-expressing CHO-K1 cells induced by the treatment with **CBtBHD**. The cells were irradiated with UV light for 5 min followed by incubation for 30 min at 37°C. The cells were fixed and permeabilized, and then F-actin was stained with phalloidin-TRITC. Arrows shows representative lamellipodia (sheet-like plasma membrane protrusions formed by actin reorganization). Scale bar: 20 μm.

**Cell migration assay induced by UV light irradiation**

Activation of EGFR stimulates cell migration through the PI3K/Akt and STAT pathways.[8] The author examined whether cell migration can be induced by **CBtBHD** and UV irradiation. BL- and Halo-EGFR were cotransfected into CHO-K1 cells. Next, the cells were incubated under serum-starved conditions for 24 h and were partially scraped using a pipette tip. **CBtBHD** was added and the cells were incubated for 30 min followed by UV light irradiation for 5 min. Next, the cells were incubated for 48 h and cell migration was observed using a confocal laser scanning microscope (10× lens, phase contrast image). The decrease in wound area by cell migration was analyzed using a scratch assay (Figure 3-20). After treatment with **CBtBHD** and UV irradiation,

an approximately 3-fold decrease in wound closure area was observed compared to that of cells that had not been irradiated with UV light. There was no significant difference in the wound closure area between non-treated cells and **CBtBHD**-treated cells. Activation of EGFR and signal transduction can be induced only by UV light irradiation. However, a small amount of cell migration was detected from non-treated cells. This is because BL-EGFR was overexpressed in the cells and a slight amount of EGFR activation was induced without the dimerizer and UV light irradiation. Moreover, the wound closure area of cells irradiated with UV light (without **CBtBHD** treatment) was slightly smaller than that of non-treated cells. Thus, some cells were damaged by UV light irradiation.

Based on these results, local activation of EGFR may be achieved using the system presented in this thesis. This method is applicable for studying intercellular communication by stimulation of target proteins expressed in a cell.

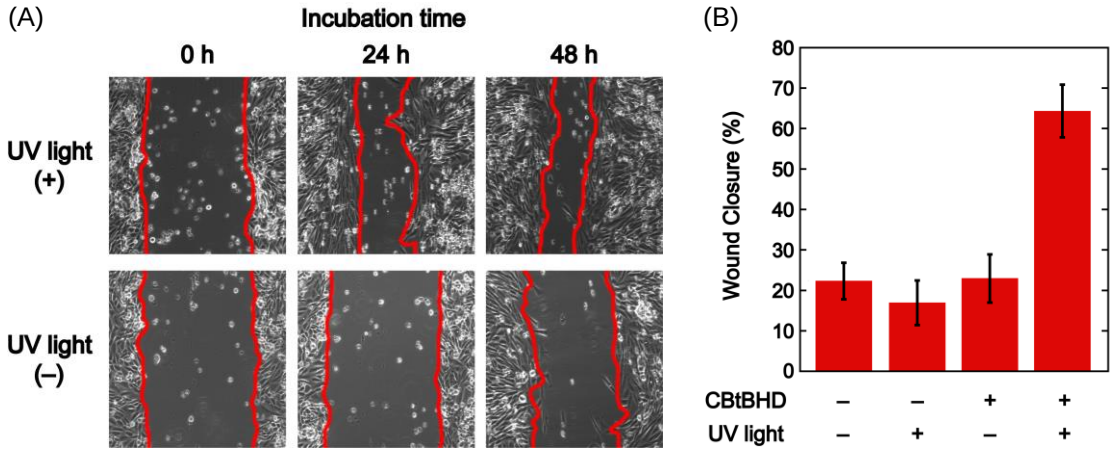


***Figure 3-20.*** (A) Migration of BL- and Halo-EGFR-expressing CHO-K1 cells treated with 500 nM **CBtBHD** for 30 min at 37°C. Then, the cells were irradiated with UV light followed by incubation for 48 h at 37°C. The cells were observed using an FV-10i confocal laser scanning microscope. (B) Average wound closure area of BL- and Halo-EGFR-expressing CHO-K1 cells treated with **CBtBHD** (500 nM) and irradiated with UV light. Average wound closure area during **CBtBHD** stimulation was calculated using ImageJ software. Data are means ± S.E.M. of triplicate determinations from phase contrast images.

## Experimental Section

**Materials.** General chemicals for organic synthesis were of the highest grade available and were supplied by Tokyo Chemical Industries, Wako Pure Chemical, and Sigma-Aldrich. Chemicals were used without further purification. Anti-β-lactamase antibody was purchased from Abcam (ab12251). Anti-HaloTag antibody was purchased

from Promega (G9281). Streptavidin-conjugated horseradish peroxidase (HRP) was purchased from Thermo Scientific (21130). Anti-EGFR antibody was purchased from Abcam (ab2430) and anti-EGFR-pY1197 antibody was purchased from DAKO (M7299). HRP-linked secondary antibody was purchased from GE Healthcare (anti-rabbit NA934, anti-mouse NA931). Fluorescein-conjugated goat anti-rabbit IgG was purchased from Calbiochem (401314). TRITC conjugated phalloidin was purchased from Life Technologies (R415). Plasmid DNA was isolated using a QIAprep Spin Miniprep kit (Qiagen). All labeling probes and dimerizers were dissolved in DMSO (biochemical grade; Wako Pure Chemical) to facilitate solubilization in aqueous solvents. Silica gel column chromatography was performed using BW-300 (Fuji Silysia Chemical, Ltd.). pFN21A-Halo-EGFR was purchased from Promega.

**Instruments.** NMR spectra were recorded on a JEOL JNM-AL400 instrument at 400 MHz for $^{1}H$ and at 100.4 MHz for $^{13}C$ NMR using tetramethylsilane as an internal standard. Mass spectra were measured on a JEOL JMS-700 mass spectrometer for FAB and on a Waters LCT-Premier XE mass spectrometer for electrospray ionization. Uncaging of synthesized compounds was performed using UV light (9.3 mW/cm$^2$) with an Asahi Spectra MAX-302 xenon lamp and a band path filter (250–385 nm).

## Synthesis of Compounds

**Synthesis of 15.** 4-Methyl-7-diethylaminocoumarin (1.00 g, 4.33 mmol) was dissolved in *p*-xylene (200 mL) and $SeO_2$ (957 mg, 8.62 mmol) was added. The reaction mixture was refluxed under vigorous stirring under Ar. After 24 h, the mixture was cooled to room temperature, filtered using a pad of celite, and the organic solvent was removed by evaporation. The residue was dissolved in anhydrous EtOH (200 mL), after which $NaBH_4$ (80.8 mg, 2.14 mmol) was added at 0°C. The reaction mixture was stirred at room temperature for 3 h under Ar. Next, the suspension was carefully neutralized with 2N HCl aq., diluted with water, and ethanol was removed by evaporation. The mixture was extracted with $CH_2Cl_2$ and washed with water, then dried with brine and $Na_2SO_4$. The organic solvent was removed by evaporation and the product was purified using flash column chromatography to yield compound **15** (310 mg, 1.17 mmol, y. 27%). $^{1}H$ NMR (400 MHz, $CDCl_3$) $\delta$ 7.31 (d, 1H, $J$ = 8.5 Hz), 6.56 (dd, 1H, $J$ = 8.5 Hz, 2.1 Hz), 6.52 (d, 1H, $J$ = 2.1 Hz), 6.25 (s, 1H), 4.83 (s, 2H), 3.40 (q, 4H), 1.20 (t, 6H); $^{13}C$ NMR (100 MHz, $CDCl_3$) $\delta$ 162.8, 156.7, 155.5, 149.7, 125.1, 108.8, 105.7, 104.9, 98.0, 61.9, 44.7, 12.5; HRMS (FAB$^+$) *m/z*: 266.0950 (Calcd for $[M+H]^+$: 266.0942).

**Synthesis of 16.** Compound **15** (48.8 mg, 0.197 mmol) was dissolved in anhydrous

THF (8 mL) and $PBr_3$ (107 mg, 0.394 mmol) was added at 0°C. The reaction mixture was stirred at room temperature under Ar. After 6 h, the reaction mixture was neutralized with 10% $Na_2CO_3$ aq. and extracted with ethyl acetate. Next, the organic layer was washed with water and dried with brine and $Na_2SO_4$. The organic solvent was removed by evaporation and the product was purified by flash column chromatography to yield compound **16** (18.9 mg, 0.0611 mmol, y. 31%). $^1$H NMR (400 MHz, $CDCl_3$) $\delta$ 7.49 (d, 1H, $J$ = 8.5 Hz), 6.62 (dd, 1H, $J$ = 8.5 Hz, 2.5 Hz), 6.51 (d, 1H, $J$ = 2.5 Hz), 6.14 (s, 1H), 4.40 (s, 2H), 3.42 (q, 4H), 1.21 (t, 6H); $^{13}$C NMR (100 MHz, $CDCl_3$) $\delta$ 161.3, 155.4, 154.7, 149.2, 124.8, 109.8, 107.8, 103.8, 98.5, 48.7, 43.1, 12.3; HRMS ($FAB^+$) *m/z*: 310.0464 (Calcd for $[M+H]^+$: 310.0437).

**Synthesis of 17.** Compound **8** (300 mg, 1.08 mmol) and *N*-hydroxysuccinimide (249 mg, 2.16 mmol) were dissolved in anhydrous DMF (5 mL) and then WSCD·HCl (414 mg, 2.16 mmol) was added at 0°C. The mixture was stirred at 0°C for 6 h under Ar. The organic solvent was removed by evaporation and the residue was dissolved in ethyl acetate. The organic layer was washed with 10% citric acid aq. and water and dried with brine and $Na_2SO_4$. The organic solvent was removed by evaporation to yield compound **17** (242 mg, 0.648 mmol, y. 60%). $^1$H NMR (400 MHz, $CDCl_3$) $\delta$ 4.32–4.18 (m, 4H), 3.71–3.55 (m, 14H), 3.42–3.30 (m, 2H), 2.86 (s, 4H); $^{13}$C NMR (100 MHz, $CDCl_3$) $\delta$ 172.1, 170.8, 72.3, 71.5, 70.8, 70.7, 70.2, 69.6, 67.7, 62.3, 26.6; HRMS ($FAB^+$) *m/z*: 375.1534 (Calcd for $[M+H]^+$: 375.1510).

**Synthesis of 18.** Ampicillin (280 mg, 0.802 mmol) was dissolved in anhydrous DMF (5 mL) and then TEA (162 mg, 1.60 mmol) and compound **17** (200 mg, 0.535 mmol) were added at 0°C. The mixture was stirred for 16 h under Ar and then the organic solvent was removed by evaporation. The residue was dissolved in ethyl acetate and washed with 10% citric acid aq., sat. $NaHCO_3$ aq. and water and was dried with brine and $Na_2SO_4$. The organic solvent was removed by evaporation. The residue was dissolved in anhydrous DMF (5 mL) and then TEA (108 mg, 1.07 mmol) and 4-bromomethyl-7-diethylaminocoumarin (248 mg, 0.803 mmol) were added. The mixture was stirred for 5 h under Ar and then organic solvent was removed by evaporation. The residue was dissolved in ethyl acetate and washed with sat. $NaHCO_3$ aq. and water, and then dried with brine and $Na_2SO_4$. The organic solvent was removed by evaporation and the product was purified by flash column chromatography to yield compound **18** (139 mg, 0.1166 mmol, y. 31%). $^1$H NMR (400 MHz, $CDCl_3$) $\delta$ 7.93(dd, 1H, 8.5, 2.4 Hz), 7.42–7.35 (m, 5H), 6.72 (d, 1H, $J$ = 8.5 Hz), 6.58 (d, 1H, $J$ = 2.4 Hz), 6.52 (s, 1H), 5.65 (d, 1H, $J$ = 6.4 Hz), 5.59 (dd, 1H, $J$ = 3.8 Hz, 9.3 Hz), 5.50 (d, 1H, $J$ = 4.0 Hz), 4.50 (s, 1H), 4.06 (s, 2H), 3.72–3.61 (m, 18H), 3.41 (q, 4H), 1.56 (s, 3H), 1.45

(s, 3H), 1.21 (t, 3H); $^{13}$C NMR (100 MHz, $CDCl_3$) $\delta$ 174.3, 171.5, 168.9, 168.6, 160.8, 156.4, 154.2, 150.1, 147.3, 135.2, 131.5, 130.2, 126.8, 125.4, 112.5, 106.8, 97.8, 77.5, 72.3, 71.2, 70.9, 70.5, 70.1, 69.7, 65.5, 64.4, 65.5, 60.9, 60.4, 47.1, 30.4, 29.7, 18.5, 13.7, 12.7; HRMS ($FAB^+$) *m/z*: 838.3445 (Calcd for $[M+H]^+$: 838.3440).

**Synthesis of 19.** Ampicillin (280 mg, 0.802 mmol) was dissolved in anhydrous DMF (5 mL) and then TEA (162 mg, 1.60 mmol) and compound **17** (200 mg, 0.535 mmol) were added at 0°C. The mixture was stirred for 16 h under Ar and then organic solvent was removed by evaporation. The residue was dissolved in ethyl acetate and washed with 10% citric acid aq., sat. $NaHCO_3$ aq. and water, and then was dried with brine and $Na_2SO_4$. The organic solvent was removed by evaporation. The residue was dissolved in anhydrous DMF (5 mL) and then TEA (108 mg, 1.07 mmol) and 2, 3-dimethoxy-5-nitrobenzene (220 mg, 0.803 mmol) were added. The mixture was stirred for 10 h under Ar. The organic solvent was removed by evaporation. The residue was dissolved in ethyl acetate and washed with sat. $NaHCO_3$ aq. and water and then dried with brine and $Na_2SO_4$. The organic solvent was removed by evaporation and the product was purified by flash column chromatography to yield compound **19** (189 mg, 0.235 mmol, y. 44%). $^1$H NMR (400 MHz, $CDCl_3$) $\delta$ 7.93 (s, 1H), 7.80–7.71 (m, 2H), 7.40–7.28 (m, 6H), 5.68–5.41 (m, 5H), 4.43 (s, 1H), 3.90 (s, 3H), 3.80 (s, 3H), 3.78–3.50 (m, 18H), 1.55 (s, 3H), 1.46 (s, 3H); $^{13}$C NMR (100 MHz, $CDCl_3$) $\delta$174.4, 172.5, 171.0, 169.7, 155.7, 143.2, 140.0, 134.7, 129.4, 128.7, 128.4, 127.4, 127.3, 120.1, 79.0, 72.1, 71.8, 70.6, 70.4, 70.3, 70.1, 70.0, 69.6, 69.5, 64.4, 63.7, 60.1, 60.0, 56.8, 29.9, 28.1; HRMS ($FAB^+$) *m/z*: 804.2896 (Calcd for $[M+H]^+$: 804.2868).

**Synthesis of FPA-Caged 1.** Compound **18** (18.0 mg, 0.0215 mmol) and 6-carboxyfluorescein-alkyne (13.3 mg, 0.0322 mmol) were dissolved in a solvent mixture consisting of DMF (1.6 mL) and water (0.4 mL), and then sodium ascorbate (6.40 mg, 0.0322 mmol) and $CuSO_4$ (5.2 mg, 0.0322 mmol) were added. The reaction was continued for 6 h at room temperature and the solvent was removed by evaporation. The product was purified by flash column chromatography to yield **FPA-Caged 1** (6.48 mg, 5.18 µmol, y. 25%). $^1$H NMR (400 MHz, $CDCl_3$) $\delta$ 10.1 (s, 2H), 8.34 (d, $J$ = 8.4 Hz, 1H), 8.28 (d, $J$ = 8.4 Hz, 1H), 7.75 (s, 1H), 7.54 (d, 1H, $J$ = 8.5 Hz), 7.52 (a, 1H), 7.40-7.29 (m, 5H), 6.75 (d, 2H, $J$ = 2.1 Hz), 6.65 (dd, 1H, $J$ = 8.5 Hz, 2.0 Hz), 6.60 (d, 2H, $J$ = 8.5 Hz), 6.56 (dd, 2H, $J$ = 8.5, 2.1 Hz), 6.51 (d, 1H, $J$ = 2.0 Hz), 6.07 (s, 1H), 5.53 (d, 1H, $J$ = 6.4 Hz), 5.44 (dd, 1H, $J$ = 3.8 Hz, 9.3 Hz), 5.28 (d, 1H, $J$ = 4.0 Hz), 4.53 (s, 1H), 4.40 (s, 2H), 4.12 (s, 2H), 3.59–3.37 (m, 22H), 1.49 (s, 3H), 1.38 (s, 3H), 1.14 (t, 6H); $^{13}$C NMR (100 MHz, $CDCl_3$) $\delta$ 174.4, 172.1, 171.0, 169.5, 169.0, 167.5, 159.7, 155.6, 155.3, 152.4, 150.7, 148.8, 147.1, 139.5, 134.0, 130.7, 130.4, 13.3, 129.7,

129.0, 128.1, 126.7, 125.7, 123.8, 122.7, 111.0, 110.7, 109.1, 108.8, 107.4, 104.7, 98.1, 83.1, 77.0, 71.9, 71.1, 70.7, 70.3, 70.1, 70.0, 69.6, 69.3, 64.5, 62.0, 61.2, 50.4, 52.8, 46.1, 43.7, 29.7, 28.8, 13.7; HRMS ($FAB^+$) *m/z*: 1251.4358 (Calcd for $[M+H]^+$ 1251.4339).

**Synthesis of FPA-Caged 2.** Compound **19** (111 mg, 0.138 mmol) and 6-carboxyfluorescein-alkyne (57.3 mg, 0.138 mmol) were dissolved in a solvent mixture consisting of DMF (1.6 mL) and water (0.4 mL), and then sodium ascorbate (41.1 mg, 0.207 mmol) and $CuSO_4$ (33.1 mg, 0.207 mmol) were added. The reaction was continued for 6 h at room temperature and the solvent was removed under vacuum. The product was purified by reversed-phase HPLC and eluted with $H_2O$/acetonitrile containing 0.1% formic acid to yield **FPA-Caged 2** (6.48 mg, 5.33 μmol, y. 4%). $^1H$ NMR (400 MHz, $CDCl_3$) $\delta$ 10.2 (s, 2H), 9.23–9.28 (m, 2H), 8.20 (d, 1H, $J$ = 7.6 Hz), 8.09–8.06 (m, 2H), 7.90 (s, 1H), 7.71 (d, 2H), 7.41–7.27 (m, 6H), 6.69 (s, 2H), 6.60–6.54 (m, 4H), 5.75 (d, 1H, $J$ = 8.4 Hz), 5.56–5.43 (m, 4H), 4.46 (s, 1H), 4.43 (s, 1H), 3.90–3.42 (m, 24H), 1.51 (s, 3H), 1.36 (s, 3H); $^{13}C$ NMR (100 MHz, $CDCl_3$) $\delta$174.2, 173.2, 172.1, 169.8, 168.8, 168.0, 167.0, 164.4, 159.7, 153.1, 151.8, 148.3, 144.3, 140.1, 137.9, 128.3, 126.9, 124.8, 123.4, 122.9, 112.5, 109.2, 108.3, 102.2, 72.2, 72.5, 71.7, 71.2, 70.4, 70.0, 69.6, 69.5, 69.4, 69.3, 68.7, 67.2, 64.8, 63.9, 60.7, 58.2, 56.4, 56.3, 56.1, 54.7, 52.4, 51.4, 49.2, 34.9, 29.8, 26.4; HRMS ($FAB^+$) *m/z*: 1217.3784 (Calcd for $[M+H]^+$ 1217.3768).

**Synthesis of 20.** Compound **12** (85.0 mg, 0.263 mmol) was dissolved in $CH_2Cl_2$ (2 mL) and then TFA (233 μL) was added at 0°C. The mixture was stirred for 3 h at 0°C and then the solvent was removed by evaporation. The residue was dissolved in anhydrous DMF. Boc-Lys (Z) (120 mg, 0.289 mmol), TEA (78.0 mg, 0.771 mmol), WSCD·HCl (74.0 mg, 0.386 mmol), and HOBt (52.0 mg, 0.385 mmol) were added to the solution at 0°C. The mixture was stirred under Ar for 6 h, after which the organic solvent was removed by evaporation and the residue was dissolved in ethyl acetate and washed with sat. $NaHCO_3$ aq., 10% citric acid aq. and water. The sample was dried with brine and $Na_2SO_4$. The organic solvent was removed by evaporation and the residue was purified by flash column chromatography to yield compound **20** (90.8 mg, 0.155 mmol, y. 59%). $^1H$ NMR(400MHz, $CDCl_3$) $\delta$ 7.42-7.31 (m, 5H), 6.53 (br, 1H), 5.12 (br, 1H), 5.09 (s, 2H), 4.91 (br, 1H), 4.04 (m, 1H), 3.59–3.41 (m, 12H), 2.80 (t, $J$ = 7.2 Hz), 1.72–1.58 (m, 14H), 1.43 (s, 9H); $^{13}C$ NMR (100 MHz, $CDCl_3$) $\delta$ 172.0, 161.1, 136.7, 128.4, 127.8, 127.0, 80.1, 70.8, 70.4, 70.2, 69.1, 67.0, 57.3, 45.5, 41.3, 40.0, 32.1, 29.9, 29.3, 28.4, 27.0, 26.7, 25.1, 21.7; HRMS ($FAB^+$) *m/z*: 586.3268 (Calcd for $[M+H]^+$ 586.3254).

**Synthesis of 21.** Compound **20** (52.8 mg, 90.3 μmol) was dissolved in MeOH (5 mL)

and Pd-C (15.5 mg) was added. The mixture was stirred at room temperature under $H_2$ for 3 h. After filtration using a pad of celite, the organic solvent was removed by evaporation to yield compound **21** (40.8 mg, y. quant.). $^1$H NMR (400 MHz, $CDCl_3$) $\delta$ 6.98 (br, 1H), 5.29 (br, 1H), 4.55 (t, 2H, $J$ = 6.8 Hz), 4.11 (m, 1H), 3.58–3.42 (m, 12H), 2.79 (t, $J$ = 7.2 Hz), 1.82–1.60 (m, 14H), 1.42 (s, 9H); $^{13}$C NMR (100 MHz, $CDCl_3$) $\delta$ 171.9, 160.2, 80.7, 71.0, 70.6, 70.2, 70.0, 68.9, 45.6, 43.1, 41.2, 31.9, 30.3, 28.9, 28.6, 26.9, 26.8, 25.0, 23.6; HRMS ($FAB^+$) *m/z*: 452.2807 (Calcd for $[M+H]^+$ 452.2886).

**Synthesis of 22.** Biotin (33.3 mg, 0.136 mmol) was dissolved in anhydrous DMF (3 mL) and WSCD·HCl (34.9 mg, 0.182 mmol), HOBt (24.6 mg, 0.182 mmol) and TEA (36.8 mg, 0.364 mmol) were added. Next, compound **21** (41.1 mg, 0.0909 mmol) was added to the reaction mixture and the mixture was stirred under Ar for 8 h. The organic solvent was removed by evaporation and the residue was dissolved in ethyl acetate. The organic solvent was washed with sat. $NaHCO_3$ aq., 10% citric acid aq. and water, and then dried with brine and $Na_2SO_4$. The organic solvent was removed by evaporation and the residue was purified by flash column chromatography to yield compound **22** (18.5 mg, 0.0273 mmol, y. 30%). $^1$H NMR (400 MHz, $CDCl_3$) $\delta$ 6.60 (br, 1H), 6.40 (s, 1H), 5.95 (s, 1H), 5.44 (s, 1H), 4.52 (m, 1H), 4.31 (m 1H), 4.10 (m, 1H), 3.78–3.38 (m, 14H), 3.35–3.16 (m, 4H), 2.02 (t, 2H, $J$ = 7.6 Hz), 1.69–1.21 (m, 29H); $^{13}$C NMR (100 MHz, $CDCl_3$) $\delta$ 172.6, 171.3, 165.6, 160.0, 81.1, 71.3, 70.3, 70.0, 64.1, 62.4, 57.3, 56.1, 41.8, 41.3, 41.2, 38.9, 37.3, 30.8, 30.1, 29.8, 28.9, 28.8, 27.0, 26.3, 26.1, 25.3, 25.1, 24.5, 22.0; HRMS ($FAB^+$) *m/z*: 678.3676 (Calcd for $[M+H]^+$ 678.3662).

**Synthesis of 23.** Compound **22** (195.5 mg, 0.289 mmol) was dissolved in $CH_2Cl_2$ (10 mL) and TFA (1 mL) was added at 0°C. The reaction mixture was stirred for 1 h at 0°C and the organic solvent was removed by evaporation. The residue was dissolved in anhydrous DMF (7 mL). To this solution was added 4-pentynoic acid (83.9 mg, 0.855 mmol), TEA (87.6 mg, 0.866 mmol), and PyBOP (445 mg, 0.855 mmol) at 0°C. The mixture was stirred under Ar for 7 h, and then the organic solvent was removed by evaporation and the residue was dissolved in ethyl acetate and washed with sat. $NaHCO_3$ aq., 10% citric acid aq. and water. The sample was dried using brine and $Na_2SO_4$. The organic solvent was removed by evaporation and the residue was purified by flash column chromatography to yield compound **23** (122 mg, 0.185 mmol, y. 64%). $^1$H NMR (400 MHz, $CDCl_3$) $\delta$ 78.05 (br, 1H), 7.92 (br, 1H), 7.86 (br, 1H), 6.40 (s, 1H), 5.95 (s, 1H), 4.49 (s, 1H), 4.39 (s, 1H), 4.20 (m, 1H), 3.59–3.36 (m, 14H), 3.27 (m, 2H), 3.07 (s, 2H), 2.83 (t, $J$ = 6.4 Hz), 2.60 (1, $J$ = 6.4 Hz), 2.40 (s, 1H), 2.10 (t, $J$ = 7.8 Hz), 1.78-1.15 (m, 20H); $^{13}$C NMR (100 MHz, $CDCl_3$) $\delta$ 172.9, 172.6, 172.0. 165.1, 84.6, 71.3, 70.4, 70.1, 70.0, 64.2, 62.3, 58.1, 55.9, 44.3, 42.3, 41.2, 39.7, 36.4, 32.1, 31.6,

31.0, 30.5, 29.8, 28.1, 26.9, 25.3, 25.1, 24.3, 23.1, 18.4; HRMS ($FAB^+$) *m/z*: 658.3430 (Calcd for $[M+H]^+$ 658.3400).

**Synthesis of CBtBHD.** Compounds **19** (43.4 mg, 54.0 µmol) and **23** (39.1 mg, 59.5 µmol) were dissolved in a solvent mixture consisting of DMF (5.6 mL) and water (1.4 mL), and then sodium ascorbate (21.4 mg, 108 µmol) and $CuSO_4$ (17.2 mg, 108 µmol) were added. The reaction was continued for 8 h at room temperature and the solvent was removed by evaporation. The product was purified by reversed-phase HPLC and eluted with $H_2O$/acetonitrile containing 0.1% formic acid to yield **CBtBHD** (8.68 mg, 5.94 µmol, y. 11%). $^1H$ NMR (400 MHz, $CDCl_3$) $\delta$ 8.03 (s, 1H), 7.90 (br, 1H), 7.82 (s, 1H), 7.75 (s, 1H), 7.66 (s, 1H), 7.56 (s, 1H) 7.53–7.32 (m, 5H), 7.14 (s, 1H), 5.58–5.43 (m, 6H), 4.47–4.39 (m, 4H), 4.20 (m, 1H), 3.97–3.78 (m, 10H), 3.76–3.43 (m, 24H), 3.39 (t, 2H, *J* = 7.6 Hz), 3.04–3.24 (m, 5H), 2.61 (t, *J* = 6.4 Hz), 2.58 (t, *J* = 6.4 Hz), 2.10 (t, 2H, *J* = 8.1 Hz), 1.72–1.37 (m, 26H); $^{13}C$ NMR (100 MHz, $CDCl_3$) $\delta$ 174.5, 171.9, 171.3, 167.0, 162.3, 153.2, 148.6, 145.9, 140.3, 138.2, 131.1, 129.3, 128.3, 126.9, 125.0, 122.5, 112.6, 108.4, 104.7, 70.4, 70.2, 70.0, 69.9, 69.8, 69.7, 69.6, 69.5, 69.4, 69.3, 69.2, 68.9, 68.7, 67.2, 64.1, 64.0, 63.9, 61.0, 59.2, 56.4, 56.2, 55.4, 52.6, 49.2, 45.4, 35.2, 34.6, 32.0, 29.8, 29.0, 28.9, 28.2, 28.0, 26.4, 26.2, 25.3, 24.9, 23.2, 22.9, 21.2, 17.0; HRMS ($FAB^+$) *m/z*: 1461.6169 (Calcd for $[M+H]^+$ 1461.6190).

## Experimental Procedures

**HPLC analysis.** HPLC analyses were performed with an Inertsil ODS-3 column (4.6 × 250 mm; GL Sciences, Inc.) using an HPLC system composed of a pump (PU-2080; JASCO) and a detector (MD-2010 and FP-2020, JASCO). Preparative HPLC was performed using an Inertsil ODS-3 column (10.0 × 250 mm; GL Sciences Inc.) with an HPLC system with a pump (PU-2087, JASCO) and a detector (UV-2075; JASCO).

**Fluorometric analysis.** A slit width of 5.0 nm was used for both excitation and emission with a photomultiplier voltage of 700 V. All fluorescent probes were dissolved in DMSO to obtain 1 mM stock solutions; these solutions were diluted to the desired final concentrations with the appropriate aqueous buffer. The relative fluorescence quantum yields of the compounds were obtained by comparing the area under the emission spectrum of the sample with that of a 100 mM NaOH solution of fluorescein (fluorescence quantum yield of 0.85 when excited at 492 nm).[9]

**Confocal laser scanning fluorescence microscopy.** Confocal fluorescence microscopic images were recorded using a confocal laser scanning microscope (Olympus; FLUOVIEW FV10i) equipped with a 60× lens. Fluorescein-conjugated goat

anti-rabbit IgG was excited at 473 nm. TRITC-conjugated phalloidin was excited at 559 nm. The emission filter sets used were Olympus BA490–540 for fluorescein-conjugated goat anti-rabbit IgG; BA570–620 for TRITC-conjugated phalloidin.

**Detection of protein labeling by SDS-PAGE.** BL-tag (10 μM) was added to a solution of probes (15 μM) in 100 mM HEPES buffer (pH 7.4) and the mixture was irradiated with UV light (9.3 mW/cm$^2$) for 5 min. The samples were then incubated for 1 h at 25°C and denatured in 2× SDS gel loading buffer (100 mM Tris-HCl buffer (pH 6.8), 2.5% SDS, 20% glycerol, and 10% mercaptoethanol) and resolved by 15% SDS-PAGE. Fluorescence images of the gels were captured using a digital camera (Nikon COOLPIX P6000). The gels were stained with Coomassie Brilliant Blue prior to capturing the images.

**Cell culture.** HEK293T cells were cultured in high-glucose DMEM +Gluta Max-I (Invitrogen) supplemented with 10% FBS (Gibco), penicillin (100 U/mL), and streptomycin (100 μg/mL) (Invitrogen). CHO-K1 cells were cultured in Ham's F-12 Nutrient Mix (F-12) (Life Technologies) supplemented with 10% FBS. Cells were incubated at 37°C in a humidified atmosphere of 5% $CO_2$ in air. A subculture was performed every 2–3 days from subconfluent (<80%) cultures using a trypsin-EDTA solution (Invitrogen). Transfection of plasmids was carried out in a glass-bottomed dish (Matsunami) 24-well plate (Falcon) using Lipofectamine 2000 (Invitrogen) according to the manufacturer's protocol.

**Confocal fluorescence microscopy of BL-EGFR with FPA-Caged 1 and 2.** HEK293T cells maintained in a poly-L-lysine-coated glass-bottomed dish with DMEM containing 10% FBS at 37°C under 5% $CO_2$ were transfected with BL-EGFR using Lipofectamine 2000. After 5 h, the culture medium was replaced with DMEM, and the cells were incubated at 37°C for 24 h. Next, the cells were washed three times with Hank's balanced salt solution (HBSS; Invitrogen) and incubated with 100 nM probes irradiated by UV light (9.3 mW/cm$^2$, for 5 min) in DMEM for 30 min in a $CO_2$ incubator. The cells were then washed three times with HBSS and fluorescence microscopic images were captured using appropriate filter sets. The cells were washed three times with HBSS and observed by confocal fluorescence microscopy.

**Induction of protein heterodimerization by UV light.** HEK293T cells maintained in a 24-well plate with DMEM (Invitrogen) containing 10% FBS at 37°C under 5% $CO_2$ were co-transfected with BL-GPI and Halo-GPI using Lipofectamine 2000. After 5 h, the culture medium was replaced with DMEM, and the cells were incubated at 37°C for 20 h. Next, the cells were washed once with PBS and **CBtBHD** (500 nM) was added. The samples were incubated for 30 min and washed three times with PBS. The cells

were then irradiated with UV light (9.3 mW/cm$^2$) for 5 min and incubated for 30 min at 37°C. The cells were washed with PBS three times and lysed with 250 µL of 1× SDS sample buffer (50 mM Tris-HCl buffer (pH 6.8), 1.3% SDS, 10% glycerol, and 200 mM dithiothreitol). After scraping, the lysates were boiled at 95°C for 3 min. Subsequently, the samples were electrophoresed on a 12% SDS-polyacrylamide gel and transferred to PVDF membranes for western blotting analysis. The membranes were blocked by 1 h of incubation with TBST buffer (0.01% Tween 20, 138 mM NaCl, 20 mM Tris, pH 7.6) containing 2% skim milk at room temperature. Next, anti-β-lactamase (1:100 dilution), anti-HaloTag (1:1000 dilution) antibody or streptavidin-conjugated HRP (1:5000 dilution) was added to each membrane. After incubation for 16 h at 4°C with shaking, the membrane was washed three times with TBST buffer, incubated with HRP-linked secondary antibody (anti-rabbit (1:20000 dilution), washed three times with TBST buffer, and visualized using ECL Prime Western Blotting Detection Reagent (GE Healthcare; RPN2232).

**Induction of EGFR dimerization by UV light.** CHO-K1 cells maintained in a 24-well plate with F-12 containing 10% FBS at 37°C under 5% $CO_2$ were transfected with a plasmid encoding BL-EGFR using Lipofectamine 2000. After 5 h, the culture medium was replaced with F-12 and the cells were incubated at 37°C for 20 h. Next, the cells were washed with PBS and incubated with **CBtBHD** (500 nM) for 30 min at 37°C. The cells were irradiated with UV light (9.3 mW/cm$^2$) for 5 min and incubated for 30 min at 37°C. The cells were then washed with PBS three times and were lysed with 250 µL of 1× SDS sample buffer. After scraping, the lysates were boiled at 95°C for 3 min. Subsequently, samples were electrophoresed on a 7.5% SDS-polyacrylamide gel and transferred to PVDF membranes for western blotting. The membranes were blocked by 1 h incubation with TBST buffer containing 2% skim milk at room temperature. Anti-EGFR (1:500 dilution) antibody or streptavidin-conjugated HRP (1:5000 dilution) was added to the membrane. After incubation for 16 h at 4°C with shaking, the membrane was washed three times with TBST buffer, incubated with HRP-linked secondary antibody (anti-rabbit; 1:20,000 dilution), washed three times with TBST buffer, and visualized using ECL Prime Western Blotting Detection Reagent.

**Induction of EGFR autophosphorylation by UV light.** CHO-K1 cells maintained in a 24-well plate with F-12 containing 10% FBS at 37°C under 5% $CO_2$ were transfected with a plasmid encoding BL-EGFR using Lipofectamine 2000. After 5 h, the culture medium was replaced with F-12 and the cells were incubated at 37°C for 20 h. Next, the cells were washed three times with PBS and the culture medium was replaced with F-12 (FBS−) and incubated for 24 h at 37°C. The cells were washed with PBS and incubated

with **CBtBHD** (500 nM) for 30 min at 37°C. The cells were then washed three times with PBS and incubated for 30 min at 37°C. The cells were lysed with 250 µL of 1× SDS sample buffer. After scraping, the lysates were boiled at 95°C for 3 min. Subsequently, samples were electrophoresed on a 7.5% SDS-polyacrylamide gel and transferred to PVDF membranes for western blotting. The membranes were blocked by 1 h incubation with TBST buffer containing 2% skim milk at room temperature. Next, anti-EGFR (1:500 dilution) or anti-EGFR-pY1197 (1:500 dilution) antibody was added to each membrane. After incubation for 16 h at 4°C with shaking, the membrane was washed three times with TBST buffer, incubated with HRP-linked secondary antibody (anti-rabbit; 1:20,000 dilution, anti-mouse; 1:10,000), washed three times with TBST buffer, and visualized using ECL Prime Western Blotting Detection Reagent.

**Induction of EGFR internalization by UV light.** CHO-K1 cells maintained in a glass-bottomed dish with F-12 containing 10% FBS at 37°C under 5% $CO_2$ were transfected with BL-EGFR, using Lipofectamine 2000. After 5 h, the culture medium was replaced with F-12 and the cells were incubated at 37°C for 20 h. Next, the cells were washed with PBS and the culture medium was replaced with F-12 (−) followed by incubation for 24 h at 37°C. The cells were washed three times with PBS and incubated with **CBtBHD** (500 nM) for 30 min at 37°C. The cells were then washed three times with PBS, irradiated with UV light for 5 min, and incubated for 30 min at 37°C. Next, the cells were fixed with 4% paraformaldehyde (Wako) at 4°C for 30 min and treated with 0.5% Triton X-100 (Wako) in PBS at room temperature for 2 min. After three rinses with PBS, the cells were blocked with blocking buffer (PBS containing 3% BSA) at room temperature for 1 h. Anti-EGFR antibody followed by fluorescein-conjugated goat anti-mouse antibody was used to stain BL-EGFR. Microscopic images were acquired using a filter set for fluorescein.

**Induction of cell ruffling by UV light.** CHO-K1 cells maintained in a glass-bottomed dish with F-12 containing 10% FBS at 37°C under 5% $CO_2$ were transfected with BL-EGFR using Lipofectamine 2000. After 5 h, the culture medium was replaced with F-12 and the cells were incubated at 37°C for 20 h. Next, the cells were washed three times with F-12 (−) medium and incubated with the medium for 24 h at 37°C. After two washings with F-12 (−) medium, the cells were treated with **CBtBHD** (500 nM) in F-12 (−) medium for 30 min at 37°C under 5% $CO_2$. The cells were then washed three times with PBS, irradiated by UV light for 5 min, and incubated for 30 min at 37°C. The cells were then fixed with 4% paraformaldehyde at 4°C for 30 min, and treated with 0.5% Triton X-100 in PBS at room temperature for 2 min. The cellular F-actin was stained with phalloidin-TRITC (4.8 units/mL) for 1 h at room temperature, followed by

observation using a confocal fluorescence microscope (FV-10i; Olympus) equipped with a 60× objective.

**Cell migration assay induced by UV light.** CHO-K1 cells maintained in a glass-bottomed dish with F-12 containing 10% FBS at 37°C under 5% $CO_2$ were transfected with BL-EGFR using Lipofectamine 2000. After 5 h, the culture medium was replaced with F-12 and the cells were incubated at 37°C for 20 h. Next, the cells were washed with F-12 (−) medium and incubated with the medium for 24 h at 37°C. A scratch wound was made using a 20-μL pipette tip. The cells were treated with **CBtBHD** (500 nM) in F-12 (−) medium for 30 min at 37°C followed by irradiation by UV light for 5 min and incubated for 24 h at 37°C under 5% $CO_2$. The culture medium was then removed and the cells were treated with fresh medium dissolved with **CBtBHD** (500 nM). The cells were irradiated with UV light for 5 min and incubated for 24 h at 37°C under 5% $CO_2$. The cells were observed using an FV10i confocal scanning laser microscope equipped with a 10× objective before and after treatment of **CBtBHD**. Migration of cells was analyzed using ImageJ software.

## References


1. (a) C.W. Riggsbee, A. Deiters, *Trends Biotechnol.* **2010**, *28*, 468–475. (b) A. Deiters, *ChemBioChem* **2010**, *11*, 47–53. (c) H. Yu, J. Li, D. Wu, Z. Qin, Y. Zhang, *Chem. Soc. Rev.* **2010**, 39, 464–473.
2. (a) A. Borchardt, S.D. Liberles, S.R. Biggar, G.R. Crabtree, S.L. Schreiber, *Chem. Biol.* **1997**, *4*, 961–968. (b) N. Umeda, T. Ueno, C. Pohlmeyer, T. Nagano, T. Inoue, *J. Am. Chem. Soc.* **2011**, *133*, 12–14. (c) A.V. Karginov, Y. Zou, D. Shirvanyants, P. Kota, N.V. Dokholyan, D.D. Young, K.M. Hahn, A. Deiters, *J. Am. Chem. Soc.* **2011**, *133*, 420–423.
3. A. Matagne, J.L. Brasseur, J.-M. Frère, *Biochem. J.* **1998**, *330*, 581–598.
4. C. Brieke, F. Rohrbach, A. Gottschalk, G. Mayer, A. Heckel, *Angew. Chem. Int. Ed.* **2012**, *51*, 8446–8476.
5. (a) J. Schlessinger, *Biochemistry* **1988**, *27*, 3119–3123. (b) A. Ullrich, J. Schlessinger, *Cell* **1990**, *61*, 203–211.
6. (a) Q. Wang, G. Villeneuve, Z. Wang, *EMBO Rep.* **2005**, 6, 942–948. (b) Z. Wang, L. Zhang, T. K. Yeung, X. Chen, *Mol. Biol. Cell* **1999**, *10*, 1621–1636.
7. (a) M. Nogami, M. Yamazaki, H. Watanabe, Y. Okabayashi, Y. Kido, M. Kasuga, T. Sasaki, T. Maehama, Y. Kanaho, *FEBS Lett.* **2003**, *536*, 71–76. (b) R.S. Dise, M.R. Frey, R.H. Whitehead, D.B. Polk, *Am. J. Physiol. Gastrointest. Liver Physiol.*

**2008**, *294*, G276–G285.

8. (a) Y. Wang, S. Pennock, X. Chen, Z. Wang, *Mol. Cell. Biol.* **2002**, *22*, 7279–7290. (b) Y. Gan, C. Shi, L. Inge, M. Hibner, J. Balducci, Y. Huang, *Oncogene* **2010**, *29*, 4947–4958. (c) C.D. Andl, T. Mizushima, K. Oyama, M. Bowser, H. Nakagawa, A.K. Rustgi, *Am. J. Physiol. Gastrointest. Liver Physiol.* **2004**, *287*, G1227–G1237.
9. C.A. Parker, W.T. Rees, *Analyst* **1960**, *85*, 587–600.

# Conclusions and Perspectives

This thesis described the development of multilateral protein research tools by using BL-tag and other protein labeling systems (Figure 1).

In Chapter 1, a biotin-modified labeling probe for BL-tag was developed and multilateral detection of cell surface proteins was performed using a combination of streptavidin-conjugated functional nanoparticles. Both fluorescence imaging and magnetic resonance imaging of cell surface proteins were successfully conducted using streptavidin-conjugated QDs and SPIO.

In Chapter 2, the structure of the cell-permeable probe was optimized in order to suppress non-specific adsorption onto endogenous proteins in living cells. Localization of the optimized probe in living cells was dramatically improved by introduction of a hydrophilic linker. Using the developed probe, fluorescence imaging of intracellular proteins with a high S/N ratio was successful.

Next, the probe was applied to single-molecule imaging using a TIRF microscope. Multi-color single-molecule imaging was performed with BL-tag and HaloTag systems, and immune system proteins were analyzed. The behavior change of labeled proteins derived from protein-protein interaction during signal transduction was detected. It is expected that the technology is effective for analyzing protein-protein interactions in living cells.

In Chapter 3, the protein-labeling systems were applied to induce protein dimerization. By combining BL-tag system with HaloTag system, protein homodimers and heterodimers were induced by synthesized dimerizers in living cells. Using the developed dimerizer, activation of EGFR was successful following homodimerization of the protein. Subsequently, downstream signal transduction of EGFR can be activated. Moreover, a photoactivatable dimerizer was developed and the ability to regulate EGFR activity using light was demonstrated.

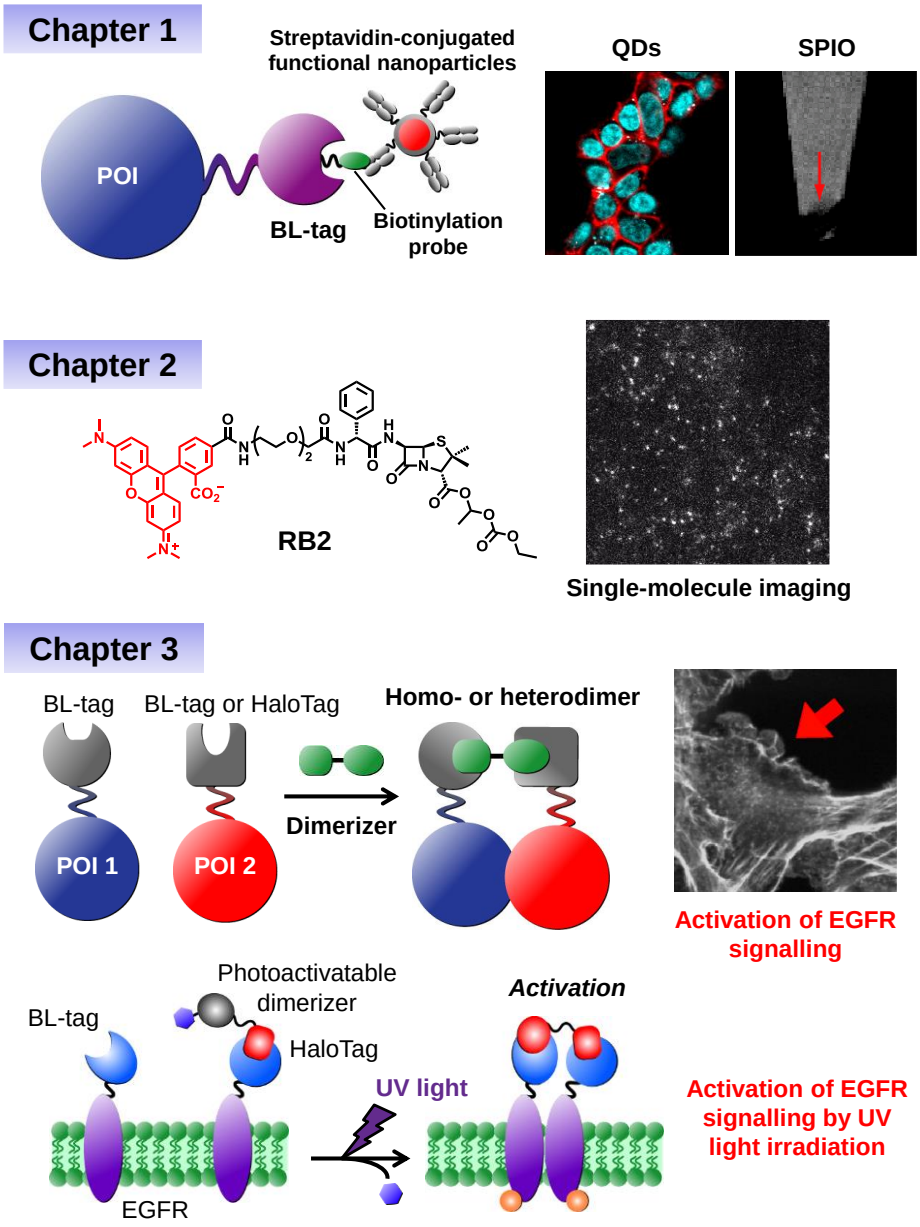


***Figure 1.*** Protein research tools developed in this research.

To fully utilize photoactivatable dimerizers, spatiotemporal activation of cell signaling using local irradiation with UV light should be adopted. Moreover, the developed dimerizers can be used to selectively activate cell surface proteins because they show poor cell permeability. In the future, dimerizers with high cell permeability should be developed and applied to control the function of intracellular proteins. These protein research tools will increase the understanding of biological phenomena and advance biological research across several fields.

# Appendix

## Protein translocation in living cells by using BHD

In Chapter 3, protein dimerization system based on protein labeling systems and synthetic dimerizer was developed. With the system, dimerization of proteins of interest (POIs) expressed inside of cells was successful. The author thought that translocation of POIs was achieved by the dimerizer. Activation of cell signaling by using a small molecule-dependent translocation of POIs was previously reported. For example, activation of small GTPases and downstream processes were achieved by rapamycin-based protein dimerization system.[1]

Protein translocation in living cells by **BHD** was performed. BL-tag fused to $Lyn_{11}$ and EGFP ($Lyn_{11}$-EGFP-BL), and HaloTag fused to mCherry (Halo-mCherry) were coexpressed in HEK293T cells. Then, the cells were treated with **BHD** for 3 h at 37°C and were observed by a confocal laser scanning microscopy (Figure A-1). The author expected that translocation of Halo-mCherry from cytosol to plasma membrane was observed by **BHD** addition. However, the fluorescence of mCherry was detected from cytosol uniformly and translocation of the protein was not observed.

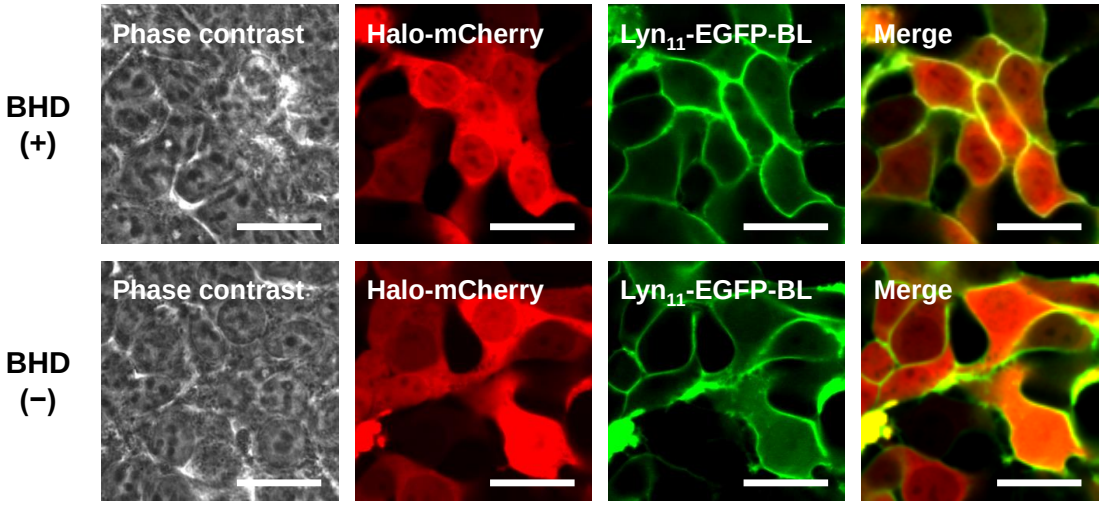


***Figure A-1.*** HEK293T cells coexpressing $Lyn_{11}$-EGFP-BL and Halo-mCherry were treated with **BHD**. The cells were transfected with plasmids encoding $Lyn_{11}$-EGFP-BL and Halo-mCherry. The cells were incubated with 500 nM of **BHD** at 37 °C for 3 h. For fluorescence microscopic images, the cells were excited at 473 nm for EGFP, and 559 nm for mCherry. Scale bar: 20 μm.

The author thought that translocation of POI was not observed because dimerization efficiency was low because of the dimerizer's poor cell permeability. Threfore, redesign of the dimerizer is needed. **BHD** has hydrophilic linker between BL-tag and HaloTag

ligand. This may decrease the cell permeability of the dimerizer. Fluorinated groups have been reported to modulate physiochemical properties of molecules.[2] Therefore, introduction of fluorinated groups into dimerizer is effective method to increase cell permeability. The groups work as an entry point into plasma membrane. If protein translocation of intracellular proteins can be achieved with the author's protein dimerization system, multiple protein translocations will be possible by combining with reported dimerizer such as rapamycin. With these systems, it is expected that analysis and elucidation of complex biological phenomena will be achieved.

## Intracellular protein dimerization induced by CBtBHD and UV light

Induction of intracellular protein dimerization was performed by **CBtBHD** and UV light irradiation. BL-tag and HaloTag were coexpressed in cytosol of HEK293T cells. Then, the cells were incubated with **CBtBHD** for 30 min. Next, the cells were irradiated with UV light for 5 min and incubated for 30 min at 37°C. The cells were lysed with SDS sample buffer and the cell lysate was analyzed by western blotting. The protein was detected by anti-β-lactamase antibody, anti-HaloTag antibody, or streptavidin-conjugated HRP (Figure A-2). When the cells were irradiated with UV light, few protein heterodimers were detected by the antibodies. Moreover, when the cells were not irradiated with UV light, very weak HaloTag protein signal was detected by streptavidin-conjugated HRP. This indicates that **CBtBHD** has poor cell permeability and little intracellular protein dimerization with **CBtBHD** can be induced by UV light irradiation. This molecule can be applied only to dimerization of cell-surface protein;

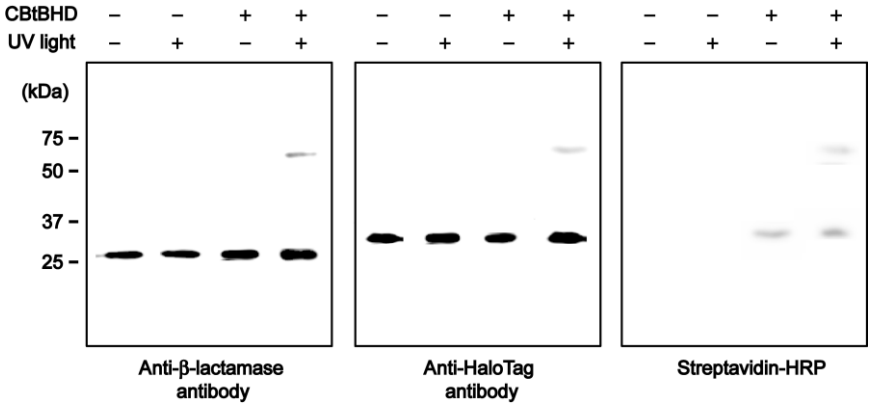


***Figure A-2.*** Dimerization of BL-tag and HaloTag in HEK293T cells using **CBtBHD** and UV light irradiation. BL-tag and HaloTag were coexpressed in HEK293T cells and treated with 500 nM **CBtBHD** for 30 min at 37°C. Next, the cells were irradiated with UV light followed by incubation for 30 min. Samples were analyzed by western blotting. Primary antibody was anti-β-lactamase, anti-HaloTag antibody, or streptavidin-conjugated HRP. Secondary antibody was HRP-conjugated anti rabbit IgG. UV light: 365 ± 5 nm. Intensity: 9.3 mW/cm$^2$, Time: 5 min.

therefore, the design of **CBtBHD** should be modified in order to increase cell permeability as well as **BHD**.

## Experimental Section

**Construction of pkmcl-EGFP-BL and pkmcl-BL-mCherry.** These plasmids were kind gifts from Dr. Atsushi Miyawaki.

**Construction of pcDNA3.1(+)-Lyn$_{11}$-EGFP-BL.** A DNA fragment of EGFP-BL was amplified from pkmcl-EGFP-BL by PCR and was digested with *Bam*HI and *Eco*RI. The DNA fragment was ligated to pcDNA3.1(+)-Lyn$_{11}$-BL, which was digested with the same restriction enzymes, to yield pcDNA3.1(+)-Lyn$_{11}$-EGFP-BL.

**Construction of pcDNA3.1(+)-Halo-mCherry.** A DNA fragment of mCherry was amplified from pkmcl-BL-mCherry by PCR and was digested with *Hind*III and *Eco*RI. The DNA fragment was ligated to pcDNA3.1(+)-Halo-EGFP, which was digested with the same restriction enzymes, to yield pcDNA3.1(+)-Halo-mCherry.

**Protein translocation in living cells by BHD.** HEK293T cells maintained in glass with DMEM (Gibco) containing 10% FBS (Gibco) at 37°C under 5% $CO_2$ were transfected with a plasmid encoding Lyn$_{11}$-EGFP-BL and Halo-mCherry, using Lipofectamine 2000 (Invitrogen). After 5 h, the culture medium was replaced with DMEM, and the cells were incubated at 37°C for 20 h. Then, the cells were washed with HBSS (Gibco) and incubated with **BHD** (500 nM) for 3 h at 37°C in DMEM. The cells were then washed three times with HBSS and microscopic images were acquired using a filter set for EGFP and mCherry.

**Induction of intracellular protein dimerization by UV light.** HEK293T cells maintained in a 24-well plate with DMEM containing 10% FBS at 37°C under 5% $CO_2$ were co-transfected with BL-tag and HaloTag using Lipofectamine 2000. After 5 h, the culture medium was replaced with DMEM, and the cells were incubated at 37°C for 20 h. Next, the cells were washed once with PBS and **CBtBHD** (500 nM) was added. The samples were incubated for 30 min and washed three times with PBS. The cells were then irradiated with UV light (9.3 mW/cm$^2$) for 5 min and incubated for 30 min at 37°C. The cells were washed with PBS three times and lysed with 250 µL of 1× SDS sample buffer (50 mM Tris-HCl buffer (pH 6.8), 1.3% SDS, 10% glycerol, and 200 mM dithiothreitol). After scraping, the lysates were boiled at 95°C for 3 min. Subsequently, the samples were electrophoresed on a 12% SDS-polyacrylamide gel and transferred to PVDF membranes for western blotting analysis. The membranes were blocked by 1 h of incubation with TBST buffer (0.01% Tween 20, 138 mM NaCl, 20 mM Tris, pH 7.6)

containing 2% skim milk at room temperature. Next, anti-β-lactamase (1:100 dilution) (Abcam; ab12251), anti-HaloTag (1:1000 dilution) (Promega; G9281) antibody or streptavidin-conjugated HRP (1:5000 dilution) (Thermo Scientific; 21130) was added to each membrane. After incubation for 16 h at 4°C with shaking, the membrane was washed three times with TBST buffer, incubated with HRP-linked secondary antibody (anti-rabbit; 1:20000 dilution) (GE Healthcare; NA934), washed three times with TBST buffer, and visualized using ECL Prime Western Blotting Detection Reagent (GE Healthcare; RPN2232).

## References


1. (a) T. Inoue, W.D. Heo, J.S. Grimley, T.J. Wandless, T. Meyer, *Nat. Methods*, **2005**, *2*, 415–418. (b) T. Komatsu, I. Kukelyansky, J.M. McCaffery, T. Ueno, L.C. Varela, T. Inoue, *Nat. Methods* **2010**, *7*, 206–208. (c) F. Castellano, P. Montcourrier, P. Chavrier, *J. Cell Sci*. **2000**, *113*, 2955–2961. (d) F. Castellano, P. Chavrier, *Methods Enzymol.* **2000**, *32*5, 285–295.
2. H.-J. Böhm, D. Banner, S. Bendels, M. Kansy, B. Kuhn, K. Müller, U. Obst-Sander, M. Stahl, *ChemBioChem* **2004**, *5*, 637–643.

# *List of Publications*

1. Cell-Surface Protein Labeling with Luminescent Nanoparticles through Biotinylation by Using Mutant β-Lactamase-Tag Technology
   A. Yoshimura, S. Mizukami, Y. Hori, S. Watanabe, and K. Kikuchi.
   *ChemBioChem* **2011**, *12*, 1031–1034.

2. Covalent Protein Labeling with a Lanthanide Complex and Its Application to Photoluminescence Lifetime-Based Multicolor Bioimaging
   S. Mizukami, T. Yamamoto, A. Yoshimura, S. Watanabe, and K. Kikuchi.
   *Angew. Chem. Int. Ed.* **2011**, *50*, 8750–8752.

3. $^{1}$H MRI Detection of Gene Expression in Living Cells by Using Protein Tag and Biotinylation Probe
   A. Yoshimura, S. Mizukami, Y. Mori, Y. Yoshioka, and K. Kikuchi.
   *Chem. Lett.* **2014**, *43*, 219–221.

4. Artificial Control of Signal Transduction by Receptor Dimerization Based on Protein Labeling Systems
   A. Yoshimura *et al*.
   *In preparation.*

5. Single-Molecule Imaging Approach for Analyzing Immune Systems by Using Protein Labeling Systems
   A. Yoshimura *et al*.
   *In preparation.*

# *Supplementary Publication*

1. pH Induced dual "OFF-ON-OFF" switch: influence of a suitably placed carboxylic acid
   K. K. Sadhu, S. Mizukami, A. Yoshimura, and K. Kikuchi.
   *Org. Biomol. Chem.* **2013**, *11*, 563–568.

## *Presentations at International Conferences*

1. Biotin modification of living cell surface using mutant β-lactamase-tag technology
   A. Yoshimura, S. Mizukami, and K. Kikuchi.
   *World Molecular Imaging Congress*, Kyoto, Japan, September 2010.

2. Development of biotin-modification probe using mutant β-lactamase-tag technology
   A. Yoshimura, S. Mizukami, and K. Kikuchi.
   *Pacifichem*, Honolulu, Hawaii, USA, December 2010.

3. Development of Labeling Method for Cell-surface Protein with Functional Nanoparticles
   A. Yoshimura, S. Mizukami, and K. Kikuchi.
   *Sweden-Japan Joint Colloquium "Direct Imaging in Bio / Medical Science"*, Lund, Sweden, January 2011.

4. Development of labeling method for cell-surface protein with functional nanoparticles
   A. Yoshimura, S. Mizukami, and K. Kikuchi.
   *Gordon Research Conference –Bioorganic Chemistry*, New Hampshire, USA, June 2011.

5. Development of Labeling Method for Cell-Surface Protein with Fluorescent Nanoparticles
   A. Yoshimura, S. Mizukami, Y. Mori, Y. Yoshioka, and K. Kikuchi.
   *The 11th Global COE International Symposium: Bio-Environmental Chemistry*, Osaka, Japan, December 2011.

## *Award*

1. Chair's Outstanding Poster Award
   *Gordon Research Conference –Bioorganic Chemistry*, New Hampshire, USA, June 2011.

# Acknowledgements

The author is very grateful to Professor Kazuya Kikuchi for his continuous guidance, support, and encouragement throughout this study. The author expresses sincere thanks to Dr. Shin Mizukami for providing valuable guidance and discussion. The author also expresses his cordial thanks to Dr. Yuichiro Hori for his kind help and useful suggestions.

The author is deeply grateful to Professor Yoshichika Yoshioka and Dr. Yuki Mori at Osaka University for their cooperation and support during MRI measurements. The author expresses his gratitude to Professor Masahiro Ueda and Dr. Jun Kozuka at RIKEN Quantitative Biology Center and Dr. Yutaro Kumagai at Osaka University for their support with single-molecule imaging of the immune system.

The author would like to thank Professor Shigenori Kanaya and Professor Shinobu Itoh for their helpful discussions and suggestions. Thank you to all of the members of the Kikuchi group for their kind help, teaching, and friendship.

The author acknowledges financial support from the Japan Society for the Promotion of Science (JSPS) for Young Scientists and the Global Centers of Excellence (GCOE) Program “Global Education and Research Center for Bio-Environmental Chemistry” of Osaka University.

Finally, the author appreciates the tremendous support and continuous encouragement of his family and friends.

Osaka, Japan
January, 2014

**Akimasa Yoshimura**

*Laboratory of Chemical Biology*
*Department of Material and Life Science*
*Division of Advanced Science and Biotechnology*
*Graduate School of Engineering*
*Osaka University*